Production of dust by massive stars at high redshift

C. Gall · J. Hjorth · A. C. Andersen

Abstract The large amounts of dust detected in sub-millimeter galaxies and quasars at high redshift pose a challenge to galaxy formation models and theories of cosmic dust formation. At $z > 6$ only stars of relatively high mass (> 3 M$_\odot$) are sufficiently short-lived to be potential stellar sources of dust. This review is devoted to identifying and quantifying the most important stellar channels of rapid dust formation. We ascertain the dust production efficiency of stars in the mass range 3–40 M$_\odot$ using both observed and theoretical dust yields of evolved massive stars and supernovae (SNe) and provide analytical expressions for the dust production efficiencies in various scenarios. We also address the strong sensitivity of the total dust productivity to the initial mass function. From simple considerations, we find that, in the early Universe, high-mass (> 3 M$_\odot$) asymptotic giant branch stars can only be dominant dust producers if SNe generate $\lesssim 3 \times 10^{-3}$ M$_\odot$ of dust whereas SNe prevail if they are more efficient. We address the challenges in inferring dust masses and star-formation rates from observations of high-redshift galaxies. We conclude that significant SN dust production at high redshift is likely required to reproduce current dust mass estimates, possibly coupled with rapid dust grain growth in the interstellar medium.

C. Gall
Dark Cosmology Centre, Niels Bohr Institute, University of Copenhagen, Juliane Maries Vej 30, DK-2100 Copenhagen, Denmark
Tel.: +45 353 20 519
Fax: +45 353 20 573
E-mail: christa@dark-cosmology.dk

J. Hjorth
Dark Cosmology Centre, Niels Bohr Institute, University of Copenhagen, Juliane Maries Vej 30, DK-2100 Copenhagen, Denmark
Tel.: +45 353 25 928
Fax: +45 353 20 573
E-mail: jens@dark-cosmology.dk

A. C. Andersen
Dark Cosmology Centre, Niels Bohr Institute, University of Copenhagen, Juliane Maries Vej 30, DK-2100 Copenhagen, Denmark
Tel.: +45 353 25 892
Fax: +45 353 20 573
E-mail: anja@dark-cosmology.dk

1 Introduction

The origin of the significant amounts of dust found in high-z galaxies and quasars (QSOs) remains elusive.

The detection of thermal dust emission from high-z QSOs at sub-millimeter and millimeter wavelengths (e.g., Omont et al, 2001, 2003; Carilli et al, 2001b; Bertoldi and Cox, 2002) indicates far-infrared luminosities $\geq 10^{12-13}$ L$_\odot$, implying dust masses of $\geq 10^8$ M$_\odot$ and star-formation rates up to 3000 M$_\odot$ yr^{-1} (e.g., Bertoldi et al, 2003). Observational evidence for dust in these systems has been reported by, e.g., Pei et al (1991); Pettini et al (1994); Ledoux et al (2002); Priddey et al (2003); Robson et al (2004); Chary et al (2005); Beelen et al (2006); Hines et al (2006).

The age of the Universe at $z > 6$ was less than ~1 Gyr. Early star formation is believed to have taken place at redshift 10–50 (Tegmark et al, 1997; Greif and Bromm, 2006); the highest redshift QSO known is at $z = 7.1$ (Mortlock et al, 2011) while the earliest observationally galaxies detected so far include a spectroscopically confirmed $z = 8.2$ gamma-ray burst host galaxy (Tanvir et al, 2009; Salvaterra et al, 2009), a galaxy reported to be at a spectroscopic redshift of $z = 8.6$ (Lehnert et al, 2010), a gamma-ray burst host galaxy at $z \sim 9.4$ (Cucchiara et al, 2011), and a galaxy at a photometric redshift of $z \sim 10$ (Bouwens et al, 2011). The epoch of reionization is determined at $z = 10.4 \pm 1.2$ (Komatsu et al, 2010) (~500 Myr after the Big Bang). These facts imply that the maximum time available to build up large dust masses is at most ~400–500 Myr, and possibly much less.

Hence, a fast and efficient dust production mechanism is needed. Core collapse supernovae (CCSNe) are contemplated to be the most likely sources of dust at this epoch (e.g., Dwek, 1998; Tielens, 1998; Edmunds, 2001; Morgan and Edmunds, 2003; Maiolino et al, 2004) due to their short lifetimes and large production of metals. Consequently, several theoretical models for dust formation in CCSNe have been developed, which result in dust masses of up to 1 M$_\odot$ per SN within the first ~600 days after the explosion (e.g., Kozasa et al, 1989, 1991; Clayton et al, 1999, 2001; Todini and Ferrara, 2001; Nozawa et al, 2003). Dwek et al (2007) argued that 1 M$_\odot$ of dust per SN is necessary if SNe only are to account for the inferred amounts of dust in high-z QSOs.

However, observations of dust in the ejecta of nearby SNe a few hundred days past explosion have revealed only $\sim 10^{-4}$–10^{-2} M$_\odot$ of hot (~400–900 K) dust (e.g., Wooden et al, 1993; Elmhamdi et al, 2003; Sugerman et al, 2006; Kotak et al, 2009). Larger amounts (~10^{-2} M$_\odot$ up to ~1 M$_\odot$) of cold and warm (20–150 K) dust have been reported in SNe and SN remnants (SNRs), a few 10–1000 years after explosion (e.g., Rho et al, 2008, 2009; Dunne et al, 2009; Gomez et al, 2009; Barlow et al, 2010; Matsuura et al, 2011).

The discrepancy between observationally and theoretically determined dust yields has provoked a reconsideration of SN dust formation theories (Cherchneff and Dwek, 2010) and models including dust destruction have been developed (e.g., Bianchi and Schneider, 2007; Nozawa et al, 2007; Nath et al, 2008; Silvia et al, 2010). These models demonstrate that dust grains can be effectively destroyed in a reverse shock on timescales up to $\sim 10^4$ years after the SN explosion. However, they are unable to explain the low observed dust masses at earlier epochs.

Dust production in SNe seems to depend on SN Type (e.g., Kozasa et al, 2009; Nozawa et al, 2010). Moreover, intermediate and high-mass asymptotic giant branch (AGB) stars with

masses between 3–8 M$_\odot$ have sufficiently short lifetimes of a few 10^7–10^8 years (e.g., Schaller et al, 1992; Schaerer et al, 1993; Charbonnel et al, 1993; Raiteri et al, 1996) to be potential contributors to dust production in high-z galaxies (e.g., Marchenko, 2006).

In addition to the possible influence from different types of stars on the total amount of dust in high-z systems, the prevailing initial mass function (IMF) plays an important role. In the local Universe, an IMF favouring lower mass stars is well established (e.g., Elmegreen, 2009) while the IMF in the early Universe and in starburst galaxies may be biased towards high-mass stars (e.g., Doane and Mathews, 1993; Davé, 2008; Dabringhausen et al, 2009; Habergham et al, 2010).

In this review we summarize current knowledge about the most important channels for stellar sources to produce dust towards the ends of their lives and identify the relevant stellar mass ranges contributing to the total amount of dust in galaxies. We determine the ranges of dust production efficiencies of AGB stars and SNe and address the influence of various IMFs on the dust productivity of stars between 3–40 M$_\odot$. Based on this insight we review what is currently known about the stellar contribution to dust in high-z galaxies. The review is arranged as follows: we first summarize our knowledge about the late stages of stellar evolution of massive stars (Sect. 2). In Sect. 3 some fundamentals of dust grain formation and characteristics are described. We address the complexity of determining the amount of dust theoretically and observationally in Sect. 4 (evolved massive stars) and Sect. 5 (SNe). Dust production efficiencies are quantified in Sect. 6 and the impact of the IMF on the total dust productivity is discussed in Sect. 7. The inference of large amounts of dust in massive high-z galaxies and QSOs, along with theoretical models addressing this topic, is reviewed in Sect. 8. Sect. 9 provides a summary of the main conclusions of this review and an outlook for future directions.

## 2 The late stages of massive stellar evolution

For the most likely dust producers, such as AGB stars and CCSNe, the majority of the dust production takes place at the end stages of their evolution. Therefore, pertaining to the observed presence of dust in galaxies and QSOs at $z \geq 6$, only stars which live short enough to die before the age of the Universe at this redshift are conceivable sources of dust.

In Fig. 1 we illustrate the relation between the minimum zero-age main sequence (ZAMS) mass of stars and the redshift at which they die. We have considered three different epochs for the onset of star formation. For a formation redshift of $z = 10$ we find that the lowest mass of a star to be a potential source of dust at $z = 6$ is 3 M$_\odot$. Less massive stars can be excluded because their lifetimes are longer than the age of the Universe at this redshift. The effect of the metallicity with which a star is born is small.

Owing to this ascertainment, we are solely interested in the high-mass ($\gtrsim 3$ M$_\odot$) stellar population. We therefore briefly summarize what is known about the end stages of massive stellar evolution, which eventually govern the dust production of these stars.

2.1 The first stars

The first generation of stars, so-called Population III (Pop III) stars, played an important role in reionizing the Universe and were responsible for the early enrichment with metals. They are believed to have formed in dark-matter mini halos of $\sim 10^{5-6}$ M$_\odot$ at redshift $z \sim 10$–50 (e.g., Tegmark et al, 1997; O'Shea and Norman, 2007). The very first stars (Pop III.1)
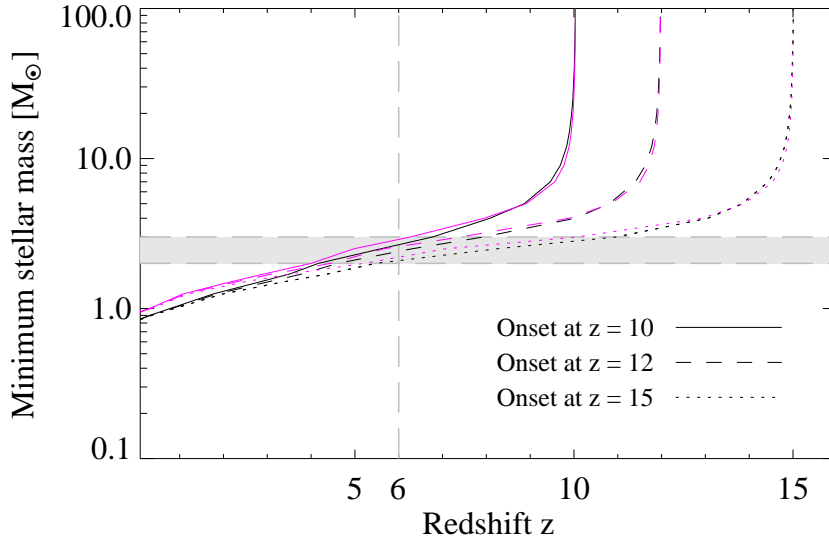
Fig. 1 Relation between stellar mass, stellar lifetime and redshift in the early Universe. The graphs show the minimum ZAMS mass of a star dying at a given redshift for an onset of star formation at three different epochs: $z = 15$ (dotted curves), $z = 12$ (dashed curves) and $z = 10$ (solid curves). The colour coding corresponds to different metallicities: $Z = 0.001$ (black) and $Z = 0.040$ (magenta). The vertical dashed line marks a star dying at $z = 6$, similar to the highest-redshift QSOs known. The grey shaded region indicates stars with masses between 2–3 $M_\odot$. The metallicity dependent lifetimes are taken from Schaller et al (1992), Schaerer et al (1993) and Charbonnel et al (1993). The cosmological model used is a ΛCDM Universe with $H_0 = 70$ km s^{-1} Mpc^{-1}, $\Omega_m = 0.3$ and $\Omega_\Lambda = 0.7$.

formed in isolation and are expected to have been relatively rare, only about 10% by mass of all generations of Pop III stars (e.g., Greif and Bromm, 2006; McKee and Tan, 2008). From simulations it is predicted that these stars are very massive, $\sim 10^{2-3}$ $M_\odot$ (e.g., Abel et al, 2002; Bromm and Larson, 2004; Schneider et al, 2006; Yoshida et al, 2006). The formation of the second generation of stars (Pop III.2) is influenced by the radiative and mechanical feedback effects of the first stars and is found to be delayed by about ~ 200 Myr (e.g., Johnson et al, 2007; Yoshida et al, 2007a). The critical mass of these stars is suggested to be lower, about ~ 30–40 $M_\odot$ (e.g., Yoshida et al, 2007b; Norman, 2010). For a review on the first stars we refer the reader to Bromm et al (2009).

According to Heger et al (2003), stars with metallicity $Z = 0$ and masses between 40–140 $M_\odot$ and above 260 $M_\odot$ collapse into black holes, while stars in the mass range 140–260 $M_\odot$ die as pair instability SNe (PISNe). The explosion will entirely disrupt the star, leaving a quite peculiar chemical signature (Heger and Woosley, 2002) which is manifested in a strong odd-even effect of the produced nuclei. So far, only one supernova, the Type Ic SN 2007bi has been reported as a PISN (Gal-Yam et al, 2009). However, theoretical modeling indicates that SN 2007bi may also be consistent with an energetic core-collapse SNe with a main sequence progenitor mass of ~ 100–280 $M_\odot$ (Moriya et al, 2010; Yoshida and Umeda, 2011). The typical PISN signature expected to be observable in the first and most metal-poor stars has not been detected yet (e.g., Beers and Christlieb, 2005). The reason for the non-detection is unclear. Ekström et al (2008) discuss the possibility that, under the conditions

of fast rotation, CNO line driven Wolf–Rayet (WR) winds and magnetic fields, the PISN stage of very massive stars can be avoided. Karlsson et al (2008) argue that stars formed out of gas enriched by primordial PISNe are more metal-rich and thus the signature of PISNe would not be expected in metal-poor stars.

The metal enrichment by Pop III stars leads to formation of low-mass Pop II stars, as soon as a critical metallicity of $Z_{cr} \sim 10^{-6}$–10^{-4} $Z_\odot$ (Bromm and Loeb, 2003; Schneider et al, 2006; Tumlinson, 2006) is reached. This transition is expected to take place fast due to a rapid metal enrichment (Maio et al, 2010), although metal-free regions survive over longer timescales. Greif et al (2010) showed in a cosmological simulation that one single PISN (at $z \simeq 30$) can enrich the mini halo in which it forms uniformly up to $Z = 10^{-3}$ $Z_\odot$ and induce Pop II star formation (at $z \simeq 10$).

The IMF for the first stars is considered to have been very top heavy with high characteristic masses > 35–100 $M_\odot$ (e.g., Bromm et al, 2002; Tumlinson, 2006; Yoshida et al, 2008). For the generation of Pop II stars, top heavy IMFs with somewhat lower characteristic masses or Salpeter-like IMFs are usually assumed. Tumlinson (2006) points out that metal-free star formation is relatively scarce at redshift $z \sim 6$. Owing to the above discussion, PISNe and the very first stars are disputable to be major dust sources for dust-rich galaxies at $z \sim 6$.

2.2 AGB stars

Stars in the AGB phase are in their late stages of evolution. They have initial masses in the range $\sim$ 0.85–8 $M_\odot$ and have completed the helium-burning phase in their centers. AGB stars have low surface temperatures (max 3500 K) but high luminosities (a few times 10^3 $L_\odot$) and have built up so-called helium- and hydrogen-burning shells around their degenerate cores of carbon and oxygen. The hydrogen burning shells deliver the energy needed to maintain the high luminosities. During the AGB evolution the stars develop quite strong winds with increasing mass-loss rates towards their late stages whereby they lose some of their matter (e.g., Schöier and Olofsson, 2001). The very late stages are characterized by intense mass-loss, which increases towards the end, when the stars enter a super-wind phase with mass-loss rates up to 10^{-4} $M_\odot$ yr^{-1} (e.g., Bowen and Willson, 1991; Schöier and Olofsson, 2001). In general, the stars lose up to $\sim$ 80 % of their masses during the AGB phase and form circumstellar envelopes of gas and dust. Low and intermediate mass stars (at the lower mass end of the AGB mass range) end their lives as white dwarfs. However, the final fate of stars with masses around 8 $M_\odot$ might be different (see Sect. 2.4).

AGB stars can be broadly divided into three distinct classes based on low-resolution spectra: (i) The oxygen-rich M-stars whose spectra are dominated by bands due to TiO molecules, (ii) the carbon-rich C-stars whose spectra are dominated by bands due to C_2 and CN molecules and (iii) S-stars which are neither rich in oxygen nor carbon, identified through their strong bands due to primarily ZrO (Lattanzio and Wood, 2003).

The distribution of C- and M-stars is a function of stellar mass and initial metal abundance. For low initial metallicities it is easier to form C-stars as less carbon needs to be dredged up. Stellar evolutionary models by Karakas and Lattanzio (2007) predict that for Large Magellanic Cloud (LMC)-like metallicities, M-stars evolve from low (1.0–1.5 $M_\odot$) and high (5.0–8.0 $M_\odot$) mass stars, while C-stars originate from intermediate (1.5–5.0 $M_\odot$) mass stars. The latter has also been found by e.g., Vassiliadis and Wood (1993) and Zijlstra et al (2006).

Generally, AGB stars with masses above 4 $M_\odot$ experience hot-bottom burning (e.g., Blöcker and Schönberner, 1991; D'Antona and Mazzitelli, 1996) leading to a reduction of the amount of carbon which can be dredged up. Models of massive low-metallicity AGB stars (Ventura and D'Antona, 2009) show that $Z = 10^{-4}$ stars appear as C-stars during most of their AGB phase while a slightly higher metallicity of $Z = 6 \times 10^{-4}$ yields M-stars.

2.3 Core collapse supernovae

CCSNe are divided into two different classes, Type I and Type II, and their subtypes (e.g., Filippenko, 1997, and references therein). Type II SNe are defined by the presence of hydrogen lines in the optical spectra while Type I SNe are defined through their absence. The CCSNe subtypes can be aligned roughly in the order of increasing progenitor mass, starting with II-P, II-L, IIn, IIb, Ib and Ic (e.g., Anderson and James, 2008). As we discuss below, there is no one-to-one correspondence between progenitor mass and spectral Type. However, the alignment of the SN subtypes might correspond to increasing mass-loss of the hydrogen envelope (for Type II SNe) and subsequent stripping of the helium envelope (Type I SNe) of the progenitors (e.g., Nomoto et al, 1995; Maund et al, 2011). The main characteristics of the subtypes leading to the typical CCSN classification scheme are summarized in Table 1.

The most common CCSNe are Type II-P SNe. Smartt et al (2009) find, that the mass range of the progenitors of Type II-Ps is between $8.5^{+1.0}_{-1.5}$ and $17 \pm 1.5\,M_\odot$. A lower mass limit of ~8 $M_\odot$ was found independently by Anderson and James (2008). However, theoretical predictions from stellar evolution models (e.g., Heger et al, 2003; Eldridge and Tout, 2004; Poelarends et al, 2008) indicate a higher upper mass limit for II-P SNe: For solar metallicity it is ~25 $M_\odot$ and increases with decreasing metallicity. It is therefore unclear what happens with stars more massive than 17 $M_\odot$. The progenitors of II-Ps are found to be red supergiants (RSGs) (e.g., Woosley and Weaver, 1986; Smartt, 2009; Crockett et al, 2011). Confirmed examples include SN 2003gd (Smartt et al, 2004; Maund and Smartt, 2009) and SN 2008bk (Mattila et al, 2008b, 2010; Van Dyk et al, 2010). The Type II-P SN 2002hh likely arose from a RSG progenitor of around 16–18 $M_\odot$ (Pozzo et al, 2006; Smartt et al, 2009). However, RSGs up to 25 $M_\odot$ have been detected in the Local Group (e.g., Levesque et al, 2005, 2006). One possibility is that they collapse and form a black hole (Smartt et al, 2009; Heger et al, 2003; Fryer et al, 2007). In that case, they either appear as very faint SNe or no explosion is observed at all due to fallback of ^{56}Ni. Alternatively, more massive stars might end their lives as Type II-L SNe. A possible example is SN 2009kr whose progenitor could be a yellow super giant (YSG) of mass 15–24 $M_\odot$ (Elias-Rosa et al, 2010; Fraser et al, 2010).

Stars more massive than 25 $M_\odot$ evolve into WR stars and likely explode as Ib or Ic SNe (Massey and Olsen, 2003; Crowther, 2007). A small fraction of these involve a relativistic explosion (Soderberg et al, 2010) leading to broadlined Ic SNe, sometimes accompanied by a gamma-ray burst (e.g., Hjorth et al, 2003). During their precursor luminous blue variable (LBV) stage, they lose their hydrogen envelope either through massive eruptions or in periods of enhanced mass-loss and form a rather dense circumstellar disc (CSD). The WR phase lasts for approximately 10^5 years (e.g., Meynet and Maeder, 2003; Eldridge and Vink, 2006) whereupon the star finally explodes as a CCSN, leaving a black hole.

Stars more massive than 25–30 $M_\odot$ may explode during their LBV phase before entering the WR stage. This was the case for SN 2005gj (Kotak and Vink, 2006; Trundle et al, 2008) and SN 2005gl (Gal-Yam et al, 2007), which both appeared as very bright CCSNe of Type IIn. The Type IIn SN 2005ip (Smith et al, 2009) had a different progenitor, probably a RSG

Table 1 Definitions of different types of core collapse SNe[a]

SN Type	Defining characteristics	Progenitor mass range in $M_\odot$	Progenitor characteristics	Prominent examples
Type II	hydrogen present			
II-P (plateau)[b]	blue, almost featureless spectrum	(7) 8–25	RSG	SN 1969L, SN 2003gd
II-L (linear)[c]	very blue, almost featureless spectrum	~ 15–25	YSG	SN 2009kr
IIn (narrow line)	narrow emission lines on a broad base			
IIn	low luminosity	~ 8–10	SAGB	SN 2008S
IIn	very luminous	> 25–30	LBV	SN 2005gj, SN 2005gl
IIb	similar to Type Ib SN, little hydrogen present	> 25–30	WR, binary	SN 1993J, SN 2008ax
Type I	hydrogen deficient			
Ib	helium rich	> 25	WR	SN 1999dn
Ic	helium deficient, no Si II	> 25	WR, binary	SN 2007gr

Notes. [a]The types of CCSNe are classified based on their spectral appearance and photometric evolution (e.g., Filippenko, 1997). Information on the progenitor is taken from Smartt et al (2009) and Smartt (2009). [b]The lightcurve exhibits a 'plateau' for an extended periode after maximum brightness. [c]The lightcurve (in magnitudes) declines linearly with time.

of roughly 20–40 $M_\odot$. This shows that Type IIn SNe may arise from either stars with LBV-like mass ejection if they are very luminous, or from massive RSGs with a strong wind interaction if of moderate luminosity.

The fate of stars more massive than roughly 17–25 $M_\odot$ is sensitive to mass-loss effects, depending on magnetic fields, metallicity, binarity, or rotation, although the details of these dependencies are not well understood (e.g., see for a review Puls et al, 2008). As a consequence, there is no simple relation between SN Type and progenitor mass. It seems, however, that these stars rather explode as IIn, IIb, Ib or Ic SNe than ordinary Type II-P SN. The progenitor of the Type IIb SN 2008ax (Crockett et al, 2008; Pastorello et al, 2008) was a late-type 28 $M_\odot$ WR star with strong nitrogen emission lines in the spectra (a so-called WNL star). The mass of the progenitor of the Type IIb SN 2003bg was estimated to be 20–25 $M_\odot$ (Mazzali et al, 2009). The Type Ib SN 1999dn seems to be consistent with a progenitor of mass 23–25 $M_\odot$ (Benetti et al, 2011). An example of a Type Ic SN is SN 2004gt, where the progenitor mass is estimated to be $\gtrsim$ 40 $M_\odot$ (Maund et al, 2005). For the Ic SN 2002ap a single star progenitor of 30–40 $M_\odot$ has been proposed, but with very high mass-loss rates (Crockett et al, 2007).

Binary interaction between two lower mass stars has been contemplated as the progenitor for some Type IIb and Ic SNe. For the IIb SN 1993J a companion star was clearly observed (Maund et al, 2004). Other examples where this scenario has been invoked include the IIb SN 2001ig (Ryder et al, 2006), SN 2002ap (Crockett et al, 2007), SN 2004gt (Maund et al, 2005) and SN 2008ax (Crockett et al, 2008).

2.4 The critical progenitor mass range 8–10 $M_\odot$

The fate of stars in the mass range $\sim$ 8–10 $M_\odot$ is ambiguous since the mass border between high-mass AGB stars and CCSNe is smeared out. Moreover, the decisive factors for the development of stars in this mass range are unfortunately rather uncertain (e.g., Nomoto, 1984, 1987). We denote this range the critical progenitor mass range.

Stars in the critical progenitor mass range may either evolve directly into II-P SNe or form an electron-degenerate core of oxygen, neon and magnesium (O-Ne-Mg) and enter the super AGB (SAGB) phase. SAGB stars can either become O-Ne-Mg white dwarfs or turn into electron capture SNe (ECSNe).

The appearance of an ECSN could be as a faint and ^{56}Ni poor II-P SN such as SN 1994N, SN 1999eu or SN 2005cs (Pastorello et al, 2004, 2006). However, Smartt et al (2009) did not find any signature or convincing evidence that faint and ^{56}Ni poor II-P SNe are ECSNe. The inferred luminosities for progenitors in this mass range rather favour normal Type II-P SNe. A peculiar example is the faint and ^{56}Ni poor II-P SN 2007od (Andrews et al, 2010), whose spectra favour a SAGB star as the progenitor (Inserra et al, 2011).

Alternatively, a ECSN could occur as a low-luminosity Type IIn SN such as SN 2008S (Prieto et al, 2008). The progenitor mass of SN 2008S was determined to be $\sim$6–10 $M_\odot$ and the progenitor could have been a SAGB star (Prieto et al, 2008; Botticella et al, 2009; Wesson et al, 2010).

According to Wanajo et al (2009), about 30 % of all CCSNe could appear as ECSNe if all stars in the mass range of 8–10 $M_\odot$ end in the explosion channel. Poelarends et al (2008, and references therein) suggested that only the most massive (9–9.25 $M_\odot$) stars will explode as ECSNe, representing $\sim$ 4% of all SNe. Siess (2007, 2008) showed that at very low metallicity ($Z = 10^{-6}$), the mass range for stars becoming an ECSN is much broader (7.6–9.8 $M_\odot$). Thompson et al (2009) suggested the rate of ECSNe to be $\sim$ 20% of all CCSNe.

2.5 Type Ia supernovae

Type Ia SNe are characterized by the absence of hydrogen and presence of silicon in their spectra and are believed to result from a thermonuclear explosion of a carbon-oxygen white dwarf (e.g., Livio, 2000; Hillebrandt and Niemeyer, 2000). An explosion takes place when the white dwarf reaches the Chandrasekhar mass through external mass supply. However the nature of the progenitors and explosion patterns are controversial. Two scenarios are currently favoured; (i) a single-degenerate model where a main sequence or giant companion star transfers mass by Roche lobe overflow (Whelan and Iben, 1973; Fink et al, 2007) and (ii) a double degenerate model where the companion star is also a white dwarf and the two objects merge (Iben and Tutukov, 1984; Webbink, 1984; Pakmor et al, 2010). The mass range of stars possibly exploding as Type Ia SN is 3–8 $M_\odot$ (e.g., Maoz, 2008) which means that the stars become C-O white dwarfs after having evolved as AGB stars. This gives rise to rather long delay times between the formation of the progenitor system and the explosion due to the long lifetimes of these stars. From explosion models (e.g., Greggio and Renzini, 1983; Matteucci and Recchi, 2001; Greggio, 2005) different delay times are predicted. Observations indicate that there may be two different progenitor channels, resulting in SNe Ia with delays of either $\lesssim$ 400 Myr or $\gtrsim$ 2.4 Gyr since progenitor formation (Brandt et al, 2010). Mannucci et al (2006) suggest that half the SNe Ia explode already after about 100 Myr while the other half have longer delay times of about 3 Gyr.

Table 2 Main characteristics of some prominent dust species

Dust species	Chemical definition	T_c [K][a]	Spectral characteristics, prominent bands [μm][b]	Reference
Carbon-rich environment				
Amorphous carbons, a-C:H	sp^2/sp^3, H	$\gtrsim 1700$	$\approx 0.2, 3.4, 6.85, 7.25$	1–8
PAH[c]	fusions of C_6H_6[d]	$\lesssim 1700$	0.2–0.26, 2–50	7, 9, 10
Graphitic carbon	sp^2	~ 1600	~ 0.22	11, 12
Silicon carbide	SiC	$\gtrsim 1700$	~ 10–13	12–14
Oxygen-rich environment				
Olivine	$[Mg, Fe]_2SiO_4$[e]	~ 1300	~ 0.7–1.5, 9, 10–11.6, 18, 20	15–19
Forsterite	Mg_2SiO_4	~ 1300	$\sim 10, 11.3, 69$	15, 17, 20, 21
Fayalite	Fe_2SiO_4	~ 1000	$\sim 10.6, 11.4, 93$–94, 110	15, 17, 20, 22, 23
Pyroxene	$[MgFe]SiO_3$[e]	~ 1300	~ 10–20, 40.5	15, 24
Enstatite	$MgSiO_3$	~ 1300	$\sim 9.7, 19.5, 26$–30	15, 24
Magnetite	Fe_3O_4	~ 800	$\sim 17, 25$	15, 25
Corundum	Al_2O_3	~ 1700	broad at ~ 13 (12.5–14)	15, 26
Spinel	$MgAl_2O_4$	~ 1200	$\sim 0.3, 0.5, 2, 13, 17, 32$	15, 19, 27
Calcite	$CaCO_3$	~ 800	$\sim 6.8, 11.4, 44, 92$	28
Dolomite	$CaMg[CO_3]_2$	~ 800	$\sim 6.6, 11.3, 60$–62	28
Iron	Fe	~ 900	featureless	15, 29, 30

References. (1) Jäger et al (1998b); (2) Duley and Williams (1981); (3) Jones and Nuth (2011); (4) Dartois et al (2004); (5) Frenklach et al (1989); (6) Pascoli and Polleux (2000); (7) Jäger et al (2009a); (8) Mennella et al (1997); (9) Cherchneff (2011); (10) Cherchneff et al (1991); (11) Draine and Lee (1984); (12) Sharp and Wasserburg (1995); (13) Lodders and Fegley (1995); (14) Mutschke et al (1999); (15) Gail (2010); (16) Koike et al (1993); (17) Jäger et al (1998a); (18) Pitman et al (2010); (19) Zeidler et al (2011); (20) Koike et al (2003); (21) Koike et al (2010); (22) Hofmeister (1997); (23) Pitman and Hofmeister (2006); (24) Koike et al (2000); (25)Koike et al (1981); (26)Koike et al (1995); (27) Fabian et al (2001); (28) Posch et al (2007); (29) Palik (1985); (30) Kemper et al (2002);
Notes. [a]T_c is an *approximate* dust condensation temperature which varies with different properties, such as the proximity to thermodynamic equilibrium, the prevailing pressure or the composition of the gas (e.g., Sharp and Wasserburg, 1995; Gail, 2010). [b]The exact peaks depend in most cases on properties of the grains such as temperature, crystallinity, size, morphology or impurities. Most silicates and oxides are highly transparent in the ultraviolet (UV), visual and NIR and absorption data are either hardly available or laboratory data are not reliable since the values are often too small to be measured with standard methods of spectroscopy (Zeidler et al, 2011). [c]Polycyclic aromatic hydrocarbon (PAH). [d]benzene (C_6H_6) is an aromatic hydrocarbon (AH) and PAHs consist of several fused aromatic benzene rings, e.g., pyrene ($C_{16}H_{10}$), pentacene ($C_{22}H_{14}$), coronene ($C_{24}H_{12}$) [e]Olivine and pyroxene are non-stoichiometric compounds with the chemical formulation for olivine: $Mg_{2x}Fe_{2(1-x)}SiO_4$ and for pyroxene: $Mg_xFe_{(1-x)}SiO_3$, with $0 < x < 1$.

Having discussed the end-stages of massive stellar evolution, we next address the dust formation processes associated with massive stars (Sect. 3, 4 and 5).

3 Fundamentals of dust formation and grain species

Dust is formed by a series of chemical reactions in which atoms or molecules from the gas phase combine into clusters of increasing size. The molecular composition of the gas phase determines which atoms and molecules are available for grain formation and grain growth. The sizes of dust grains are in the range of a few 0.01–1 μm (e.g., Mathis et al, 1977; Weingartner and Draine, 2001).

The dust formation process is typically described as a two-step process, i.e., the condensation of critical seed clusters out of the gas phase and the subsequent growth to macroscopic dust grains of certain sizes and species. The nucleation process in the majority of current models is based on the so-called *classical nucleation theory* (Feder, 1966), which was developed to explain the formation of water droplets in the Earth's atmosphere. It has been found that at temperatures between ~ 700 K and ~ 2000 K and densities in the range $\sim 10^{-13}$–10^{-15} g cm^{-3} (Feder, 1966; Clayton, 1979; Sedlmayr, 1994) thermodynamically stable clusters can form. Note, however, that the applicability of this theory to astrophysical environments has been questioned (e.g., Donn and Nuth, 1985). An alternative theory based on chemical kinetics has also been applied to describe dust formation in diverse environments (e.g., Frenklach and Feigelson, 1989; Cherchneff et al, 1992).

Dust grain formation depends on various critical parameters such as for example the sticking probability, α. This parameter depends on, e.g., the material under consideration, the internal energy of the grains, the impact energy or the temperature of the gas. However, the exact sticking probability is uncertain (Draine, 1979; Leitch-Devlin and Williams, 1985; Gail, 2003) and is therefore often taken to be unity, for simplicity. In this case all colliding particles stick together, leading to a maximum amount of dust to be formed under the given nucleation and growth conditions.

The resulting dust species depend on the environment. Stellar environments are mainly rich in either carbon or oxygen and depending on the most abundant element, predominantly either carbonaceous dust or silicates will form (see Table 2 for an overview of some common dust species).

Carbonaceous dust mainly consists of the element carbon (C) and has manifold forms of appearance defined by the types of carbon hybrid orbitals (sp, sp^2 and sp^3) leading to different bond structures between the C atoms (e.g., Henning et al, 2004). Amorphous carbon is typically characterized by the ratio of sp^2 to sp^3 hybridized bonds. Graphitic grains are composed solely of sp^2 and nano-diamonds of sp^3 hybridized bonds, respectively. Dependent on the ratio of sp^2 to sp^3 and the impurity of other elements in the single bonds (i.e., H, N), various subtypes of either amorphous carbon, such as hydrogenated amorphous carbon (a-C:H) or nano-diamonds are created (e.g., Duley and Williams, 1981; Molster and Waters, 2003; Henning et al, 2004; Jones and D'Hendecourt, 2004). In an environment which is not only carbon-rich but also H-rich, polycyclic aromatic hydrocarbon (PAH) can form at low temperatures ($T_c \lesssim 1700$ K) (e.g., Cherchneff et al, 1991; Jäger et al, 2009a; Cherchneff, 2011). Typically, PAHs are fusions of several aromatic benzene (C_6H_6) rings (e.g., Cherchneff et al, 1992) and constitute the building blocks for the condensing solid particles, so-called soot grains (e.g., Jäger et al, 2011). The largest PAH molecules condensing together with the soot grains are found to have 222 C atoms ($C_{222}H_{42}$) (e.g., Jäger et al, 2009a,b, and references therein).

Other dust grains found in a carbon-rich environment are for example FeS, MgS or different polytypes of silicon carbide (SiC), such as α-SiC or β-SiC (e.g., Borghesi et al, 1985; Orofino et al, 1991), which condense at high temperatures (e.g., $T_c \gtrsim 1700$ K) (e.g., Daulton et al, 2002, and references therein).

Silicates are the most stable condensates. Typically, silicate grains consist of $[SiO_4]^{4-}$ tetrahedra in conjunction with Mg^{2+} or Fe^{2+} cations. For reviews on cosmic silicates we refer to Henning (2010a,b). Overall, silicate grains can be categorized into amorphous silicates or crystalline silicates. The crystalline lattice structure allows the tetrahedra to share their oxygen atoms with other tetrahedra. This leads to the formation of different types of silicates (Molster and Kemper, 2005), such as forsterite, fayalite, olivine, enstatite, ferrosilite or pyroxene (see Table 2 for details). Forsterite and enstatite are the most abundant crystalline

silicates (Molster and Waters, 2003, and references theirein). Carbonates are chemical compounds of the characteristic carbonate ion CO_3^{2-} with elements such as e.g., Ca, Mg or Fe. Common examples are calcite ($CaCO_3$), magnesite ($MgCO_3$), dolomite ($CaMg[CO_3]_2$) or siderite $FeCO_3$. Other dust grains formed in an oxygen-rich environment include corundum (Al_2O_3), grains of the group of spinels (i.e., spinel ($MgAl_2O_4$), magnetite (Fe_3O_4)), silica (SiO_2) or metallic iron (Fe).

4 Dust from evolved massive stars

4.1 Dust from AGB stars

In the local Universe, AGB stars are the prime sources of dust injected into the interstellar medium (ISM) (Gehrz, 1989; Sedlmayr, 1994; Dorschner and Henning, 1995). The dust is injected as part of the intense mass-loss during the late stages of AGB stellar evolution (see Sect. 2.2). The driving mechanism of the mass-loss is believed to be a combination of thermal pulsation and radiation pressure on dust grains resulting in slow dust driven winds (e.g., Höfner et al, 1998; Höfner and Andersen, 2007) with typical velocities between 3–30 km s^{-1}.

The dust composition in AGB stars depends on the C/O ratio in the photosphere of the star which is directly connected to the nucleosynthesis in the stellar interior. Newly formed elements like carbon and oxygen are mixed to the surface by a deep convective zone. The mixing processes occur during the thermally pulsing AGB (TPAGB) phase and also involves the external layers (Iben and Renzini, 1981). The TPAGB phase lasts approximately 10^{4-6} yr depending on the stellar mass and number of thermal pulses (Blöcker, 1995). The stellar pulsations cause atmospheric shock waves propagating through the atmosphere. Subsequently, gas is lifted above the stellar surface, producing dense, cool layers favourable for possible solid particle formation (e.g., Höfner et al, 1998). The ongoing nuclear burning and dredge-up changes the relative abundance of carbon and oxygen as the stars evolve. A change in the C/O ratio results in a change of the spectral type (see Sect. 2.2) and the composition of the dust (see Sect. 3).

- M-type: C/O < 1 results in an oxygen excess since all carbon is bound in CO molecules creating an oxygen rich environment where either silicates or carbonates are formed
- S-type: C/O ≈ 1 leads to an exhaustion of C and O which are almost completely bound in CO. For this type no abundant grain forming elements are available and grain species are defined by the less abundant elements.
- C-type: C/O > 1 creates a carbon rich environment (all oxygen bound in CO) where predominantly hydrocarbon molecules and carbonaceous dust forms together with some silicon carbide.

Deriving the dust driven mass-loss characteristics of AGB stars is difficult and the current understanding is based on numerical models. Detailed time-dependent dynamical models featuring a frequency-dependent treatment of the radiative transfer have successfully explained the mass-loss mechanism for C-stars (e.g., Höfner et al, 2003; Höfner, 2006; Winters et al, 2000). In such stars, amorphous carbon grains form from the excess of carbon at high temperatures. Mass-loss is enhanced by the radiation pressure on such grains which efficiently accelerates the dust particles away from the star, dragging the gas along. Models involving C-rich dust driven mass-loss are well tested and are consistent with observations (e.g., Gautschy-Loidl et al, 2004; Nowotny et al, 2005, 2010).

In the case of M-stars the oxygen environment leads to formation of preferentially Fe-free silicates (Woitke, 2006; Höfner and Andersen, 2007), in particular olivine and pyroxene type grains. Such grains are consistent with observed features in infrared (IR) spectra of cool giants (Molster et al, 2002a,b,c). However, small (< 1 μm) grains of Fe-free silicates would result in insufficient radiation pressure to drive a wind due to their transparency at wavelengths corresponding to the flux maximum of AGB stars. Höfner (2008) and Mattsson and Höfner (2011) have shown that larger grains of sizes in a very narrow range around 1 μm can drive a wind. This grain size range is also consistent with grain sizes observed in the ISM.

Dust formation and mass-loss in S-type stars pose substantial problems (Höfner, 2009). According to observations, S-stars show circumstellar physical properties similar to C- and M-stars (e.g., Ramstedt et al, 2009). However, the equality between the most abundant elements O and C inhibits the formation of known mass-loss driving dust species such as amorphous carbon or micron-sized silicates in sufficient abundances. Several minor dust species have been proposed which however are either not abundant enough or of too low opacity to enhance mass-loss (e.g., Ferrarotti and Gail, 2002, 2006). While some of these species possibly play an important role, it remains uncertain which dust types or processes drive the winds.

AGB stars are important suppliers of molecules which play a crucial role in forming dust and are important for mass-loss mechanisms (e.g., Olofsson, 1996, 1997; Knapp et al, 1998, and references therein). IR and sub-millimeter observations of AGB stars have revealed many different types of molecules (e.g., CO, SiO, PAHs, etc.) (e.g., Justtanont et al, 1996; Yang et al, 2004). In theoretical studies of M-, S- and C-stars, using a chemical kinetic approach (e.g., Cherchneff et al, 1991, 1992; Cherchneff, 2006), a wide variety of the observed molecules could be reproduced. Apart from the molecules formed only in specific environments (C- or O-rich), species such as CO, SiO, HCN and CS have been found theoretically and observationally in all types of AGB stars (e.g., Cherchneff, 2006; Decin et al, 2008, 2010).

Studying the influence of metallicity on the mass-loss and dust formation processes in AGB stars is important to understand their role in the early Universe. Theoretical investigations by Wachter et al (2008) showed that the wind velocity decreases with lowering the metallicity of low-mass AGB stars, while the mass-loss rate remains unaffected. The latter also resulted from models by Mattsson et al (2008) under the condition that the amount of condensable carbon in low-metallicity AGB stars is comparable to that of the more metal-rich counterparts. Using the James Clerk Maxwell Telescope, Lagadec et al (2009) performed CO observations of six carbon stars in the Galactic Halo and the Sagittarius stream and came to similar conclusions: The mass-loss rates of C-stars are unaffected by metallicity but the expansion velocities for metal-poor C-stars are lower. *Spitzer Space Telescope* observations of the LMC, the Small Magellanic Cloud (SMC) and the Fornax Dwarf Spheroidal indicate that mass-loss rates for M-type stars are more sensitive to metallicity while metal-poor C-stars are unaffected (e.g., Zijlstra et al, 2006; Groenewegen et al, 2007; Lagadec et al, 2007; Matsuura et al, 2007; Sloan et al, 2009). The amount of dust produced by M stars is found to decrease with decreasing metallicity while for C stars it remains unchanged (Groenewegen et al, 2007; Sloan et al, 2008). van Loon et al (2008) present ESO/VLT spectra of a sample of dusty C stars, M stars and red supergiants in the SMC. A comparison of the properties of molecular bands to similar data in the LMC indicates that dust formation in M-stars as well as in C-stars is less efficient at lower metallicities.

Typical mass-loss rates obtained observationally and theoretically are between 10^{-7} and 10^{-5} M$_\odot$ yr^{-1} (e.g., Schöier and Olofsson, 2001; Willson, 2007; Mattsson et al, 2008;

Matsuura et al, 2009). The mass-loss rates and the dust-mass-loss rates are linked via the gas-to-dust mass ratio, for which a canonical value of 200 is often assumed (e.g., Lagadec et al, 2009; Sloan et al, 2009). Estimated values of the gas-to-dust mass ratio obtained from CO observations coupled with either radiative transfer or dynamical modeling range between $\sim$ 200 and 700 (e.g., Groenewegen et al, 1998b,a; Ramstedt et al, 2008).

It is important to stress that the models discussed above are developed for low and intermediate mass stars. A theoretical dust formation model for AGB stars in the mass range of 1–7 $M_{\odot}$ has been developed by Ferrarotti and Gail (2006). Dust yields are calculated for several metallicities and result in total dust masses up to a few times 10^{-2} $M_{\odot}$. The considered grain species are silicates, iron dust, SiC and carbon, which are the most abundant grain types in M-, S- and C-type AGB stars. The model combines synthetic stellar evolution models with a non-equilibrium dust formation prescription. The dynamical treatment of the stellar outflows is simplified in that stationary flows are assumed and hence the mass-loss rate is an input parameter because it cannot be determined self-consistently. Nevertheless, the model of Ferrarotti and Gail (2006) is currently the only available source which provides dust yields for AGB stars covering a large range of stellar masses and metallicities.

4.2 Dust from red super giants and Wolf–Rayet stars

RSGs are evolved O or B stars at the He-burning stage and arise from massive stars (< 40 $M_{\odot}$). Stellar evolution models by Meynet and Maeder (2003) suggest that the RSG phase lasts for about 0.4 Myr for a $\sim$ 25$M_{\odot}$ star or 2 Myr for a $\sim$ 10$M_{\odot}$ star. Massey et al (2005) estimated a dust production rate of about 3×10^{-8} $M_{\odot}$ yr^{-1} kpc^{-2} for RSGs in the solar neighbourhood which is about 1% of the dust return rate of AGB stars.

For RGSs with a luminosity $\lesssim$ 1000 $L_{\odot}$ no evidence for dust production has been found in studies of the globular cluster 47 Tuc (Boyer et al, 2010; McDonald et al, 2011) (contrary to the findings of Origlia et al, 2007, 2010). However, stars more luminous than $\sim$ 1–2 $\times 10^3$ $L_{\odot}$ do appear dusty (e.g., McDonald et al, 2009, 2011).

From observations of the H II region NGC 604 in M33, it was found that RSGs appear more extinguished than WR stars, indicating large amounts of dust around the RSGs (Eldridge and Relaño, 2011). WR stars are the successors to massive RSGs which undergo strong winds which drive away the dust created prior to the WR phase (Eldridge et al, 2006). Thus WR stars appear less extinguished.

Although the above examples show that dust is produced around evolved massive stars, it is unclear how much of the dust survives the subsequent SN explosion. There is evidence for ongoing dust destruction in the expanding SN blast wave of the SNR Cas A, as well as dust evaporation due to the UV flash from the SN (Dwek et al, 2008).

5 Supernova dust

As outlined in the following, on average, a few times 10^{-4} $M_{\odot}$ of relatively hot dust ($\sim$ 500–1000 K) has been reported from CCSNe at early epochs while large amounts of cold dust (< 50 K) have been claimed in SN 1987A and SNRs which are a few 100–1000 yr old. In contrast, theoretical models predict that a high amount of dust in the SN ejecta can form within the first 600–1000 days (Kozasa et al, 1989, 1991; Clayton et al, 1999, 2001; Todini and Ferrara, 2001; Nozawa et al, 2003; Bianchi and Schneider, 2007; Cherchneff and Dwek,

2010). The calculated dust masses are of order 10^{-1}–1 M$_\odot$ for SNe in the mass range 12–40 M$_\odot$, for metallicities between 0–1 Z$_\odot$.

Pertaining to this controversy, we next address the difficulties of deriving dust masses in SNe from either theory or observations and provide a status of the current observational situation.

5.1 Theory

The first models to investigate dust formation in SNe were developed by e.g., Cernuschi et al (1965) and Hoyle and Wickramasinghe (1970). More recent work has addressed the various dust species and amounts of dust formed in SN ejecta, but the models are still in their infancy. The applied theories (standard nucleation theory or chemical kinetics) for dust formation in SNe is similar to that used in models for other stellar environments such as (i) stellar outflows of AGB stars (Sect. 4.1) or LBVs (e.g., Ferrarotti and Gail, 2001; Gail et al, 2005), but also (ii) substellar atmospheres (e.g., Helling et al, 2008) or (iii) brown dwarfs (e.g., Burrows, 2009, and references therein).

In addition to the uncertainties in the applied dust formation theories (Sect. 3), the SN dust models are hampered by complex physical processes which are not well understood, such as the SN explosion and subsequent expansion of the ejecta. The amount of dust and the variety of dust species formed in the theoretical models thus strongly depend on the assumptions made.

5.1.1 Dust formation models based on standard nucleation theory

Todini and Ferrara (2001, hereafter TF01) investigated the formation of dust in Type II SN arising from progenitors with 12–35 M$_\odot$ and metallicities between zero and solar. The nucleation of dust grains is based on the classical nucleation theory. For the formation of CO and SiO molecules chemical equilibrium is assumed. The ejecta are considered to be spherically symmetric and the chemical elements are fully mixed. The gas temperature and density are uniform throughout the considered volume. The temporal evolution of the temperature is defined by the assumption of an adiabatic expansion of the ejecta. For the kinetic energy of the explosion two different values are considered. In most models, amorphous carbon grains are typically the first grains which condense out of the gas phase about 300–400 days past explosion. Large seed clusters made of N monomers are able to condense and amorphous carbon grains grow to large grain sizes of about 300 Å.

Most of the amorphous carbon dust is formed at a gas temperature in the ejecta of about $T = 1800$ K. As the ejecta expand other dust species condense at lower gas temperatures, i.e., corundum at $T \sim 1600$ K, and then magnetite, enstatite and forsterite at $T \sim 1100$ K. Typically fairly small dust grains of about 10–20 Å of these species form. At zero metallicity, and in the lower energy case, the calculated total dust masses per SN are in the range 0.08 M$_\odot < M_d < 0.3$ M$_\odot$, but are increased when a higher explosion energy is assumed. The dust masses per SN increase with increasing metallicity, e.g., the amount is three times higher for Z$_\odot$ relative to zero metallicity. The obtained log-normal grain size distribution is found to be rather insensitive to metallicity.

The model of TF01 has been revisited by Bianchi and Schneider (2007) to study the effect of a reverse shock on the dust grains. Another grain species, SiO$_2$, is added to those already considered by TF01. Moreover, only clusters with a minimum number of monomers

of either $N \geq 2$ or $N \geq 10$, and discrete accretion of these, are considered. These modifications lead to an alteration of the log-normal grain size distribution of all dust species except for amorphous carbon grains and result in a larger mean grain size (and less numerous grains). With increasing N, less Si-bearing grains of large grain sizes form while amorphous carbon grains are not affected. In the case of solar and sub-solar metallicity, around 0.1–0.6 $M_\odot$ of dust is formed per SN. However for $Z = 0$ no dust is produced for progenitors more massive than 35 $M_\odot$. The final dust masses per SN are sensitive to varying the sticking probability α between 1 and 0.1. Assuming $\alpha = 0.1$ leads to significantly reduced total dust masses (0.001–0.1 $M_\odot$ of dust for progenitor masses below 20 $M_\odot$). Higher α leads to larger grains. Si-bearing grains are significantly more affected by lower values of α than amorphous carbon grains, and in some cases the amount of dust in Si-bearing grains becomes negligible. A shift of the size distribution of carbonaceous dust grains towards larger grains with higher α has also been found by Fallest et al (2011).

Bianchi and Schneider (2007) used a simple semi-analytical model to treat the dynamics of the reverse shock. The model is based on analytical approximations by Truelove and McKee (1999) for the velocity and radius of the forward and reverse shocks in the non-radiative ejecta-dominated phase and subsequent Sedov–Taylor phase of SNRs. For the energy and ejecta mass, values similar to the TF01 formation model are adopted and three different values for the ISM density are investigated. Furthermore, a uniform density distribution inside the spherically symmetric ejecta is assumed along with a uniform distribution of the dust grains. The grain size distribution is considered to be the same throughout the ejecta. It has been found that due to erosion caused by thermal and non-thermal sputtering, the grain size distribution is shifted towards smaller grains. Depending on the density of the ISM about 2–20 % of the initially formed dust mass survives (higher fraction at lower density). About 4–8×10^4 years after explosion the reverse shock has penetrated 95 percent of the original volume of the ejecta.

Nozawa et al (2003, hereafter N03) studied dust formation in the SN ejecta of zero metallicity stars (13–40 $M_\odot$) taking also PISNe (with masses of 170 or 200 $M_\odot$) into account. The classical nucleation theory is assumed, but following Gail et al (1984), a non-steady state nucleation rate is calculated. The temporal evolution of the density and temperature are calculated following hydrodynamical models by Shigeyama and Nomoto (1990) and a multifrequency radiative transfer code coupled with the energy deposition from radiative elements (Iwamoto et al, 2000), respectively. The models distinguish between unmixed ejecta and mixed ejecta. In the unmixed case, the ejecta are divided into different layers, each of different elemental composition, i.e., the innermost regime (consisting of elements such as Fe, Si and S) followed by oxygen-rich layers (composed of elements such as O, Si and Mg), and outermost, a He layer. The mass of each layer varies with progenitor mass. In the mixed case, all elements are assumed to be uniformly distributed. For either case, a formation efficiency of unity is assumed for the key molecules CO and SiO, and the total amount of freshly formed dust is found to increase with progenitor mass. The total amount of dust per SN for the mixed ejecta generally is found to be larger than for the unmixed ejecta. For SNe between 13–40 $M_\odot$ about 2–5 % of the progenitor mass condenses into dust while the corresponding fraction for for PISNe between 140–260 $M_\odot$ is 15–30 %. In the mixed case the ejecta are oxygen rich due to the assumption that the formation of CO molecules is complete. Consequently, only oxide grains such as forsterite, corundum, enstatite, SiO_2 or magnetite condense. The most abundant grain species for SNe are SiO_2 and forsterite. In the unmixed case various different grain species condense in each layer depending on the elemental composition of those. The main grain types formed are carbon, Fe, Si and forsterite.

The average grain radius of each grain species depends on the elemental composition and the gas density at the formation site.

Similar to the study of Bianchi and Schneider (2007), Nozawa et al (2007) investigate dust destruction caused by the impact of the reverse shock in the SNR phase of zero metallicity stars. The ejecta are assumed to be spherical and to expand into a uniform ISM with primordial composition, where three different cases for the hydrogen number density are considered. For the density and velocity structure of the ejecta the hydrodynamical models of Umeda and Nomoto (2002) together with the dust models (mixed and unmixed) of N03 are adopted. Three different radiative cooling processes are included. Dust destruction by sputtering and the deceleration of dust grains due to gas drag are taken into account while the effect of charge of the dust grain is neglected.

Initially, very large grains (> 0.2 μm) are found to be expelled into the ISM through the forward shock while their size is only marginally reduced through sputtering. Smaller grains are either destroyed through sputtering in the post-shock flow or are trapped and remain behind the forward shock. The critical grain size below which dust particles are fully destroyed is sensitive to the density of the ISM and is found to be in the range 0.01–0.2 μm for a hydrogen number density in the range 0.01–10 cm^{-3}. The grain size distribution of the surviving dust is therefore dominated by large grains. The fraction of dust destroyed is found to be higher for the mixed grain model than for the unmixed, as the mixed model lacks grains larger than > 0.01–0.05 μm. Furthermore, the final fate of the dust grains depends on the thickness of the hydrogen envelope of the progenitor star (Nozawa et al, 2010). In the case of a thin hydrogen envelope (as expected for Type IIb SNe) smaller grains form. Moreover, the reverse shock encounters the ejecta much earlier than for SNe with a thick hydrogen envelope (as is the case for Type II-P SNe). In the latter case the reverse shock encounters the dust $\sim 10^{3-4}$ yr after explosion, depending on the density of the ISM.

5.1.2 Dust formation model based on chemical kinetics

Models for dust formation in the SN outflow of a zero metallicity star of 20 M$_\odot$ and PISNe (170 and 270 M$_\odot$) have been accomplished by Cherchneff and Dwek (2009, 2010). For the temperature and density structure of the SN ejecta, the models of N03 are adopted. The temporal evolution of those quantities is calculated by assuming that the ejecta follow an adiabatic expansion similar to the models described above. The ejecta velocity is for simplicity kept constant and a mixed (Umeda and Nomoto, 2002) and unmixed case (N03) are considered. It has been argued that the commonly adopted assumptions of thermodynamic equilibrium as well as the standard nucleation theory are inappropriate for describing dust formation in the dynamical flows of SN ejecta (see Sect. 3). Cherchneff and Dwek (2009, 2010) therefore use a chemical kinetic approach for the formation of molecules and dust grains. The chemical kinetic description of the ejecta is based on (i) the initial chemical composition of the gas and (ii) a set of chemical reactions describing the chemical processes in the ejecta. This new approach leads to smaller dust masses by a factor of ~ 5 and to a different chemical composition of the formed dust compared to the models of either TF01, N03 or Schneider et al (2004). The most abundant grain species which form in these models are pure silicon, silica and silicates, while carbon dust is negligible.

5.2 Inferring dust masses from observations

Deriving the mass of dust from observations is equally complex. Warm dust emits in the near-infrared (NIR) and mid-infrared (MIR) wavelength range, whereas the emission from cold dust is shifted to far-infrared (FIR) or sub-millimeter wavelengths and is often difficult to differentiate from cold foreground material. In addition, it is impossible to infer the structure of dust grains and their spatial distribution within the ejecta from observations. Hence, the derived dust masses rely on the models and techniques used to interpret the data.

The methods mainly used to infer the existence of dust are based on observations of either (i) the attenuation of the red wings of spectral lines at optical/NIR wavelengths or (ii) the thermal emission from dust grains. Most observations of SNe and SNRs have been made with the *Spitzer Space Telescope* since its launch in 2003, because ground-based MIR observations are difficult. The instruments onboard of *Spitzer* cover in the wavelength range 3.6–160 μm. Earlier observations, e.g., of SN 1987A (Wooden et al, 1993) were performed with the *Kuiper Airborne Observatory* operating in the 1–500 μm spectral range. The start of operation of the *Herschel Space Observatory* in 2009 has facilitated FIR and sub-millimeter observations (detectors sensitive to wavelengths between 55–625 μm) of SNe and SNRs as has already been accomplished, e.g., for Cas A and SN 1987A (Barlow et al, 2010; Matsuura et al, 2011).

5.2.1 Dust masses in SN ejecta

The attenuation of broad and intermediate spectral emission lines, e.g., the He I, Ca II IR triplet or O I line, is a relatively reliable and usually pronounced signature of the presence of dust. Using this method direct confirmation of newly formed dust in the ejecta has been presented for some SNe, including SN 1987A (e.g., Danziger et al, 1989; Lucy et al, 1989), SN 1990I (e.g., Elmhamdi et al, 2004), SN 1999em (e.g., Elmhamdi et al, 2003), and SN 2004et (e.g., Sahu et al, 2006; Kotak et al, 2009). Evidence for formation of new dust not only in the ejecta but also in the post-shocked shell of IIb/IIn SNe was revealed for example for SN 1998S (e.g., Pozzo et al, 2004), SN 2005ip (e.g., Smith et al, 2009), SN 2006jc (e.g., Smith et al, 2008b; Mattila et al, 2008a) and SN 2007od (Andrews et al, 2010; Inserra et al, 2011). Unfortunately, it is difficult to quantitatively derive the amount of dust, or its composition or geometry (e.g., Kotak, 2008), with this method.

Thermal emission from dust is typically detected in IR observations of SNe as a NIR or MIR 'excess'. Such an 'excess' may arise from newly formed dust in the SN ejecta or in the cool, dense shell of post-shocked gas within the forward and reverse shock. The new dust may be collisionally heated by hot gas in the reverse shocks, or heated due to radioactivity or optical emission from circumstellar interaction. Alternatively, thermal emission could be caused by pre-existing dust in the circumstellar medium. In this case the dust is either collisionally heated by hot, shocked gas, the flash from the SN or it is heated due to the interaction between the ejecta and the circumstellar matter. The latter two cases result in an 'IR echo' due to light travel time effects. It is challenging to differentiate between newly and pre-existing dust from observations of thermal emission, although thermal emission caused by an echo seems to appear at earlier epochs than emission due to dust formation, which takes place a few hundred days past explosion.

Studies of SN light curves are also useful since, in case of an echo, the light curve shows characteristic features. However, either scenario might contribute to the late-time IR flux as was the case for SN 2004et, SN 2006jc, SN 2007it and SN 2007od (e.g., Kotak et al, 2009; Mattila et al, 2008a; Andrews et al, 2010, 2011b).

5.2.2 Dust masses in SN remnants

In old SNRs (see Sect. 5.3.1) it is possible that most of the dust is cold and has escaped detection in MIR studies. Sub-millimeter observations with SCUBA have been accomplished for the Cas A (Dunne et al, 2003) and Kepler (Morgan et al, 2003) SNRs. The first measurements resulted in very large derived dust masses ($\sim$ 0.3–3 $M_\odot$) at cool temperatures of about 17–18 K. However, in particular for Cas A it has been suggested that most of the sub-milimeter emission likely arises from foreground molecular clouds (Krause et al, 2004; Wilson and Batrla, 2005). Similar considerations and new calculations led to a downwards revision of the dust mass for Kepler of about a factor of two (Gomez et al, 2009). Using either sub-millimeter polarimetry (Dunne et al, 2009) or the *Herschel Space Observatory* instruments (Barlow et al, 2010), lower dust masses were obtained for Cas A as well, although for either remnant the obtained amount of dust is well above the average results of MIR-studies in SNe at early and late epochs.

5.2.3 Caveats and uncertainties

Deriving the dust masses in SN ejecta and remnants is basically similar to the method used for deriving the amount of dust in galaxies (see Sect. 8.1). Based on the method discussed by Hildebrand (1983), the dust mass for a single temperature component is determined from the flux density observed at some frequency, λ, as

$$M_{\mathrm{d}} = \frac{F(\lambda)D_{\mathrm{L}}^2}{\kappa_{\mathrm{d}}(\lambda, a)B(\lambda, T_{\mathrm{d}})},$$ (1)

where $F(\lambda)$ is the total flux, D_{L} is the luminosity distance to the object, T_{d} is the dust temperature, $B(\lambda, T_{\mathrm{d}})$ is the black-body Planck function and $\kappa_{\mathrm{d}}(\lambda, a) = (3/4)Q(\lambda, a)/(\rho a)$ is the dust absorption coefficient for a (spherical) grain type. Here $Q(\lambda, a)$ is the dust absorption efficiency, ρ is the dust bulk density and a is the dust particle radius. The temperature T_{d} can be derived from a spectral fit. The luminosity of a single spherical grain of radius a and temperature T_{d} is given as $L_{\mathrm{d}}(\lambda) = 4\pi a^2 \pi B(\lambda, T_{\mathrm{d}})Q(\lambda, a)$.

In the Rayleigh limit, $a < \lambda$, the absorption coefficient κ is independent of the particle radius a, thus $\kappa \equiv \kappa_{\mathrm{d}}(\lambda)$, which is usually adopted since exact grain sizes and grain size distributions are unknown.

The main uncertainties in deriving the dust mass are (i) the considered dust species, (ii) the optical constants, i.e., the dust absorption coefficients for the considered dust species and (iii) the unknown grain size distribution. For reported dust mass estimates the adopted dust grain composition often varies. In addition, different optical constants are often applied for similar dust species i.e., (i) for graphite and silicate grains the optical constants are taken from Draine and Lee (1984), Draine (1985), Ossenkopf et al (1992) or Laor and Draine (1993), (ii) for Mg protosilicates from Dorschner et al (1980a) or Jäger et al (2003) and (iii) for amorphous carbon grains values from Hanner (1988) or Rouleau and Martin (1991) are assumed. While Bouchet et al (2004) preferred silicate dust for SN 1987A, Ercolano et al (2007) adopt large amounts of graphite grains. For more recent SNe, Fox et al (2010) rule out silicates and use only graphite for SN 2005ip as do Mattila et al (2008a) for SN 2006jc. Andrews et al (2010) and Andrews et al (2011b) favour an amorphous carbon dominated model for SN 2007it and SN 2007od. Spectroscopic evidence for silicate dust was revealed through a large, but declining SiO mass in SN 2004et (Kotak et al, 2009). For Cas A, Hines et al (2004) adopted a magnesium protosilicate-based grain model from Dorschner et al

(1980b) and Arendt et al (1999). Rho et al (2008) fit the spectra with a variety of different grain species based on the theoretical models of N03 and TF01 but favour magnesium proto-silicates, while Dunne et al (2003, 2009) assume grains which are either amorphous or have a clumpy, aggregate structure. Silicates and graphite dust have been assumed in the Crab and the SNR B0540 (Green et al, 2004; Temim et al, 2006; Williams et al, 2008). Assuming silicate rather than graphite dust typically leads to higher inferred dust masses. It is evident from the above highlighted examples that the determination of the grain type composition is not trivial.

Further complications in deriving the amount of dust from SNe arise from ambiguous considerations about the SN ejecta physics. In most cases it is unclear whether the ejecta are mixed or unmixed, and additionally a uniform dust and gas distribution is often assumed, while there seemingly is evidence for mixing and clumpy ejecta, as we explain below. Mixing in the ejecta likely can be explained by the theoretically observed instability of the nickel bubble during explosion of the SN leading to Rayleigh–Taylor instabilities forming in the post-shocked ejecta (e.g., Chevalier and Klein, 1978; Arnett, 1988; Herant and Benz, 1991; Herant and Woosley, 1994; Kifonidis et al, 2003). This might also support suggestions for the presence of undetected larger amounts of dust at early epochs, if dust grains are assembled in optically thick clumps (e.g., Lucy et al, 1989, 1991; Elmhamdi et al, 2003; Wooden et al, 1993; Sugerman et al, 2006; Ercolano et al, 2007; Meikle et al, 2007). According to Meikle et al (2007), dust in the ejecta of SNe can become optically thick in the MIR for dust masses exceeding a few times 10^{-3} M$_\odot$. However, in most of the cases where clumpy models have been applied, significantly larger dust masses than for smooth models were not found. In particular also these models fail to explain the large dust masses predicted by theoretical models (Wooden et al, 1993; Ercolano et al, 2007; Meikle et al, 2007; Andrews et al, 2010, 2011b).

A scenario of dust grain growth in SN and SNRs over longer timescales of a few 10–1000 yr could explain the difference in dust mass at early and late epochs. Once a stable cluster has formed, further growth to macroscopic dust grains can take place. The growth regime of dust grains extends to lower temperatures and densities than for the nucleation regime (see Sect. 3). However, significant growth is restricted by the available condensable material and dilution of the SN ejecta (Draine, 1979; Sedlmayr, 1994). The amount and timescale of grain growth might also be dependent on the Type of the SN, examples of which are the SNRs B0540−69.3, Cas A or the Crab nebula. For the latter, an extended dust grain growth phase could possibly explain the presence of large dust grains (Temim et al, 2006).

5.3 Quantitative evidence of dust from supernovae

Bearing in mind the caveats discussed in Sect. 5.2, we now proceed to summarize current reported observational evidence for dust arising from SNe.

5.3.1 SNe and SN remnants with reported dust properties

Direct evidence for dust formed in SN ejecta and remnants has been reported for only a few cases so far.

– In the peculiar Type II supernova SN 1987A at most a few times 10^{-4}–10^{-3} M$_\odot$ of dust at epochs between 615–6067 days past explosion was found (Dwek et al, 1992;

Wooden et al, 1993; Bouchet et al, 2004; Ercolano et al, 2007). FIR and sub-millimeter observations with the *Herschel Space Observatory* 8476 and 8564 days after its explosion reveal about 0.4–0.7 $M_\odot$ of cold (17–23K) dust formed in the SN outflow (Matsuura et al, 2011; Lakicevic et al, 2011).

– At epochs between 214–1393 days past explosion, dust masses of at most a few times 10^{-4} $M_\odot$ at temperatures of a few hundred K was inferred for the Type II-P supernovae SN 1999em, SN 2003gd, SN 2004dj, SN 2004et, SN 2005af, SN 2007it and SN 2007od (e.g., Elmhamdi et al, 2003; Sugerman et al, 2006; Meikle et al, 2007; Kotak, 2008; Kotak et al, 2009; Andrews et al, 2010, 2011b; Meikle et al, 2011; Szalai et al, 2011).

– For SN 2003gd, Sugerman et al (2006) derived a maximum dust mass on day 499 of 1.7 $\times 10^{-3}$ $M_\odot$ and 2.0×10^{-2} $M_\odot$ on day 678 with a clumpy model. In contrast, Meikle et al (2007) inferred only 4×10^{-5} $M_\odot$ of hot dust and concluded that the mid-IR emission from this SN cannot support a dust mass of 2.0×10^{-2} $M_\odot$. They also argue that the difference in the results may be due to the presence of a larger component of cold dust in the smooth model of Sugerman et al (2006).

– A quite peculiar case is SN 2006jc. Two years before explosion, a LBV-like outburst was detected and associated with the progenitor of SN 2006jc (Nakano et al, 2006; Pastorello et al, 2007), which has been suggested to be a very massive star (Foley et al, 2007; Pastorello et al, 2007). Evidence for ongoing dust formation in a CSD behind the forward shock already at 55 days after explosion was reported by e.g., Di Carlo et al (2008); Smith et al (2008b), but just a modest amount of 3×10^{-4} $M_\odot$ of dust was inferred (Mattila et al, 2008a). Interestingly, also larger dust masses of $\sim 8 \times 10^{-3}$ $M_\odot$ (Mattila et al, 2008a) or $\sim 3 \times 10^{-3}$ $M_\odot$ (Sakon et al, 2009) condensed in the mass-loss wind of the progenitor prior to explosion was observed.

In SNRs, at an age of a few 100–1000 yr, larger masses of rather cold dust seem to be present. For example, observations of the SNR Cas A result in a few times 10^{-5} $M_\odot$ of hot dust (>170 K) and a few times 10^{-2} $M_\odot$ of warm and cold dust (< 150 K) for the entire SNR (e.g., Arendt et al, 1999; Douvion et al, 2001b; Hines et al, 2004; Krause et al, 2004; Rho et al, 2008). An amount of $\sim 1M_\odot$ of dust at a temperature of ~ 20 K was recently suggested by Dunne et al (2009). Observations with the *Herschel Space Observatory* result in a resolved cool dust component (~ 35 K) in the unshocked interior of Cas A with an estimated mass of 7.5×10^{-2} $M_\odot$ of dust (Barlow et al, 2010). For the SNR 1E0102.2−7219 observations by Sandstrom et al (2008) have shown that 3×10^{-3} $M_\odot$ at 70 K are present as newly formed dust in the ejecta, which has already encountered the reverse shock. From observations in SNRs arising from Type II-P SNe such as B0540, SN 1987A or the Crab nebula (Williams et al, 2008; Bouchet et al, 2004; Green et al, 2004; Temim et al, 2006) an average of a few times 10^{-3}–10^{-2} $M_\odot$ of dust has been inferred.

5.3.2 Type IIn supernovae and LBVs

There is growing evidence for dust from IIn SNe and LBVs. SNe of Type IIn arise from stars at the lower mass end of CCSNe (8–10 $M_\odot$) or from stars with higher masses in connection with LBVs (> 20 $M_\odot$). In either case they have undergone strong mass-loss and are surrounded by a dense and hydrogen-rich circumstellar disc.

In the case of ECSNe (see Sect. 2.4) appearing as Type IIn SNe, dust formation seems to be quite efficient. SN 2008S was embedded in a dust enshrouded circumstellar shell and the progenitor was likely a SAGB star. The dust enshrouded phase lasted for $\sim 10^4$ years prior

to explosion (Thompson et al, 2009) and could be associated with the super-wind phase of SAGB stars.

The Type IIn SN 2005ip is an example where dust was formed in the post-shocked shell (Fox et al, 2009; Smith et al, 2009). A pre-existing large dust shell containing ~ 1–5×10^{-2} $M_\odot$ of warm (~ 400 K) dust and a hot (~ 800 K) dust component of about 5×10^{-4} $M_\odot$ arising from newly formed dust in the ejecta has been found by Fox et al (2010). For the Type IIn SN 1998S, Pozzo et al (2004) inferred a dust mass of $> 2 \times 10^{-3}$ $M_\odot$.

SN 2006gy was classified as the most luminous IIn event known (Ofek et al, 2007; Smith et al, 2007; Kawabata et al, 2009), but the explosion mechanism remains uncertain (Ofek et al, 2007; Smith et al, 2007, 2008a, 2010a). NIR observations two years past explosion (Miller et al, 2010) showed a growing NIR excess which can be explained by a massive shell of around 10 $M_\odot$ containing around 0.1 $M_\odot$ of dust heated by the SN. The existence of a dusty shell has been proposed to be due to LBV eruptions lasting over ~1500 years prior to the SN explosion (Smith et al, 2008a). The large mass of the circumstellar medium (CSM) of ~10–20 $M_\odot$ and the likely SN ejecta mass of 10–20 $M_\odot$ require a progenitor mass of ~ 100 $M_\odot$ (Smith et al, 2010a).

An amount of about 0.03–0.35 $M_\odot$ of dust present in a circumstellar torus created by possible LBV-like mass-loss of mass 3–35 $M_\odot$ has been proposed to be the origin of a mid-IR excess toward SN 2010jl (Andrews et al, 2011a) at ~ 90 d. From spectropolarimetry obtained at an earlier epoch (14 d), the presence of a significant dust mass along the line of sight to the progenitor was ruled out (Patat et al, 2011), so the dust must lie in an inclined torus. A warm Spitzer/IRAC survey of 68 Type IIn SNe detected between 1999 and 2008 results in about 10 Type IIn SNe exhibiting late-time mid-IR emission caused by pre-existing dust heated through the interaction of the SN shock with the circumstellar medium (Fox et al, 2011). The progenitor mass-loss histories are consistent with those of LBVs.

Smith et al (2003) measured the mass of a 19th century eruption from the well-known LBV η Car to be about 12–20 $M_\odot$. A dust mass of 0.4 ± 0.1 $M_\odot$ surrounding η Car was estimated by Gomez et al (2010) who also estimated that > 40 $M_\odot$ of gas has been ejected so far. SN 1961V was tentatively classified as an η Car-like outburst with optically thick dust in a massive shell suggested to be present based on the fading of the light curve after around 4 years (Goodrich et al, 1989; Filippenko et al, 1995). However, the nature of SN 1961V is contentious (e.g., Stockdale et al, 2001; Van Dyk et al, 2002; Chu et al, 2004). Kochanek et al (2010) suggest it to be a peculiar, but real SN which has experienced enhanced mass-loss prior to explosion. Similar objects are SN 1954J (Smith et al, 2001; Van Dyk et al, 2005), SN 1997bs (Van Dyk et al, 2000), SN 2000ch (Wagner et al, 2004), SN 2002kg, and SN 2003gm (Weis and Bomans, 2005; Maund et al, 2006; Van Dyk et al, 2006).

The transients UGC 2773-OT and SN 2009ip (Smith et al, 2010b; Foley et al, 2010) were both LBV outbursts. The progenitor of SN 2009ip was serendipitously observed 10 yr prior to its outburst as an extremely luminous star and the mass was estimated to be about 50–80 $M_\odot$ (Smith et al, 2010b; Foley et al, 2010). UGC 2773-OT was less luminous with a mass of > 25 $M_\odot$, but found in a very dusty environment. Finally, a dusty nebula around the object HR Car (Umana et al, 2009) consisting of amorphous silicates indicates that dust has formed during the LBV outburst.

Smith and Owocki (2006) deduced masses for the observed nebulae of several LBVs and LBV candidates and concluded that an LBV giant eruption typically involves 10 $M_\odot$ of material. The expansion velocities of such outbursts can be as high as 750 km s^{-1} as measured for η Car (Davidson, 1971) and up to 2000–3000 km s^{-1} for SN 1961V (Goodrich et al,

**Table 3** Observed and derived properties of SNe

SN	SN Type	Progenitor	M_{P} [M$_\odot$][a]	t_{pe} [d][b]	M_d [M$_\odot$][c]	T_{d} [K][d]	Refs.
2007od	II-P	SAGB	~ 9.7–11	300	1.7×10^{-4}	580	1, 2
				455	1.9×10^{-4}	490	2
				667	1.8×10^{-4}	600	2
2007it	II-P	—	~ 16–27	351	1.6–7.3×10^{-4}	500	3
				561	7.0×10^{-5}	700	3
				718	8.0×10^{-5}	590	3
				944	4.6×10^{-5}	480	3
2006jc	pec. Ibn	LBV	~ 40	200	6.9×10^{-5}	800	4, 5
				230	3×10^{-4}	950	6
2005af	II-P	—	—	214	4×10^{-4}	—	4, 7
2004et	II-P	RSG	9	300	3.9×10^{-5}	900	4, 8, 9
				464	6.6×10^{-5}	650	8
				795	1.5×10^{-4}	450	8
2004dj	II-P	RSG	12–20	267–275	0.3–2.0×10^{-5}	710, 186	10–14
				500	2.2×10^{-5}	650	15
				652	3.2×10^{-5}	610	15
				859	3.3×10^{-5}	570	15
				849–883	0.1–3.2×10^{-4}	530, 120	10
				996	5.0×10^{-5}	520	15
				1006–1016	0.1–7.6×10^{-4}	462, 110	10
				1207	$> 1.0 \times 10^{-4}$	460	15
				1236–1246	0.1–4.2×10^{-4}	424, 103	10
				1393	$> 1.5 \times 10^{-4}$	430	15
2003gd	II-P	RSG	~ 8	499	2.0–17×10^{-4}	480	4, 16
				496	4×10^{-5}	525	17
				678	2.7–20×10^{-3}	—	16
1999em	II-P	RSG	15	510	$\sim 10^{-4}$	510	4, 18
1998S	IIn	—	—	360	$> 2 \times 10^{-3}$	1250	4, 19
1987A	II-pec	BSG	~ 20	615	3.7–31×10^{-5}	422	4, 20
				615	2–13×10^{-4}	—	21
				775	5.9–50×10^{-5}	307	20
				775	2–7.5×10^{-4}	—	21
				1144	5×10^{-4}	150	22
				6067	1–20×10^{-4}	90–100	23
				8467, 8564	4–7×10^{-1}	17–23	24

References. (1) Inserra et al (2011); (2) Andrews et al (2010); (3) Andrews et al (2011b); (4) Smartt et al (2009, and references therein); (5) Sakon et al (2009); (6) Mattila et al (2008a); (7) Kotak (2008); (8) Kotak et al (2009); (9) Maguire et al (2010); (10) Szalai et al (2011); (11) Maíz-Apellániz et al (2004); (12) Kotak et al (2005); (13) Wang et al (2005); (14) Vinkó et al (2009); (15) Meikle et al (2011); (16) Sugerman et al (2006); (17) Meikle et al (2007); (18) Elmhamdi et al (2003); (19) Pozzo et al (2004); (20) Wooden et al (1993); (21) Ercolano et al (2007); (22) Dwek et al (1992); (23) Bouchet et al (2004); (24) Matsuura et al (2011)

Notes. [a] M_{P} is the mass of the progenitor. [b] t_{pe} is the time past explosion. [c] M_d is the inferred dust mass. [d] T_{d} is the inferred dust temperature.

1989). Dust formed in such LBV outbursts is likely to escape before the shock from the final SN explosion catches up with the dusty shell.
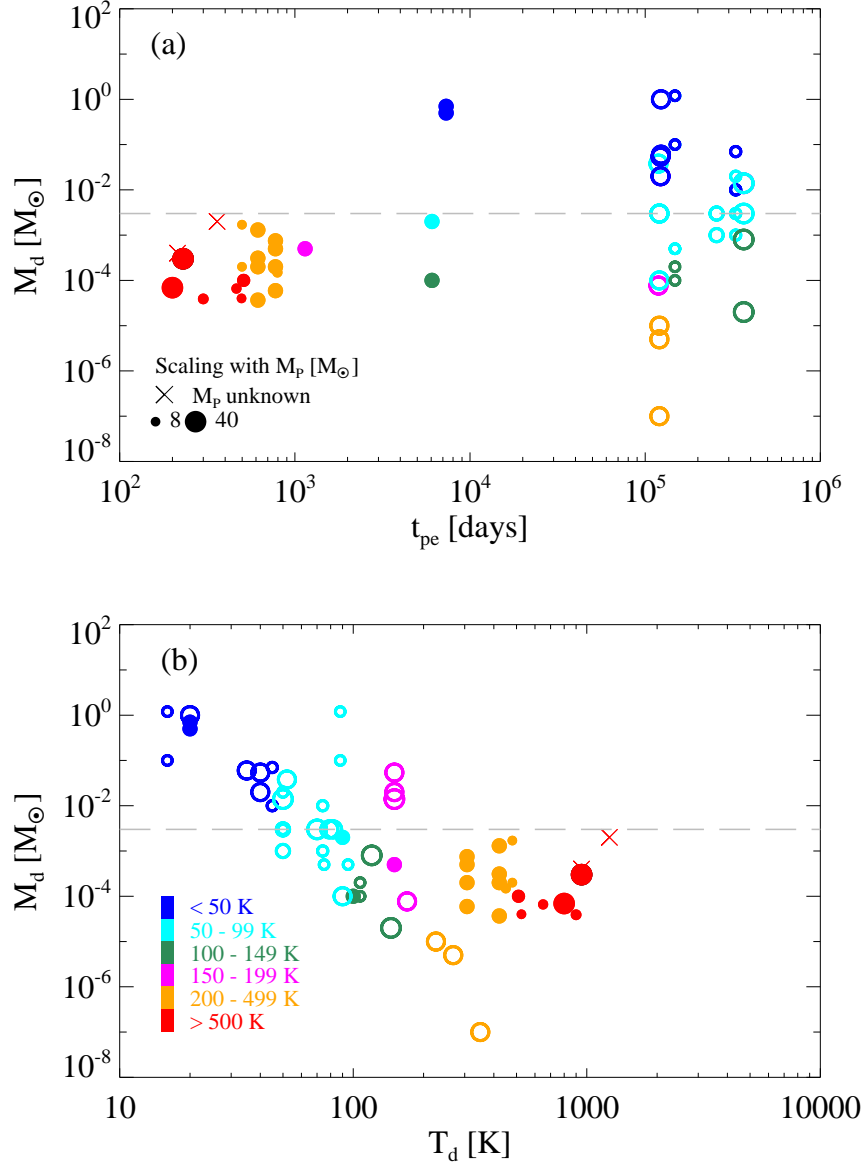
Fig. 2 Inferred amount of dust from SN and SNR observations at different (a) epochs and (b) temperatures (Tables 3 and 4). Filled circles represent observations of SNe at early and late epochs and open circles mark observations from SNRs with an age of several 100 yr. The colours denote the temperature (T_d) of the dust and t_{pe} is the time past explosion. The size of the symbols is scaled by the mass of the SN progenitor. The horizontal dashed line represents an upper limit to the dust mass of 3×10^{-3} M$_\odot$ at early epochs and is also consistent with the logarithmic average of the inferred dust masses in SNRs.

Table 4 Observed and derived properties of SNRs

SNR	SN Type	Progenitor	M_P [$M_\odot$][a]	t_{pe}[yr][b]	M_d [$M_\odot$][c]	T_d [K][d]	Refs.
Cas A	IIb	WR	15–30	326	7.7×10^{-5}	170	1,2
				326	3.8×10^{-2}	52	2
				330	$\sim 10^{-7}, \sim 10^{-4}$	350, 90	3
				330	$5 \times 10^{-6}, 1 \times 10^{-5}$	268, 226	4
				330	3×10^{-3}	79, 82	4
				330	< 1.5	—	5
				335	$2–5.4 \times 10^{-2}$	40–150	6
				337	~ 1	~ 20	7
				337	6×10^{-2}	~ 35	8
				337	7.5×10^{-2}	~ 35	9
Kepler	Ia / Ib	—	~ 8	405	$1–2 \times 10^{-4}$	107	10, 11, 12[e]
				405	5×10^{-4}	75–95	10[e]
				405	$0.1–1.2$	16, 88	13
B0540	II-P	—	15–25	700–1100	$1–3 \times 10^{-3}$	50–65	14–16
Crab	II-P or	—	8–10	950	$1–7 \times 10^{-2}$	45	16–19
	ECSN	—		950	$3–20 \times 10^{-3}$	50	19
				952	$1–10 \times 10^{-3}$	74	20
1E0102	Ib/Ic or	—	~ 30	~ 1000	1.4×10^{-2}	50–150	21–23
	II-L/b	—		~ 1000	3×10^{-3}	70	24
				~ 1000	2×10^{-5}	145	24
				~ 1000	8×10^{-4}	120	25

References. (1) Krause et al (2008); (2) Arendt et al (1999); (3) Douvion et al (2001b); (4) Hines et al (2004); (5) Wilson and Batrla (2005); (6) Rho et al (2008); (7) Dunne et al (2009); (8) Sibthorpe et al (2009); (9) Barlow et al (2010); (10) Blair et al (2007); (11) Reynolds et al (2007); (12) Douvion et al (2001a); (13) Gomez et al (2009); (14) Reynolds (1985); (15) Williams et al (2008); (16) Chevalier (2006); (17) Nomoto et al (1982); (18) Kitaura et al (2006); (19) Green et al (2004); (20) Temim et al (2006); (21) Blair et al (2000); (22) Chevalier (2005); (23) Rho et al (2009); (24) Sandstrom et al (2008); (25) Stanimirović et al (2005)

Notes. [a]M_P is the mass of the progenitor. [b]t_{pe} is the time past explosion. [c]M_d is the inferred dust mass. [d]T_d is the inferred dust temperature. [e]The derived dust masses are attributed to circumstellar dust heated by the SN blast wave.

5.3.3 Type Ia, Ib, Ic and IIb supernovae

Significant amounts of dust from Ic or Ib SNe has not been reported, and they are not currently considered to be important sources of dust.

A very clear non-detection of dust for a Ic SN was obtained by Hunter et al (2009) for SN 2007gr. Besides the peculiar Ibn SN 2006jc, the only proposed occurrence of dust formation for a Ib SN is for SN 1990I at day ~ 250 (Elmhamdi et al, 2004). The same seems to be the case for Type IIb SNe. However, Krause et al (2008) has identified the SN causing the SNR Cas A as a Type IIb. Cas A is well studied in terms of dust (see Sect. 5.3.1) and represents the only example so far of a SN of this Type where dust has been reported.

Clayton et al (1997) discuss the possibility of SiC grain formation and growth in Type Ia SNe, but the latest models (Nozawa et al, 2011) and observations (Borkowski et al, 2006) of Type Ia SNe indicate that only little or no dust forms in the ejecta. Ishihara et al (2010) attributed the thermal dust emission in parts of the Type Ia SNR Tycho SN 1572 to a possible SN shock interaction with ambient molecular clouds. On the contrary, Tian and Leahy (2011) conclude from radio and X-ray observations that the remnant is isolated. The SNR Kepler possibly constitutes an exceptional case, with inferred FIR dust masses up to $1–3$ $M_\odot$

(Morgan et al, 2003; Gomez et al, 2009). However, MIR observations rather indicate a dust mass of a few 10^{-4} $M_\odot$ of dust, suggested to arise from circumstellar dust heated by the SN blast wave (Douvion et al, 2001a; Blair et al, 2007). Moreover, the classification of the progenitor is debated. The first claim that Kepler has its origin in a SN Ia were made by Baade (1943) which was later also supported by Blair et al (2007). Bandiera (1987) suggested that the progenitor might have been a runaway star with strong winds. Further possibilities are discussed by Reynolds et al (2007), but a SN Ia event is favoured. Pertaining to the meagre evidence of dust from this Type of SN and its ambiguous nature and delay times, SNe Ia are likely not significant dust contributors in the early Universe.

5.3.4 Summary of observational status

The observational status of SNe and SNRs for which dust formation has been inferred is summarized in Tables 3 and 4. We have attempted to include all observed SNe and SNRs for which information about the derived dust mass is available. In addition, we present details about the Type of the observed SN, the nature and mass of the progenitor, the epoch of observation and the inferred dust temperature. Based on this we plot in Fig. 2 the observed dust yields from Tables 3 and 4 as a function of epoch (Fig. 2a) or temperature (Fig. 2b). From Fig. 2a it is evident that regardless of SN Type or progenitor mass, only hot dust at an amount below $\sim 3 \times 10^{-3}$ $M_\odot$ is present at early epochs, i.e., less than about 2×10^3 days past explosion At late epochs (later than $\sim 5 \times 10^3$ days past explosion) a large dispersion in the inferred dust masses is evident, spanning 7 orders of magnitude (from 10^{-7} $M_\odot$ to 1 $M_\odot$). One might speculate that the upper envelope indicates that, with aging of the SNe and SNRs, dust grains grow to larger sizes and the total amount of dust increases. However, the presence of only hot dust at early epochs might as well reflect an instrumental selection effect (see Sect. 5.2.1). At these epochs no observations at longer (FIR to (sub-)millimeter) wavelengths, sensitive to cold dust temperatures, have been accomplished so far. Thus, the presence of cold dust at early epochs cannot unambiguously be ruled out.

Higher inferred dust masses appear to be related to cold dust. This is clear from Fig. 2b which exhibits a conspicuous relation between the inferred dust mass and the temperature at which it is inferred. Independent of the epoch of observation or the progenitor mass, the amount of dust at lower temperatures is significantly larger than at warm to hot temperatures.

Finally we point out that the progenitors of the observed SNe and SNRs, which are in the mass range of 8–30 $M_\odot$, eject a total mass of heavy elements relevant for dust formation of about 0.3–2 $M_\odot$ in the SN explosion. Only stars more massive than ~ 15 $M_\odot$ eject an amount of heavy elements larger than 1 $M_\odot$ (e.g., Woosley and Weaver (1995, hereafter WW95), Nomoto et al (2006, herafter N06), Eldridge et al (2008, herafter ET08)). Thus, the observationally inferred high dust masses in e.g., SN 1987A (Table 3) or Cas A (Table 4) likely necessitate very high dust formation efficiencies if of SN origin. The possible dust formation efficiencies and their uncertainties are discussed in following section.

6 Dust production efficiency

Based on the dust yields obtained from observations and theory, summarized in previous sections, we next discuss the efficiencies of massive stellar sources in producing dust from their available metals.
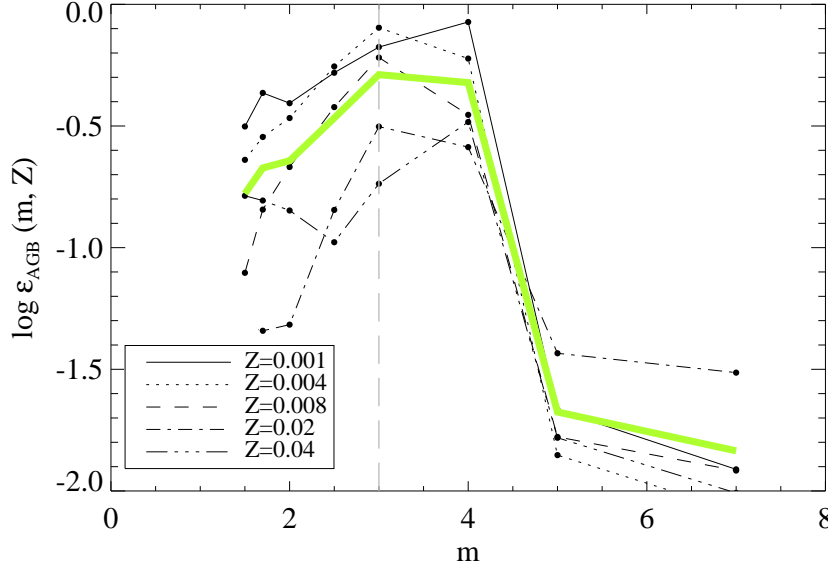
Fig. 3 Dust production efficiencies of AGB stars. The efficiencies are based on dust yields from Ferrarotti and Gail (2006) and yields of heavy elements from van den Hoek and Groenewegen (1997). The solid, dotted, dashed, dashed-dotted and dashed-dot-dotted curve are for metallicities of $Z = 0.001$, $Z = 0.004$, $Z = 0.008$, $Z = 0.02$, and $Z = 0.04$, respectively. The green line indicates the metallicity-averaged efficiency $\epsilon_{AGB}(m)$ obtained as a straight average of the five black curves. The vertical dashed line marks the boundary of 3 $M_\odot$, below which AGB stars are not considered as dust contributors at high redshift.

Following Gall et al (2011a), the dust production efficiency $\epsilon(m, z)$ per stellar mass and metallicity is defined as

$$\epsilon(m, Z) = \frac{M_d(m, Z)}{M_Z(m, Z)}, \tag{2}$$

where $M_d(m, Z)$ is the mass of dust produced and released into the ISM, $M_Z(m, Z)$ is the total ejected mass of heavy elements relevant for dust condensation per star and $m \equiv M_*/M_\odot$, where M_* is the zero age main sequence mass. It is assumed that the amount of dust is the final mass, which has formed and possibly been processed through shock interactions.

6.1 Efficiencies of AGB stars

The dust production efficiency, $\epsilon_{AGB}(m, Z)$, for AGB stars in the mass range 3–7 $M_\odot$ is calculated from theoretical values of $M_d(m, Z)$ and $M_Z(m, Z)$. The amount of dust $M_d(m, Z)$ is obtained from total dust yields of Ferrarotti and Gail (2006). Stellar yields for AGB stars have been calculated by e.g., Renzini and Voli (1981), Marigo (2001), Herwig (2004), Karakas and Lattanzio (2007) and recently by Karakas (2010). However most of the models do not provide yields covering the range of masses (3–8 $M_\odot$), elements or metallicities relevant for this investigation. For the sake of consistency, the amount of heavy elements, $M_Z(m, z)$, is obtained from the the yields of van den Hoek and Groenewegen (1997) cover-

ing a large grid of metallicities and stellar masses. The efficiency $\epsilon_{\mathrm{AGB}}(m, Z)$ is calculated for four different metallicities in accordance with calculations by Ferrarotti and Gail (2006).

The results are presented in Fig. 3. It is evident that $\epsilon_{\mathrm{AGB}}(m, Z)$ decreases quite rapidly between 4 and 5 $M_\odot$, independently of the metallicity. AGB stars in the mass range 3–4 $M_\odot$ (i.e., C-stars) apparently are the most efficient dust producers. It can also be seen that at lower metallicities ($Z \leq 0.008$) these AGB stars are more efficient in condensing their available heavy elements into dust than at higher metallicities. The green thick curve in Fig. 3 illustrates the metallicity-averaged efficiency, $\epsilon_{\mathrm{AGB}}(m)$, for AGB stars.

6.2 Efficiencies of CCSNe

As highlighted in Sect. 5 there is a discrepancy between the derived SN dust yields from observations (resulting in low amounts of dust) and theory (predicting large dust masses). It is therefore of interest to determine plausible limits for the dust production efficiency of SNe based on the dust yields obtained from either approach.

6.2.1 Maximum efficiency

An upper limit to the SN dust production efficiency can be ascertained using the mass and metallicity dependent dust yields from TF01 to determine the mass of dust $M_{\mathrm{d}}(m, Z)$. The yields for the heavy elements $M_{\mathrm{Z}}(m, Z)$ are taken from WW95, since these were also used by TF01. The efficiency for $Z = 0$ is derived from the dust yields of N03 and the total amount of metals of N06 – both yields are taken from unmixed grain models. The resulting efficiencies can be seen in Fig. 4, where we notice a clear decline of $\epsilon(m, Z)$ with increasing progenitor mass.

The efficiencies obtained by TF01 and N03 at $Z = 0$ differ significantly. For TF01, $\epsilon(m, Z)$ decreases quite drastically for stars between 20–25 $M_\odot$, whereas it remains more flat in the models of N03. The maximum SN efficiency limit can be obtained by averaging the efficiencies obtained for each Z from these models over metallicity (the average efficiency for all stellar masses is obtained via rational spline interpolation and extrapolation into the mass regime of 8–12 $M_\odot$ where no yields for heavy elements are available). This is sufficient to describe the observed tendencies and obtain an estimate of $\epsilon(m)$. We will refer to this as the 'maximum' SN dust production efficiency $\epsilon_{\mathrm{max}}(m)$, drawn as the dark blue curve with red crosses representing the averaged values in Fig. 4.

6.2.2 High efficiency

According to the predictions of Bianchi and Schneider (2007) and Nozawa et al (2007, 2010), dust grain destruction takes place when a reverse shock penetrates the dust layer at timescales up to $\sim 10^4$ years past explosion. This leads to a significant (up to 100%) reduction of the dust formed, depending on the ISM density and grain size. For example, Nozawa et al (2007) have shown that large grains in contrast to small grains remain relatively unaffected by the reverse shock. Following Bianchi and Schneider (2007), the possibility of grain destruction can be accounted for by applying a reduction of 93% to $\epsilon_{\mathrm{max}}(m)$. The resulting reduced efficiency still represents a rather high dust production efficiency in comparison to what is derived from SN observations. Hence, this will be referred to as the 'high' SN dust efficiency $\epsilon_{\mathrm{high}}(m) \equiv 0.07\epsilon_{\mathrm{max}}(m)$.
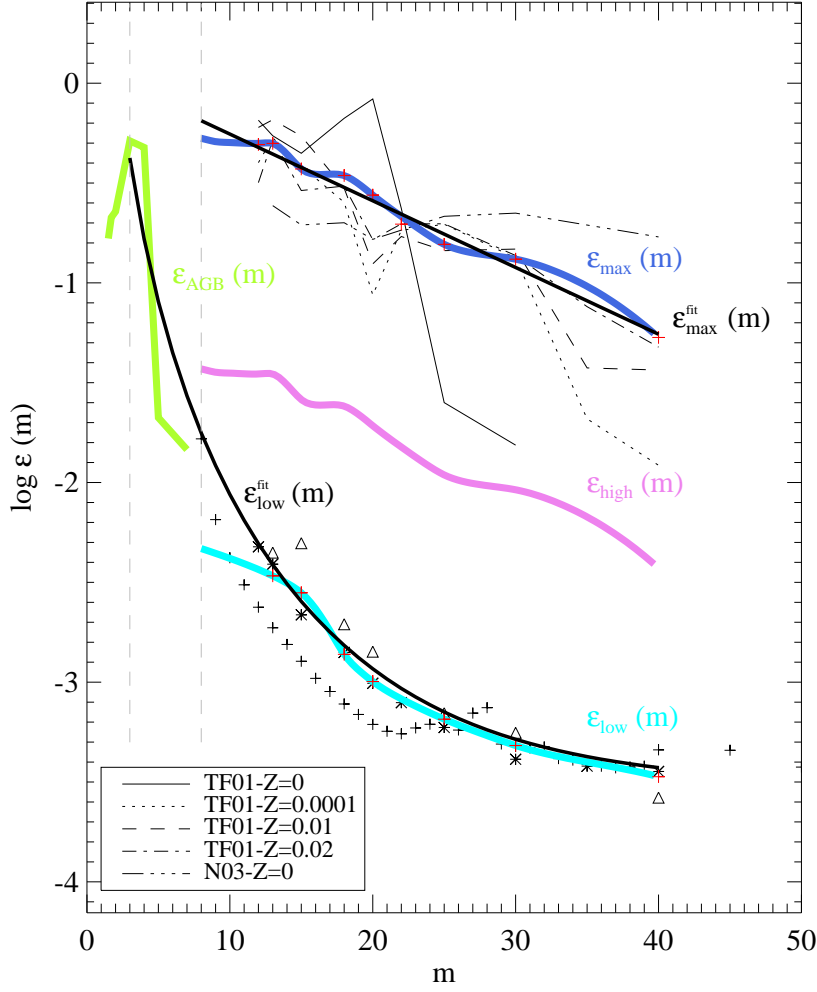
Fig. 4 Dust production efficiencies of massive stars. Upper curves: Efficiencies calculated from SN dust yields of TF01 and metal yields of WW95. The solid (thin), dotted, dashed and dashed-dotted curve are for metallicities of $Z = 0$, $Z = 0.0001$, $Z = 0.01$ and $Z = 0.02$, respectively. The dashed-dot-dotted curve represents the efficiency at $Z = 0$ derived from dust yields of N03 and metal yields from N06. The blue thick curve represents the averaged 'maximum' SN efficiency $\epsilon_{max}(m)$ and the black thick solid curve represents the fitted efficiency $\epsilon_{max}^{fit}(m)$. The thick violet curve represents the 'high' SN efficiency $\epsilon_{high}(m)$. Lower symbols: Efficiencies derived from the averaged observed dust amount of 3×10^{-3} $M_\odot$ of SNRs and the SN metal yields of WW95 (stars), N06 (crosses) and ET08 (triangles) for solar metallicity. The thick cyan curve is the averaged 'low' SN efficiency $\epsilon_{low}(m)$ and the black thick solid curve the fitted efficiency $\epsilon_{low}^{fit}(m)$. The left green curve represents the averaged AGB efficiency $\epsilon_{AGB}(m)$ (see also Fig. 3). The vertical lines mark the range of AGB stars between 3–8 $M_\odot$ and SNe more massive than 8 $M_\odot$.

We note that either $\epsilon_{\mathrm{max}}(m)$ or $\epsilon_{\mathrm{high}}(m)$ might also be interpreted as the result of longer timescale dust grain growth (see Fig. 2) in the SNR itself. The 'maximum' $\epsilon_{\mathrm{max}}(m)$ presupposes that dust destruction through shock interactions is inefficient. The 'high' SN efficiency, $\epsilon_{\mathrm{high}}(m)$, could also be the result of smaller or no destruction, depending on how much dust would initially have formed before a possible shock interaction.

6.2.3 Low efficiency

The lowest feasible limit for the efficiency of SNe dust production is generated based on observed dust yields from the SNRs Cas A, B0540−69.3, Crab nebula, and 1E0102.2−7219 at temperatures between 50–100 K (see Table 4). The inferred amount of dust $M_{\mathrm{d}}(m, Z)$ is taken to be 3×10^{-3} M$_{\odot}$ and is applied to SNe in the mass interval 8–40 M$_{\odot}$.

For the mass of heavy elements $M_{\mathrm{Z}}(m, Z)$ the yields of WW95, N06 and ET08 are used. The metallicity of most SN progenitors given in Tables 3 and 4 is estimated to be between around solar ($Z = 0.02$) or LMC-like ($Z = 0.008$) (Smartt et al, 2009). Solar metallicity for all SNe in the mass range of 8–40 M$_{\odot}$ can therefore be assumed. The metal yields $M_{\mathrm{Z}}(m, Z)$ are also evaluated for $Z = Z_{\odot}$. To obtain the low SN efficiency limit we average the efficiencies obtained using the yields of WW95, N06 and ET08. The same interpolation and extrapolation scheme as for $\epsilon_{\mathrm{max}}(m)$ is applied and the resulting average efficiency appears as the cyan curve with average values indicated as red crosses in Fig. 4.

The resulting averaged dust production efficiency only depends on the stellar mass. We will refer to this as the 'low' SN efficiency $\epsilon_{\mathrm{low}}(m)$. Interestingly, also $\epsilon_{\mathrm{low}}(m)$ features a declining tendency with increasing stellar mass, similar to $\epsilon_{\mathrm{max}}(m)$.

There are two possible interpretations of this limit. The amount of dust produced by SNe could be similar to the low observed amount of dust at early epochs and this rather low amount of dust does not significantly grow on longer timescales. This might be the case for the SNR B0540−69.3 (Williams et al, 2008). Alternatively, $\epsilon_{\mathrm{low}}(m)$ may be the result of potential dust destruction of larger amounts of dust from shock interactions.

6.3 Analytical approximations

To illustrate the general trends of different $\epsilon(m)$ we provide simple analytical fits to the derived averaged efficiencies of AGB stars and SNe.

One notices from Fig. 4 that there might be a smooth connection of the efficiencies, $\epsilon_{\mathrm{low}}(m)$, between high-mass AGB stars and low-mass SNe. An adequate approximation covering all stars between 3–40 M$_{\odot}$ is a power law for $\epsilon(m)$,

$$\epsilon_{\mathrm{low}}^{\mathrm{fit}}(m) = a\, m^{-\beta} + c, \qquad 3 \le m \le 40, \qquad (3)$$

with $a = 15$, $\beta = 3.25$, and $c = 2.8 \times 10^{-4}$. The negative slope reflects the decreasing efficiency of stars with increasing mass to release the produced dust grains into the ISM. It also illustrates that AGB stars in this case are more efficient, closely followed by the low-mass SNe. While $\epsilon_{\mathrm{low}}^{\mathrm{fit}}(m)$ drops by roughly three orders of magnitude in the 3–40 M$_{\odot}$ mass range, the rather steep decline for stars between $\sim$ 3–12 M$_{\odot}$ over approximately two orders of magnitude is noteworthy. We also note that although $\epsilon_{\mathrm{low}}^{\mathrm{fit}}(m)$ provides a fairly good approximation to $\epsilon_{\mathrm{low}}(m)$, it does not capture the strong preference for 3–4 M$_{\odot}$ stars over 5–7 M$_{\odot}$ stars (see Fig. 3).
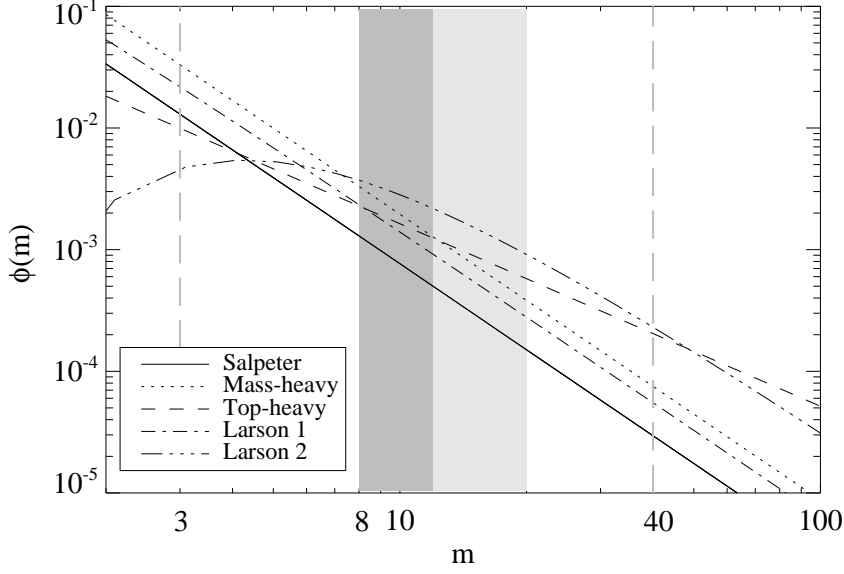
Fig. 5 The five IMFs considered. The solid, dotted, dashed, dashed-dotted, and dashed-dot-dotted curves represent the Salpeter, mass-heavy, top-heavy, Larson 1 and Larson 2 IMF, respectively. The dark grey area signifies the critical mass range of 8–12 $M_\odot$ and the light grey area signifies SNe between 12–20 $M_\odot$. The vertical dashed lines mark the limits of the range in stellar mass considered (between 3 $M_\odot$ and 40 $M_\odot$).

The 'maximum' SN dust formation efficiencies are better approximated by an exponential function,

$$\epsilon_{\max}^{\text{fit}}(m) = a\,e^{-(m/m_0)}, \qquad 8 \leq m \leq 40, \tag{4}$$

with $a = 1.2$ and $m_0 = 13$. Comparing the efficiency $\epsilon_{\text{AGB}}(m)$ of AGB stars to $\epsilon_{\max}(m)$, we find no possibility for a smooth connection. In this case, stars between 8–12 $M_\odot$ are the most efficient dust producers. The general decline of $\epsilon_{\max}^{\text{fit}}(m)$ for stars between 8–40 $M_\odot$ is about an order of magnitude, comparable to the drop of $\epsilon_{\text{AGB}}(m)$ from a 4 $M_\odot$ to a 6 $M_\odot$ AGB star. The resulting fits are shown in Fig. 4 as black solid curves.

7 Stellar dust productivity

Having reviewed the dust production efficiency of single massive stars, we next discuss the dust productivity of these massive stars in a galaxy. Besides the dust production efficiency, the total amount of dust produced in a galaxy depends on the star-formation rate (SFR), $\psi(t)$ and the IMF, $\phi(m)$.

7.1 The initial mass function

The IMF is an important parameter influencing the evolution of dust, gas and metals in a galaxy. It determines the mass distribution of a population of stars with a certain ZAMS

mass. The IMF was first proposed by Salpeter (1955), derived for Galactic field stars. Originally, the IMF was not a power law but composed of a logarithmic slope of about -1.7 for stars below 1 $M_\odot$ and -1.2 for stars between 1–10 $M_\odot$. It was suggested that a power law with slope -1.35 applied to the entire mass range is appropriate, but strictly speaking it is only valid for stars between 0.4–10 $M_\odot$. Nevertheless, the Salpeter IMF is still often applied to more extended mass ranges (e.g., 0.1–100 $M_\odot$) (for detailed reviews, see, e.g., Scalo, 2005; Chabrier, 2005). Later studies have shown that the IMF flattens for stars below 0.5 $M_\odot$ and significantly declines in the mass regime < 0.1 $M_\odot$ (e.g., Kroupa, 2002; Chabrier, 2003a,b). A steeper decline for intermediate mass stars has also been suggested (Scalo, 1986, 1998). A characteristic mass has been defined such that half the initial mass goes into stars with masses lower than the characteristic mass and half into stars more massive. The characteristic mass describes the mass at which stars are preferentially formed. For the field star IMFs described above the characteristic mass is about 1 $M_\odot$ (e.g., Larson, 2006).

A fundamental debate regarding the IMF is whether there is a systematic variation of the IMF with some physical conditions of star formation or whether it is universal (see Bastian et al, 2010, for a review). Several theoretical approaches suggest non-universality. Systematic changes of the IMF leading to a shift of the characteristic mass towards higher stellar masses are found in star-forming environments with increased ambient temperatures (e.g., Larson, 1998) or high-densities (Murray and Lin, 1996; Krumholz et al, 2010). The absence of a variation of the characteristic mass due to a change of the equation of state as a result of dust processes is suggested by Bonnell et al (2007).

Usually any IMF with a characteristic mass shifted towards high stellar masses resulting in an overabundance of high-mass stars is referred to as 'top-heavy' IMF. The possibility of a top-heavy IMF in low-metallicity environments and in particular in the early Universe was suggested already by Schwarzschild and Spitzer (1953) and plausible evidence is extensively discussed in, e.g., Larson (1998) and Tumlinson (2006). Furthermore, indirect and direct evidence for a top-heavy IMF has been found in various systems such as e.g., starburst galaxies (ee.g., Rieke et al, 1993; Doane and Mathews, 1993; Dabringhausen et al, 2009), disturbed galaxies (Habergham et al, 2010), and sub-millimeter galaxies (e.g., Baugh et al, 2005; Nagashima et al, 2005; Michałowski et al, 2010b). Evidence for IMF variations towards higher stellar masses also comes from observations of the Galactic Center region and Galactic globular clusters (e.g., D'Antona and Caloi, 2004; Ballero et al, 2007; Maness et al, 2007; Bartko et al, 2010) and star clusters (e.g., Smith and Gallagher, 2001).

However, any reference to a top-heavy IMF must be assessed critically. Usually the degree to which the IMF is 'top-heavy' varies significantly among different studies. Differences can be due to extreme assumptions of the exponent for the power law IMFs (i.e., $\alpha = 0$) or due to different characteristic masses in log-normal IMFs, but may also be due to the assumed mass interval of the IMF.

In models of dust evolution in galaxies and high-z QSOs (e.g., Morgan and Edmunds, 2003; Dwek et al, 2007) a Salpeter IMF is often used. Considering the evidence for an IMF different from the commonly adopted Salpeter IMF, it is of interest to investigate the implication on the dust productivity of five different IMFs (Table 5).

The IMF is normalized in the mass interval $[m_1, m_2]$ such that

$$\int_{m_1}^{m_2} m\,\phi(m)\,\mathrm{d}m = 1, \tag{5}$$

where m_1 and m_2 are the lower and upper limits of the IMF given in Table 5.

Table 5 IMF parameters

IMF	α	m_1	m_2	m_{ch}
Salpeter	1.35	0.1	100	—
Mass-heavy	1.35	1.0	100	—
Top-heavy	0.5	0.1	100	—
Larson 1	1.35	0.1	100	0.35
Larson 2	1.35	0.1	100	10.0

The power law IMFs (Salpeter, mass heavy and top heavy) have the form $\phi(m) \propto m^{-(\alpha+1)}$ while the log-normal Larson IMFs (Larson, 1998) are given as $\phi(m) \propto m^{-(\alpha+1)} \exp(-m_{ch}/m)$, where m_{ch} is the characteristic mass. The 'top-heavy' IMF is characterized by a flatter slope than the Salpeter IMF. The 'mass-heavy' IMF has a similar slope as the Salpeter IMF but the formation of stars with stellar masses below 1 $M_\odot$ is suppressed leading to the formation of more stars in the mass interval $[m_1, m_2]$ compared to the Salpeter IMF. The log-normal IMFs have the same slope as the Salpeter IMF in the high mass tail of the IMF, but flatten or decline for masses below the characteristic mass. The 'Larson 1' is closest to a Salpeter IMF while the 'Larson 2' IMF is biased towards higher stellar masses and can be referred to as a 'top-heavy' IMF.

In Fig. 5 we plot the IMFs considered. From the shape of the curves for $\phi(m)$ it is evident that the majority of the stars relevant for dust formation are formed in the mass range of 3–8 $M_\odot$ for all IMFs, followed by stars between 8–12 $M_\odot$. Note that this includes the critical mass range of 8–10 $M_\odot$ (see Sect. 2.4). For SNe between 10–12 $M_\odot$ dust yields or metal yields are uncertain or unavailable, leading to uncertainties in the dust production efficiency. For the purposes of the following discussion, we therefore extend the previously defined critical mass range up to 12 $M_\odot$.

7.2 Dust productivity

The amount of dust produced per star, $M_d(m)$, is calculated from the dust formation efficiencies as $M_d(m) = M_Z(m)\,\epsilon(m)$. The yields of heavy elements $M_Z(m)$ are taken from WW95 (for SNe) and van den Hoek and Groenewegen (1997) (for AGBs). We study two cases, $Z = Z_\odot$ and $Z = 0.01Z_\odot$.

To quantify the effect of the various IMFs and the dust production efficiencies on the total dust contribution from AGBs and SNe we define the total dust productivity of all stars in the mass interval $[m_L, m_U]$ as

$$\mu_D = \int_{m_L}^{m_U} \phi(m)\, \frac{M_Z(m)}{M_\odot}\, \epsilon(m)\, dm. \tag{6}$$

The lower and upper mass limits, m_L and m_U, deliniate the interval 3–40 $M_\odot$, which will be further divided into the AGB star range 3–8 $M_\odot$, and the SN ranges 8–12 $M_\odot$, 12–20 $M_\odot$ and 20–40 $M_\odot$. The total dust productivity, μ_D, depends on the IMF, the efficiency and the metal yields through the integrand $\xi_d(m) = \phi(m)\,(M_Z(m)/M_\odot)\,\epsilon(m)$, which is the specific dust productivity.

The calculated amount of dust $M_d(m)$ for each efficiency case (see Sect. 6.2) is presented in Fig. 6. We note that the amount of dust produced per AGB star is between the values of $M_d(m)$ for SNe with $\epsilon_{low}(m)$ and $\epsilon_{high}(m)$. Regarding the quality of the fitting functions
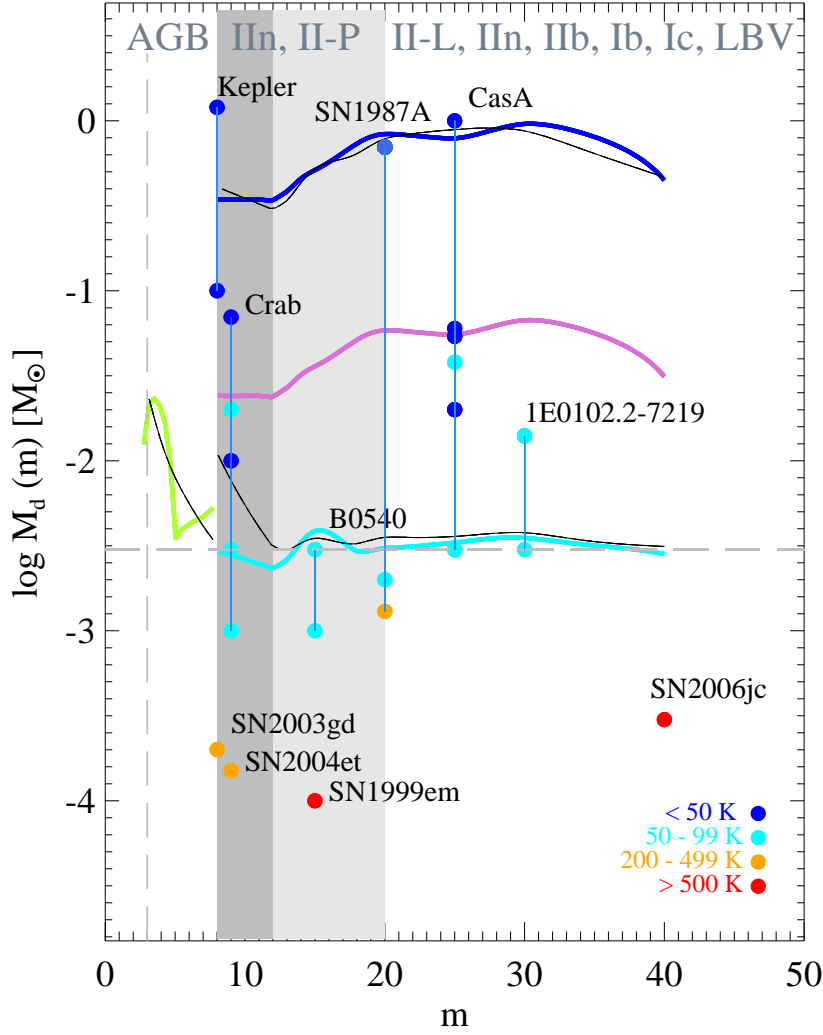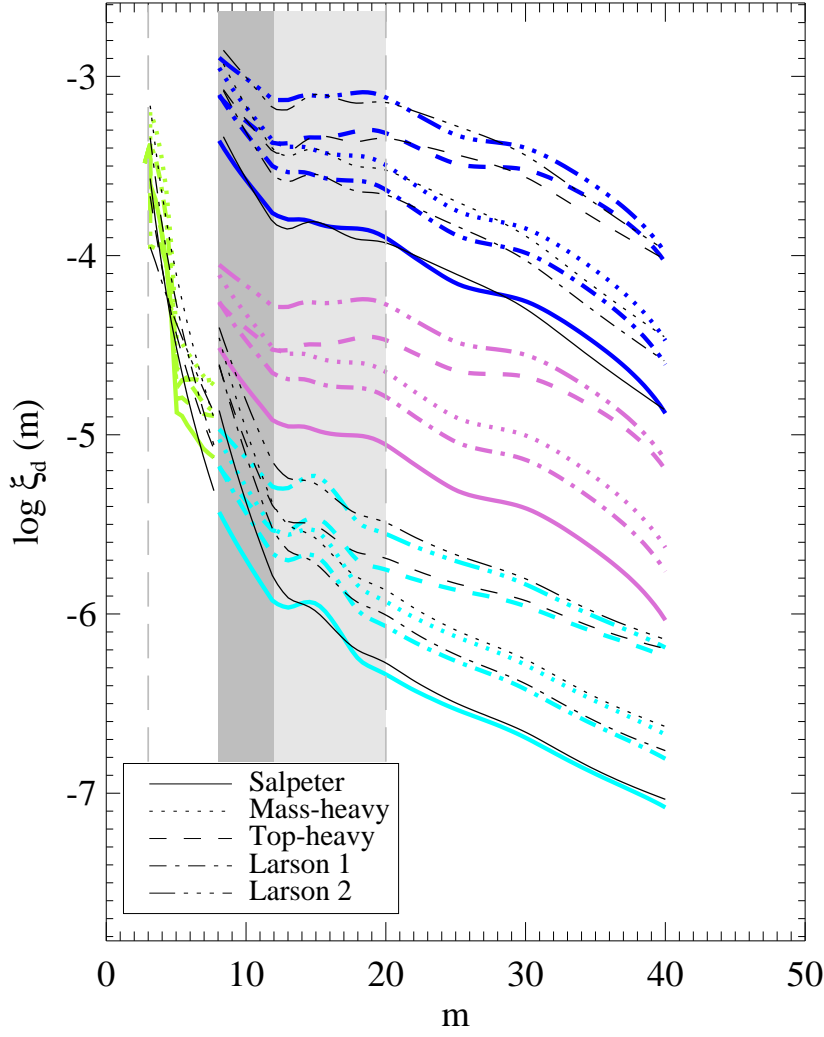
Fig. 6 Dust yields for AGB stars and SNe calculated for $\epsilon_{max}(m)$ (dark blue curve), $\epsilon_{high}(m)$ (violet curve), $\epsilon_{low}(m)$ (cyan curve), $\epsilon_{max}^{fit}(m)$ and $\epsilon_{low}^{fit}(m)$ (black curves) as well as for AGB stars (green curve). Filled circles represent observed dust yields for different SNe at different temperatures. The dark grey zone corresponds to the critical mass range (8–12 $M_\odot$) and the light grey region corresponds to the approximate mass range for Type II-P SNe.

(Eq. 4), using $\epsilon_{low}^{fit}(m)$ for all stars in the range 3–40 $M_\odot$ results in lower dust yields for stars between 6–7 $M_\odot$ and a significant overestimate of $M_d(m)$ for stars in the critical mass range 8–10 $M_\odot$, relative to using $\epsilon_{low}(m)$. Using $\epsilon_{max}^{fit}(m)$ for the 'maximum' SN efficiency is consistent with using $\epsilon_{max}(m)$

For comparison we plot the highest inferred dust yields from the observed SNe listed in Tables 3 and 4. The two upper values for Cas A (Rho et al, 2008; Dunne et al, 2009) and the

Fig. 7 Specific dust productivity. (a) Specific dust productivity $\xi_d(m)$ of stellar masses calculated for $\epsilon_{max}(m)$ (dark blue curve), $\epsilon_{high}(m)$ (violet curve), $\epsilon_{low}(m)$ (cyan curve), $\epsilon_{max}^{fit}(m)$ and $\epsilon_{low}^{fit}(m)$ (black curves) as well as for AGB stars (green curve). The dark grey zone corresponds to the critical mass range (8–12 $M_\odot$) and the light grey region corresponds to the approximate mass range for Type II-P SNe. The solid, dotted, dashed, dashed-dotted, and dashed-dot-dotted curves represent the Salpeter, mass-heavy, top-heavy, Larson 1 and Larson 2 IMFs, respectively.

upper value of SN 1987A (Matsuura et al, 2011) at low temperature match the dust yields calculated using $\epsilon_{max}(m)$ or $\epsilon_{high}(m)$. Dust masses for SNe calculated using $\epsilon_{low}(m)$ are also in good agreement with the observed dust yields from several SNRs. We also plot the highest observationally derived dust yield for the Kepler remnant (see Table 4 and discussion in Sect. 5.3.3). The inferred dust yields from the Kepler remnant may not be representative of dust from CCSNe (the SN has been suggested to be a Type Ia). However, in view of the general uncertainty about dust from stars with such a progenitor mass, this SNR provides an interesting benchmark.

Fig. 7 shows the specific dust productivity $\xi_d(m)$ for all $\epsilon(m)$ and the various considered IMFs. The slopes of $\xi_d(m)$ exhibit a declining trend with increasing stellar mass regardless of the choice of $\epsilon(m)$. SNe with masses between 30–40 $M_\odot$ are ~ 10 times less productive than SNe with masses between 8–12 $M_\odot$. For AGB stars $\xi_d(m)$ decreases steeply between 3–7 $M_\odot$, resulting in about an order of magnitude lower value for the higher mass AGB stars. The most productive AGB stars therefore are 3–4 $M_\odot$ stars, partly reflecting their higher dust production efficiencies $\epsilon_{AGB}(m)$ (see Figs. 4 and 6).

A Larson 2 IMF exhibits the highest dust productivity for SNe between 8–40 $M_\odot$, independently of the dust production efficiency, while the lowest specific productivity is obtained for a Salpeter IMF. The difference in $\xi_d(m)$ between either a Larson 2 or a top-heavy IMF and the Salpeter IMF is larger for the more massive stars (~ 30–40 $M_\odot$). For AGB stars, the largest sensitivity to the IMF occurs for 3–4 $M_\odot$ stars which exhibits the largest difference in $\xi_d(m)$ for a mass-heavy IMF (highest value) vs. a Larson 2 IMF (lowest value).

The total dust productivity μ_D of AGB stars and SNe, subdivided into 3 mass ranges, is presented in Fig. 8. For a 'low' SN efficiency, $\epsilon_{low}(m)$, the total amount of dust produced is almost exclusively manufactured by AGB stars. Dust production by SNe in this case is negligible for all considered IMFs.

The total dust productivity is increased as soon as SNe are assumed to produce dust with the 'high' SN efficiency $\epsilon_{high}(m)$. For a Salpeter, Larson 1 and mass-heavy IMF, AGB stars still dominate the dust production whereas for a top-heavy or Larson 2 IMF, SNe are the prime dust producers.

In case of the 'maximum' SN efficiency, $\epsilon_{max}(m)$, dust is primarily manufactured by SNe and the dust supply from AGB stars is negligible. For this efficiency the amount of dust produced by SNe is roughly 5–10 times higher than for $\epsilon_{low}(m)$ and $\epsilon_{high}(m)$, depending on the IMF. We find that for the IMFs favouring lower mass stars, the three SN mass ranges (8–12 $M_\odot$, 12–20 $M_\odot$, 20–40 $M_\odot$) are nearly equally important. While there is considerable uncertainty about dust production channels from stars between 30–40 $M_\odot$, the analysis indicates that this mass range is the least significant range. Hence, SN dust production is in general dominated by stars in the mass range 8–20 $M_\odot$ with an almost equal contribution from stars between 8–12 $M_\odot$ and 12–20 $M_\odot$.

For the calculations with yields for heavy elements at a metallicity of $Z = 0.01\, Z_\odot$ we find the same tendencies. This indicates that these relations most likely also apply to high-z galaxies.

7.3 An example

This simple formalism allows us to address the origin of large dust masses in QSOs at high redshift, as discussed in more detail in Sect. 8.1. In the following we estimate whether the derived dust productivities may be sufficient to account for the 2–$7 \times 10^8\, M_\odot$ of dust inferred in QSOs at $z \geq 6$ (e.g. Bertoldi et al, 2003; Robson et al, 2004; Beelen et al, 2006).
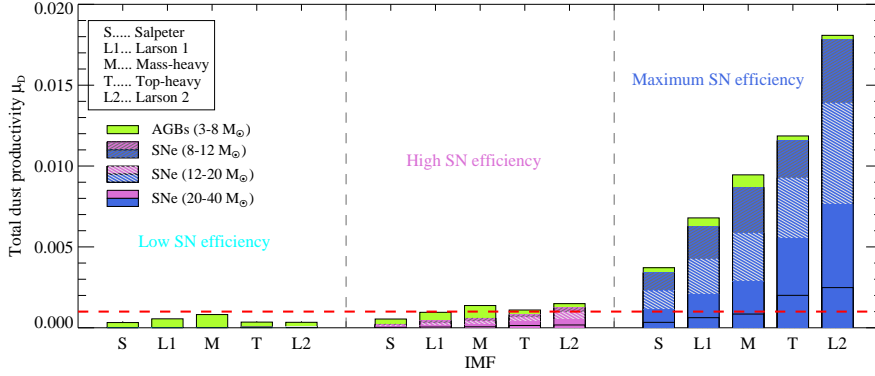
Fig. 8 Total dust productivity of AGB stars and SNe for different IMFs and SN dust production efficiencies. The height of the bars represents the total dust productivity of stars in the mass range 3–40 $M_\odot$. The contribution from AGB stars is marked in green, the SN mass ranges of 8–12 $M_\odot$, 12–20 $M_\odot$ and 20–40 $M_\odot$ are the dark grey shaded, light grey shaded and solid blue areas. The contribution from stars in the mass range of 30–40 $M_\odot$ is the area from the bottom to the black solid line in the bar. The letters S, L1, M, T, L2 stand for the Salpeter, Larson 1, mass-heavy, top-heavy and Larson 2 IMFs, respectively. The red dashed line marks the minimum estimated dust productivity of $\mu_D = 10^{-3}$ required to account for high dust masses in QSOs at $z \geq 6$.

We assume a minimum required dust mass of $M_D = 2 \times 10^8 \, M_\odot$ and a maximum available time span of $\Delta t = 400$ Myr for building up this amount of dust. The minimum required average amount of dust produced per unit time is expressed as the dust production rate in this period, $R_D = M_D/\Delta t = 0.5 \, M_\odot \, \text{yr}^{-1} = \mu_D \, \psi(t)$. We assume a high constant average SFR $\psi(t) = 500 \, M_\odot \, \text{yr}^{-1}$, based on derived SFRs from observed high-z QSOs ranging from 100–3000 $M_\odot \, \text{yr}^{-1}$ (e.g. Bertoldi et al, 2003; Dwek et al, 2007; Riechers et al, 2009; Wang et al, 2010). With these assumptions, all cases for which $\mu_D \leq 10^{-3}$ can be excluded (see Fig. 8).

For the 'low' SN dust production efficiency, $\epsilon_{\text{low}}(m)$, none of the IMFs gives a sufficiently high dust productivity. Only a mass-heavy IMF is close to the limit. Moreover, the long lifetimes of 3–4 $M_\odot$ AGB stars (see Fig. 1), which dominate the AGB dust production (see Sect. 7 and Fig. 6), is problematic. These stars will start contributing with a delay of more than ~ 200 Myr so will produce dust for only approximately half the time of the assumed maximum time span of 400 Myr. Thus, a 'low' SN dust production efficiency appears to be insufficient to account for the dust at high redshift.

In case of a 'high' SN efficiency, $\epsilon_{\text{high}}(m)$, the majority of the IMFs might lead to a sufficiently high dust productivity. Due to their short lifetimes, SNe can be assumed to release dust immediately after formation. Thus, SNe dominate the dust production for a Larson 2 or top heavy IMF. Taking into account the reduction of the AGB dust contribution due to the long lifetimes of these stars, the Salpeter or Larson 1 IMFs most likely do not lead to sufficiently large amounts of dust at high-z.

For a 'maximum' SN efficiency $\epsilon_{\text{max}}(m)$ the total dust production rates R_D of 3–18 $M_\odot$ yr^{-1} are achieved primarily through SN dust production. This leads to possible dust masses in excess of $10^9 \, M_\odot$ produced in high-z systems, even for significantly lower star formation rates than assumed in our scenario.

We note that it is unclear if a high SFR can be sustained over 400 Myr. In fact, the very high derived SFRs ($\geq 1000 \, M_\odot \, \text{yr}^{-1}$) are attributed to shorter ($\leq 10^8$ yr) durations of the starburst (e.g. Bertoldi et al, 2003; Dwek et al, 2007; Riechers et al, 2009). Assuming a

SFR $\psi(t) = 1000$ M$_\odot$ yr^{-1} and a $\Delta t = 200$ Myr leads to the same dust productivity $\mu_D = 10^{-3}$ as discussed above, although the AGB star contribution would be even more suppressed due to the long lifetimes relative to Δt.

8 Dust at high redshift

From SCUBA, MAMBO, MAMBO-2 and VLA surveys of bright high-z QSOs at $4 \lesssim z \leq 6.4$ (e.g., Carilli et al, 2001a; Omont et al, 2001; Isaak et al, 2002; Bertoldi and Cox, 2002; Bertoldi et al, 2003; Priddey et al, 2003; Robson et al, 2004; Beelen et al, 2006) very high dust masses of more than 10^8 M$_\odot$ and star formation rates of more than 10^3 M$_\odot$ yr^{-1} have been inferred from the measured sub-millimeter fluxes.

Theoretically, it has been proven difficult to explain the origin of these dust masses in QSOs at $z \gtrsim 6$, despite some attempts (e.g., Dwek et al, 2007; Valiante et al, 2009; Pipino et al, 2011; Dwek and Cherchneff, 2011; Gall et al, 2011a,b; Mattsson, 2011; Valiante et al, 2011). At this redshift the timescale available to build up large dust masses is short, which limits the possible options for sources of dust (see Sect. 2, Fig. 1).

As a consequence, massive stars have been strongly favoured, although the actual dust production by massive stars (see above discussions in Sect. 4 and 5) is afflicted with large uncertainties and other sources may play an important role as well.

Nevertheless, features in the extinction curves of various objects at high redshift have been attributed to dust of SN origin. For example, the extinction curve inferred for the QSO SDSS J1048+46 at $z = 6.2$ possesses a characteristic plateau at around 1700–3000 Å, interpreted as arising from amorphous carbon and magnetite SN dust (Maiolino et al, 2004) based on the TF01 models. A similar feature has been reported for the afterglow of GRB 071025 at $z \sim 5$ (Perley et al, 2010). Also less conspicuous features in extinction curves (notably flatter UV slopes than the SMC extinction curve) have been interpreted as evidence for dust from SNe. Several QSOs (e.g., Gallerani et al, 2010) turned out to be best fitted with a contribution from extinction curves for SN-like dust (Hirashita et al, 2008). The young infrared galaxy SST J1604+4304 at $z \sim 1$ has also been proposed to be best fitted with a SN extinction curve from Hirashita et al (2008) (Kawara et al, 2011).

The observationally derived dust masses and SFRs for high-z galaxies are naturally uncertain. Below we therefore briefly review the basic concepts and caveats in deriving dust masses and SFRs from observations. Next we summarize the theoretical models aiming to explain the observations at high redshift.

8.1 Inferring physical properties of high-z QSOs

8.1.1 Dust mass

Based on the method discussed by Hildebrand (1983), the dust mass is determined from the sub-millimeter flux density observed at frequency $\nu_o = \nu_r/(1 + z)$ as

$$M_d = \frac{S(\nu_o)D_L^2}{(1 + z)\kappa_d(\nu_r)B(\nu_r, T_d)},$$ (7)

where ν_r is the rest-frame frequency (see also Eq. 1). For definition of the parameters we refer to Sect. 5.2.

While there are uncertainties related to the cosmology entering the luminosity distance, D_L, the main uncertainties in deriving the dust mass from observations are given by T_d and $\kappa_d(\nu_r)$, which is usually parametrized as

$$\kappa_d(\nu_r) = \kappa_d(\nu_0)\left(\frac{\nu_r}{\nu_0}\right)^{\beta}, \tag{8}$$

where β is the emissivity index. From the above formalism it is clear that $\kappa_d(\nu)$ significantly depends on dust properties such as β, the grain radius a and the grain density ρ (because $\kappa_d(\nu) \equiv (3/4)Q(\nu)/(a\rho)$). None of these properties are well known.

The dust absorption coefficient at the critical frequency (wavelength), $\nu_0 = 2.4$ THz ($\lambda_0 = 125 \ \mu$m), at which a source becomes optically thin, was determined by Hildebrand (1983) to be $\kappa_d(\nu_0) = 18.75$ cm^2 g^{-1}. For values of the absorption coefficient other than that determined by Hildebrand (1983), we refer to a summary of Alton et al (2004, their Table 4). While $\kappa_d(\nu)$ increases from FIR to sub-millimeter wavelengths (Draine, 1990), it should be noted that even for similar wavelengths the inferred values for $\kappa_d(\nu)$ often vary by an order of magnitude.

Another ambiguous parameter is the emissivity index β. It has been found that β is dependent on the wavelength (or frequency) and increases with increasing wavelength. For $\lambda \lesssim 200 \ \mu$m the emissivity index $\beta \sim 1$ and for $\lambda \gtrsim 1000 \ \mu$m, $\beta \sim 2$ (e.g., Erickson et al, 1981; Schwartz, 1982). However, β might also depend on the dust composition, the grain size and possibly also the temperature. For a detailed discussion we refer to Dunne and Eales (2001) and references therein. The emissivity index β as well as the dust temperature, T_d, can be determined by fitting the spectral energy distribution (SED). According to Hildebrand (1983) the flux density, $S(\nu)$, is defined as

$$S(\nu) = \Omega_d Q(\nu) B(\nu, T_d), \tag{9}$$

where $\Omega_d = N(\sigma_d/D_L^2)$ is the solid angle subtended by the dust source in the sky, with N the number of spherical grains, each of cross section σ_d. For high-z objects the SEDs are fitted in the rest-frame and Eq. 9 needs to be modified accordingly.

For a simultaneous determination of T_d and β many flux measurements at different wavelengths are necessary. This however is often not possible for high-z objects and values for either T_d or β are simply assumed. Priddey and McMahon (2001) found that the composite SED of a sample of QSOs at $z > 4$ are best fitted with a single temperature of $T_d \sim 40$ K and an emissivity index $\beta \sim 1.95$, while Hughes et al (1997) and Benford et al (1999) found $T_d \sim 50$ K and $\beta \sim 1.5$ for high-z objects. From a study similar to Priddey and McMahon (2001), but with a larger sample of high-z QSOs ($1.8 \le z \le 6,4$), Beelen et al (2006) obtain a higher temperature $T_d \sim 47$ K but a lower $\beta \sim 1.6$ for a combined SED of all QSOs (see Fig. 9).

The SED can in principle be fitted using either a single temperature model (as described above) or a two-temperature component model as accomplished by e.g., Dunne and Eales (2001), Vlahakis et al (2005) or Ivison et al (2010). For a two-component model the equation for the dust mass can be expressed as

$$M_d = \frac{S(\nu_o)D_L^2}{(1+z)\kappa_d(\nu_r)}\left[\frac{N_w}{B(\nu_r, T_w)} + \frac{N_c}{B(\nu_r, T_c)}\right], \tag{10}$$

where N_w and N_c represent the mass fractions of the warm and cold components. While the uncertainties in deriving the dust mass from observations are normally large, it has

been found that using a two-component dust model, the derived dust masses are usually a factor of ~ 2 higher than what can be obtained from a single temperature model (e.g., Dunne and Eales, 2001; Vlahakis et al, 2005) due to the larger amount of cold dust.
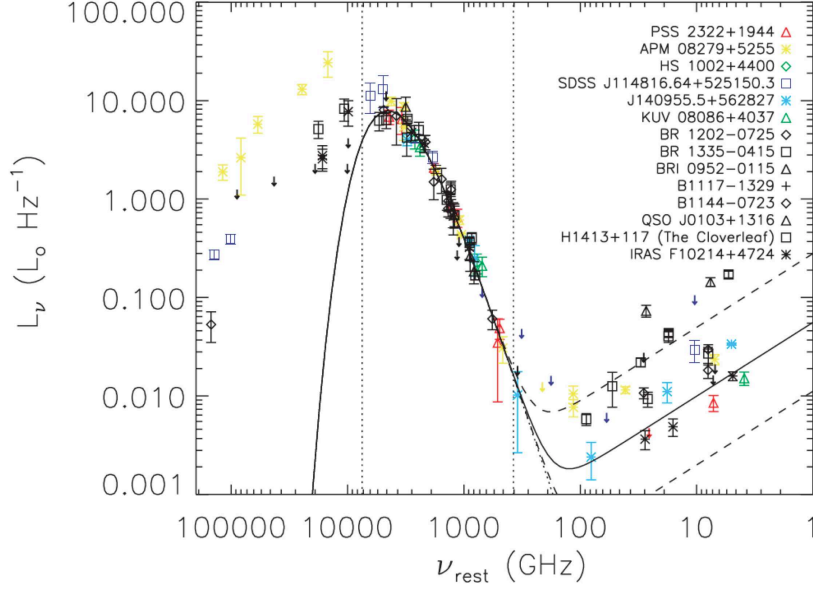
Fig. 9 Combined SED, in the rest frame, of high-z QSOs taken from Beelen et al (2006). The plot comprises data from sources discussed in Benford et al (1999), Priddey and McMahon (2001) and Beelen et al (2006). The mean FIR data points are best fitted with a graybody of temperature $T_d \sim 47$ K and emissivity index $\beta \sim 1.6$.

8.1.2 Star-formation rate

The SFR of a galaxy, ψ, can be related to its dust continuum spectrum through the FIR luminosity, L_{FIR}, as

$$\psi = \delta_{MF}\delta_{SB}(L_{FIR}/10^{10}\,L_\odot)\,M_\odot yr^{-1} \tag{11}$$

(e.g., Gallagher et al, 1984; Thronson and Telesco, 1986; Omont et al, 2001). Here $\delta_{MF} = (\Delta t_{FIR}/Myr)^{-1}(\bar{M}/M_\odot)/(\bar{L}/L_\odot)$, where Δt_{FIR} accounts for the (assumed) duration of the starburst, and $\bar{M}/\bar{L}$ is the mass-to-luminosity ratio, which is determined from an assumed IMF. δ_{SB} is the fraction of the FIR emission due to dust heated by the starburst.

The FIR luminosity can be obtained (see e.g., Yun and Carilli, 2002) by integrating the SED (Eq. 9) over the emitting area Ω_d and the corresponding frequency range,

$$L_{FIR} = 4\pi D_L^2 \int_{\Omega_d} \int S(\nu)d\nu d\Omega. \tag{12}$$

Alternatively, once the dust mass is known, L_{FIR} can be obtained by integrating the SED using Eq. (7),

$$L_{FIR} = 4\pi M_d \int \kappa_d(\nu) B(\nu, T_d) d\nu, \tag{13}$$

which emphasizes the relation between the FIR luminosity and the dust mass. For bright high-z objects, FIR luminosities of the order of 10^{12-13} $L_\odot$ are usually derived (e.g., Omont et al, 2001; Bertoldi and Cox, 2002; De Breuck et al, 2003; Robson et al, 2004; Beelen et al, 2006; Wang et al, 2010; Ivison et al, 2010; Leipski et al, 2010).

Evidently, the calculated value of the SFR sensitively depends on the assumed IMF through δ_{MF}. In most cases a Salpeter IMF is assumed, but, as pointed out by Dwek et al (2007) and Dwek and Cherchneff (2011), the IMF constitutes one of the major uncertainties. For example, the derived SFR of ~ 3400 $M_\odot$ yr^{-1} for QSO SDSS J1148+5251 (Fan et al, 2003), using a Salpeter IMF, decreases to about 380 $M_\odot$ yr^{-1} for a top-heavy IMF. The range of the SFR in some high-z objects might therefore be between 10^{2-4} $M_\odot$ yr^{-1}.

Another critical parameter is the assumption of the duration of the starburst, Δt_{FIR}. Commonly either values of $\delta_{MF} \sim 0.8$–2.1 (Scoville and Young, 1983; Thronson and Telesco, 1986) or simply $\delta_{MF} = 1$ are adopted. However, these values have been derived using a Salpeter IMF and an assumed starburst age of for example $\Delta t_{FIR} = 2$ Myr (Thronson and Telesco, 1986). As pointed out by Omont et al (2001), these assumptions might in fact be inappropriate for massive starbursts in high-z galaxies. Considering a continuous starburst of 100 Myr and a Salpeter IMF with different low mass cutoffs, Omont et al (2001) derive $\delta_{MF} \sim 1.2$–3.8. Assuming a flat IMF ($\alpha = 1$) at low masses and $\Delta t_{FIR} = 10$–100 Myr results in $\delta_{MF} \sim 0.8$–2, similar to the values of Thronson and Telesco (1986).

Regarding the fraction of the FIR emission heated by the starburst, δ_{SB}, it is unknown whether the FIR luminosity arises solely from the starburst and if the entire stellar radiation is absorbed and re-emitted by warm dust or whether heating by an active galactic nucleus (AGN) must to be taken into account. The common view is that the heating source is the starburst and a contribution of the AGN is usually neglected, thus δ_{SB} is set to 1. Taking a contribution of the AGN into account would result in a smaller amount of dust and lower star formation rates. For a more detailed discussion we refer to, e.g., Omont et al (2001) and Isaak et al (2002).

8.2 Theoretical models

To address the issue of the inferred large dust masses in high-z galaxies, chemical evolution models so far have been the preferred approach for following the temporal progression of the physical properties of a galaxy. The range of applications is large, e.g., the models can be used to investigate the temporal evolution of the abundance of different elements and dust influenced by formation and destruction processes, the abundance distribution of elements, stellar masses, the metallicity, SFR and other physical properties. The models are mainly regulated by the interplay between processes such as star formation, gas and dust flows, stellar feedback, and the considered dust destruction and growth processes. Another important input is the IMF. However, most of the processes governing the models are uncertain and various simplifications must be made. For a profound review on chemical evolution models see Tinsley (1980), Dwek (1998), Dwek et al (2009) or Piovan et al (2011a,b). Over the past years several dust evolution models addressing the above presented issue have been developed. Below we discuss the main findings.

The first attempt to explain the large derived dust masses in the $z = 6.4$ QSO J1148+5251 (Fan et al, 2003) was carried out by Dwek et al (2007), who concluded that at least 1 $M_\odot$ of dust per SN is required to account for the observed dust mass in this QSO (if SNe are the only sources of dust). The total mass of the QSO host galaxy is considered to be about 5×10^{10} $M_\odot$ to match the suggested dynamical mass for this QSO (e.g. Walter et al, 2004).

Valiante et al (2009) include AGB stars in their models and claim that 10^8 $M_\odot$ of dust can predominantly be produced by AGB stars in QSO J1148+5251. The considered mass of the galaxy of about 1×10^{12} $M_\odot$ in the study, however, exceeds the plausible dynamical mass derived from observations by more than about an order of magnitude. The model includes a star-formation history resulting from a hierarchical galaxy merger tree scenario (Li et al, 2007) and neglects gas in- and outflows. Star formation commenced at $z = 15$, resulting in about 550 Myr available for stars to evolve, and the SFR reached values up to 10^4 $M_\odot$ yr^{-1}.

Pipino et al (2011) adopted models developed by Calura et al (2008) for elliptical galaxies. The models comprise dust contribution from different stellar sources, a QSO wind and dust grain growth in the ISM. A model galaxy as massive as 10^{12} $M_\odot$ was applied to J1148+5251. Although the predicted SFR exceeds 3×10^3 $M_\odot$ yr^{-1}, the observed large dust masses could only be reproduced with a strong contribution from dust grain growth in the ISM in addition to dust produced by SNe and massive AGB stars. The results are strongly affected by a very high assumed dust destruction due to SN shocks in the ISM. Moreover, the models assume dust from SNe Ia, even though there is no clear evidence for significant dust production by these Types of SNe (see Sect. 5.3.3). The dust contribution by the QSO wind of a few times 10^7 $M_\odot$ is insufficient.

Dwek and Cherchneff (2011) constructed scenarios comprising star-formation histories with a dominant dust production by either AGB stars or SNe. An average dust yield of about 0.15 $M_\odot$ (Cherchneff and Dwek, 2010) for all SNe, independent of their progenitor mass, was assumed. Only in cases of short-duration and intense bursts with SFRs in excess of 10^4 $M_\odot$ yr^{-1}, SNe are found to be sufficient to produce the observed dust masses.

Pertaining to the discrepancies of the claims made in previous models, Gall et al (2011a) ascertained the impact of diverse astrophysical conditions governing the evolution of the total dust mass in galaxies. The model takes into account AGB stars, different Types of core collapse SNe, and stellar yields from different groups. The dependence of stellar lifetimes on stellar masses and dust destruction due to SN shock interactions are considered. A simple treatment to estimate the impact of the formation of a supermassive black hole is introduced. It is shown that the amount of dust reached in galaxies and the significance of the contribution by either AGB stars or SNe strongly depend on the assumed mass of the galaxy and is sensitive to the interplay between the IMF, the SFR, the dust production efficiency of SNe and the degree of dust destruction. Overall, larger dust masses are achieved with increasing mass of the galaxies or IMFs biased towards higher stellar masses. The calculations show that for increasing mass of the galaxies (and fixed SFR and IMF) either an increasing degree of dust destruction or a lower SN dust production efficiency can be accommodated.

Gall et al (2011b) identified plausible scenarios capable of reproducing the large observed dust masses for different QSOs at $z \gtrsim 6$. They found that large quantities of dust can be generated in QSOs as early as 30–170 Myr after the onset of the starburst if the SFR of the starburst is $> 10^3$ $M_\odot$ yr^{-1}. An initial gas mass of the galaxy of about 1–3×10^{11} $M_\odot$ was found to be sufficiently large. However, SNe are required to be very efficient while at these early epochs AGB stars contribute only marginally (see also this work, Sect. 7.2, Fig 8).

It is worth stressing that the predictions of chemical evolution models partly reflect the initial assumptions made about physical conditions and processes. For example, the prediction of a major AGB star contribution (Valiante et al, 2009) can be reproduced by the

models of Dwek and Cherchneff (2011) and Gall et al (2011a,b) when similar galaxy mass, SFR, IMF and dust production of stellar sources are assumed.

Chemical dust evolution models face many uncertainties constituting various caveats in the aferomentioned approaches. Apart from the ambiguous dust production by stellar sources discussed in this review, the unknown formation and evolution of the QSOs and the associated star formation history, pose a fundamental problem (e.g., Dwek and Cherchneff, 2011; Gall et al, 2011a). The composition and shape of dust grains produced by stellar sources or reprocessed in the ISM are relatively unknown. Commonly, carbon or silicate type dust are assumed, but other grain species might be considered as well (e.g., Dwek, 2004).

Furthermore, destruction and growth processes of dust in the ISM, which decisively influence the lifetime of dust grains, are poorly understood (e.g., Liffman and Clayton, 1989; McKee, 1989; Jones, 2004; Dwek et al, 2007). Estimates of grain lifetimes resulting from calculations for the Milky Way range between 100 and 1000 Myr (e.g., Jones et al, 1994), although these predictions are uncertain (e.g., Jones and Nuth, 2011). However, taking these lifetimes for granted, it has been shown that AGB stars together with SNe can account for only $\sim 10\%$ of the interstellar dust (Draine, 2009) in the ISM of the Milky Way and leads to a 'missing dust source problem' in the LMC similar to that in high-z galaxies (Matsuura et al, 2009).

Major outstanding questions for high-z QSOs thus include the effects of (i) dust grain growth in the ISM (e.g., Draine, 2009; Michałowski et al, 2010a; Dwek and Cherchneff, 2011), which is the preferred scenario in the Milky Way (e.g., Zhukovska et al, 2008; Draine, 2009), and (ii) dust formation in QSO outflows (e.g., Elvis et al, 2002; Pipino et al, 2011; Gall et al, 2011a).

9 Summary and Conclusion

This review has been devoted to dust formation by massive stars progenitors, including their role as dust producers in galaxies with emphasis on the early Universe. At very high redshift ($z \gtrsim 6$) the minimum stellar mass of potential dust sources is ~ 3 M$_\odot$ (see Fig. 1).

In Sect 2 we have discussed the many different channels in which stars with masses ~ 3 M$_\odot$ can evolve towards their dust producing end stages. Stars at the lower mass end (3–8 M$_\odot$) evolve to AGB stars and release dust through intense mass-loss, most efficiently at the very end stages of evolution. Observationally, mass-loss rates can be obtained and linked to dust-mass-loss rates via gas-to-dust mass ratios, but it is difficult to determine the mass of the AGB stars. Thus, current information about the mass dependency of gas and dust yields from AGB stars relies on theoretical models (Sect 4). The current state of affairs indicates that 3–4 M$_\odot$ AGB stars are dominant dust producers among the AGB stars due to a higher dust production efficiency convolved with the IMF (see Fig. 7). However, the theoretical models are still rather simplistic, because e.g., the driving mechanism for mass-loss, the chemical composition of the atmospheres and hence the details of dust formation are poorly understood.

Stars more massive than ~ 8 M$_\odot$ explode as SNe but there is no clear one-to-one correspondence between the mass of the progenitor, the Type of the SN and the amount of dust produced. The most common Type of observed SNe with reported dust masses are Type II-P SNe. However, as discussed in Sec. 5 there are other promising channels (i.e., ECSN, Type IIn SNe, LBV stars) for producing significant amounts of dust. On the other hand, there is no strong indication or evidence for significant dust formation in other SN Types (i.e., Ia, Ib,

Ic, and IIb). Based on the currently available sample of observed SNe and SNRs (Tables 3 and 4) there is a correlation between the observationally derived dust temperature and the amount of dust (see Fig. 2b). The amount of inferred cold dust (< 100 K) is higher than that of hot dust (> 100 K). While there is no evidence for cold dust in SNe at early epochs, small amounts of hot dust are present in SNRs (see Fig. 2a).

The results of theoretical models developed for dust formation in SNe are not in agreement with observations, predicting higher dust masses to be formed than observed. To account for this discrepancy, models have been developed to investigate the effect of a SN reverse shock initiated by the collision of the SN forward shock with the ISM. However, the timescales for destruction (up to 10^4 years) are too long to affect the dust masses in SNe, when observed at earlier epochs.

In most models, the investigated SNe are considered to be Type II-P SN-like in the mass range 12–40 $M_\odot$, but the many complex physical and chemical processes involved are not yet well understood. Stars in the mass range 8–12 $M_\odot$ have not been considered in the theoretical models for dust formation. The reasons are the lack of calculations of stellar yields due to the very complex evolution of these stars as discussed in Sect. 2.4. Substantial work has been devoted to model PISNe and zero-metallicity stars in the mass range 12–40 $M_\odot$, even though so far there is little observational evidence for such stars. On the contrary, there is evidence for supersolar metallicity in very dusty high-z QSOs (e.g., Fan et al, 2003; Freudling et al, 2003; Juarez et al, 2009). However, there are no models of dust production by SNe at supersolar metallicity.

In Sect 6 we have parameterized the dust production efficiency of AGB stars and SNe using currently available observations and models. For operational purposes, we have ascertained a 'low', 'high' and 'maximum' case for the dust production efficiency of SNe. Using these efficiencies we have evaluated the total dust productivity of AGB stars and SNe in the mass interval 3–40 $M_\odot$ for five different IMFs. We find that the dust production efficiency for AGB stars and SNe exhibit a decreasing tendency with increasing progenitor mass (see Fig. 4). The dust productivity of stars between 3–40 $M_\odot$ is sensitive to the choice of IMF (Sect. 7.2). This is more pronounced when stars between 8–40 $M_\odot$ form dust with 'maximum' SN efficiency. The contribution from AGB stars to the total dust productivity prevails when SNe are assumed to produce dust with a 'low' efficiency, but becomes insignificant for 'high' to 'maximum' SN dust production efficiency and for IMFs biased towards high stellar masses. The SN mass ranges of 8–12 $M_\odot$ and 12–20 $M_\odot$ are equally important and together dominate the dust production from all SNe between 8–40 $M_\odot$. Dust produced by stars between 20–40 $M_\odot$ depends on the fractions of the various types of CCSNe.

The present situation at high redshift is that large dust masses ($\gtrsim 10^8$ $M_\odot$) have been inferred from detection of thermal dust emission at sub-millimeter and millimeter wavelengths in the most distant QSOs. The issue about the origin of these high dust masses remains elusive and poses many unanswered questions. The most intriguing but also most uncertain ones concern the main dust sources, dust destruction and growth processes, the star formation history and the formation and evolution of the galaxies itself. On the other hand, deducing the dust masses from observations is challenging and afflicted with uncertainties (Sect. 8). Biases arising from assumptions about the IMF, the duration of the star formation, the absorption coefficient, the dust emissivity or the possible AGN heating could possibly lead to revisions of the dust masses currently quoted. Finally, the outcome of galactic chemical evolution models also exhibit important differences, e.g., regarding the adequacy of AGB stars to produce sufficient amounts of dust at high redshift. The main reason for this is that the models greatly differ with respect to the assumptions made for the mass of the galaxy,

dust contribution from stellar sources as well as the treatment of the star formation history (Sect. 8.2).

Future progress on the theoretical side should involve more refined models for (i) dust formation in stellar outflows and (ii) dust evolution models for galaxies. For example, models involving a more detailed account of the diverse possible end-stages of massive stars (e.g., ECSN, IIn, LBV) and the physical conditions leading to dust formation (SN ejecta, stellar winds in AGB stars, LBV outbursts) must be developed. Dust formation models should also allow for supersolar metallicity. Future galaxy models must be self-consistently connected to the mechanisms of the formation and evolution of the host galaxy impacting the evolution of the dust. Alternative dust sources complementing the stellar dust production such as dust grain growth in the ISM or dust production in QSO outflows might also be of relevance.

From an observational point of view it is necessary to increase the currently small sample of observations of dust in SNe and extend it to different SN Types with indications of dust formation. Concerning the reliability of the observationally derived properties in the high-z QSOs, studies enlightening the possible influence of the uncertain parameters on e.g., the derived dust mass, SFR or stellar mass will be of relevance.

References

Abel T, Bryan GL, Norman ML (2002) The Formation of the First Star in the Universe. Science 295:93–98, DOI 10.1126/science.295.5552.93, `arXiv:astro-ph/0112088`

Alton PB, Xilouris EM, Misiriotis A, Dasyra KM, Dumke M (2004) The emissivity of dust grains in spiral galaxies. A&A 425:109–120, DOI 10.1051/0004-6361:20040438, `arXiv:astro-ph/0406389`

Anderson JP, James PA (2008) Constraints on core-collapse supernova progenitors from correlations with H alpha emission. MNRAS 390:1527–1538, DOI 10.1111/j.1365-2966.2008.13843.x, `0809.0236`

Andrews JE, Gallagher JS, Clayton GC, Sugerman BEK, Chatelain JP, Clem J, Welch DL, Barlow MJ, Ercolano B, Fabbri J, Wesson R, Meixner M (2010) SN 2007od: A Type IIP Supernova with Circumstellar Interaction. ApJ 715:541–549, DOI 10.1088/0004-637X/715/1/541, `1004.1209`

Andrews JE, Clayton GC, Wesson R, Sugerman BEK, Barlow MJ, Clem J, Ercolano B, Fabbri J, Gallagher JS, Landolt A, Meixner M, Otsuka M, Riebel D, Welch DL (2011a) Evidence for Pre-Existing Dust in the Bright Type IIn SN 2010jl. ArXiv e-prints `1106.0537`

Andrews JE, Sugerman BEK, Clayton GC, Gallagher JS, Barlow MJ, Clem J, Ercolano B, Fabbri J, Meixner M, Otsuka M, Welch DL, Wesson R (2011b) Photometric and Spectroscopic Evolution of the IIP SN 2007it to Day 944. ApJ 731:47–+, DOI 10.1088/0004-637X/731/1/47, `1102.2431`

Arendt RG, Dwek E, Moseley SH (1999) Newly Synthesized Elements and Pristine Dust in the Cassiopeia A Supernova Remnant. ApJ 521:234–245, DOI 10.1086/307545, `arXiv:astro-ph/9901042`

Arnett WD (1988) On the early behavior of supernova 1987A. ApJ 331:377–387, DOI 10.1086/166564

Baade W (1943) Nova Ophiuchi of 1604 AS a Supernova. ApJ 97:119–+, DOI 10.1086/144505

Ballero SK, Kroupa P, Matteucci F (2007) Testing the universal stellar IMF on the metallicity distribution in the bulges of the Milky Way and M 31. A&A 467:117–121, DOI 10.1051/0004-6361:20066786, arXiv:astro-ph/0702047

Bandiera R (1987) The origin of Kepler's supernova remnant. ApJ 319:885–892, DOI 10.1086/165505

Barlow MJ, Krause O, Swinyard BM, Sibthorpe B, Besel M, Wesson R, Ivison RJ, Dunne L, Gear WK, Gomez HL, Hargrave PC, Henning T, Leeks SJ, Lim TL, Olofsson G, Polehampton ET (2010) A Herschel PACS and SPIRE study of the dust content of the Cassiopeia A supernova remnant. ArXiv e-prints 1005.2688

Bartko H, Martins F, Trippe S, Fritz TK, Genzel R, Ott T, Eisenhauer F, Gillessen S, Paumard T, Alexander T, Dodds-Eden K, Gerhard O, Levin Y, Mascetti L, Nayakshin S, Perets HB, Perrin G, Pfuhl O, Reid MJ, Rouan D, Zilka M, Sternberg A (2010) An Extremely Top-Heavy Initial Mass Function in the Galactic Center Stellar Disks. ApJ 708:834–840, DOI 10.1088/0004-637X/708/1/834, 0908.2177

Bastian N, Covey KR, Meyer MR (2010) A Universal Stellar Initial Mass Function? A Critical Look at Variations. ARA&A 48:339–389, DOI 10.1146/annurev-astro-082708-101642, 1001.2965

Baugh CM, Lacey CG, Frenk CS, Granato GL, Silva L, Bressan A, Benson AJ, Cole S (2005) Can the faint submillimetre galaxies be explained in the Λ cold dark matter model? MNRAS 356:1191–1200, DOI 10.1111/j.1365-2966.2004.08553.x, arXiv:astro-ph/0406069

Beelen A, Cox P, Benford DJ, Dowell CD, Kovács A, Bertoldi F, Omont A, Carilli CL (2006) 350 μm Dust Emission from High-Redshift Quasars. ApJ 642:694–701, DOI 10.1086/500636, arXiv:astro-ph/0603121

Beers TC, Christlieb N (2005) The Discovery and Analysis of Very Metal-Poor Stars in the Galaxy. ARA&A 43:531–580, DOI 10.1146/annurev.astro.42.053102.134057

Benetti S, Turatto M, Valenti S, Pastorello A, Cappellaro E, Botticella MT, Bufano F, Ghinassi F, Harutyunyan A, Inserra C, Magazzu A, Patat F, Pumo ML, Taubenberger S (2011) The Type Ib SN 1999dn: one year of photometric and spectroscopic monitoring. MNRAS 411:2726–2738, DOI 10.1111/j.1365-2966.2010.17873.x, 1010.3199

Benford DJ, Cox P, Omont A, Phillips TG, McMahon RG (1999) 350 Micron Dust Emission from High-Redshift Objects. ApJ 518:L65–L68, DOI 10.1086/312073, arXiv:astro-ph/9904277

Bertoldi F, Cox P (2002) Dust emission and star formation toward a redshift 5.5 QSO. A&A 384:L11–L14, DOI 10.1051/0004-6361:20020120, arXiv:astro-ph/0201330

Bertoldi F, Carilli CL, Cox P, Fan X, Strauss MA, Beelen A, Omont A, Zylka R (2003) Dust emission from the most distant quasars. A&A 406:L55–L58, DOI 10.1051/0004-6361:20030710, arXiv:astro-ph/0305116

Bianchi S, Schneider R (2007) Dust formation and survival in supernova ejecta. MNRAS 378:973–982, DOI 10.1111/j.1365-2966.2007.11829.x, 0704.0586

Blair WP, Morse JA, Raymond JC, Kirshner RP, Hughes JP, Dopita MA, Sutherland RS, Long KS, Winkler PF (2000) Hubble Space Telescope Observations of Oxygen-rich Supernova Remnants in the Magellanic Clouds. II. Elemental Abundances in N132D and 1E 0102.2-7219. ApJ 537:667–689, DOI 10.1086/309077

Blair WP, Ghavamian P, Long KS, Williams BJ, Borkowski KJ, Reynolds SP, Sankrit R

(2007) Spitzer Space Telescope Observations of Kepler's Supernova Remnant: A Detailed Look at the Circumstellar Dust Component. ApJ 662:998–1013, DOI 10.1086/518414, `arXiv:astro-ph/0703660`

Blöcker T (1995) Stellar evolution of low and intermediate-mass stars. I. Mass loss on the AGB and its consequences for stellar evolution. A&A 297:727–+

Blöcker T, Schönberner D (1991) A 7-solar-mass AGB model sequence not complying with the core mass-luminosity relation. A&A 244:L43–L46

Bonnell IA, Larson RB, Zinnecker H (2007) The Origin of the Initial Mass Function. Protostars and Planets V pp 149–164, `arXiv:astro-ph/0603447`

Borghesi A, Bussoletti E, Colangeli L, de Blasi C (1985) Laboratory study of SiC submicron particles at IR wavelengths - A comparative analysis. A&A 153:1–8

Borkowski KJ, Williams BJ, Reynolds SP, Blair WP, Ghavamian P, Sankrit R, Hendrick SP, Long KS, Raymond JC, Smith RC, Points S, Winkler PF (2006) Dust Destruction in Type Ia Supernova Remnants in the Large Magellanic Cloud. ApJ 642:L141–L144, DOI 10.1086/504472, `arXiv:astro-ph/0602313`

Botticella MT, Pastorello A, Smartt SJ, Meikle WPS, Benetti S, Kotak R, Cappellaro E, Crockett RM, Mattila S, Sereno M, Patat F, Tsvetkov D, van Loon JT, Abraham D, Agnoletto I, Arbour R, Benn C, di Rico G, Elias-Rosa N, Gorshanov DL, Harutyunyan A, Hunter D, Lorenzi V, Keenan FP, Maguire K, Mendez J, Mobberley M, Navasardyan H, Ries C, Stanishev V, Taubenberger S, Trundle C, Turatto M, Volkov IM (2009) SN 2008S: an electron-capture SN from a super-AGB progenitor? MNRAS 398:1041–1068, DOI 10.1111/j.1365-2966.2009.15082.x, `0903.1286`

Bouchet P, De Buizer JM, Suntzeff NB, Danziger IJ, Hayward TL, Telesco CM, Packham C (2004) High-Resolution Mid-infrared Imaging of SN 1987A. ApJ 611:394–398, DOI 10.1086/421936, `arXiv:astro-ph/0312240`

Bouwens RJ, Illingworth GD, Labbe I, Oesch PA, Trenti M, Carollo CM, van Dokkum PG, Franx M, Stiavelli M, González V, Magee D, Bradley L (2011) A candidate redshift z~10 galaxy and rapid changes in that population at an age of 500Myr. Nature 469:504–507, DOI 10.1038/nature09717, `0912.4263`

Bowen GH, Willson LA (1991) From wind to superwind - The evolution of mass-loss rates for Mira models. ApJ 375:L53–L56, DOI 10.1086/186086

Boyer ML, van Loon JT, McDonald I, Gordon KD, Babler B, Block M, Bracker S, Engelbracht C, Hora J, Indebetouw R, Meade M, Meixner M, Misselt K, Sewilo M, Shiao B, Whitney B (2010) Is Dust Forming on the Red Giant Branch in 47 Tuc? ApJ 711:L99–L103, DOI 10.1088/2041-8205/711/2/L99, `1002.1348`

Brandt TD, Tojeiro R, Aubourg É, Heavens A, Jimenez R, Strauss MA (2010) The Ages of Type Ia Supernova Progenitors. AJ 140:804–816, DOI 10.1088/0004-6256/140/3/804, `1002.0848`

Bromm V, Larson RB (2004) The First Stars. ARA&A 42:79–118, DOI 10.1146/annurev.astro.42.053102.134034, `arXiv:astro-ph/0311019`

Bromm V, Loeb A (2003) The formation of the first low-mass stars from gas with low carbon and oxygen abundances. Nature 425:812–814, DOI 10.1038/nature02071, `arXiv:astro-ph/0310622`

Bromm V, Coppi PS, Larson RB (2002) The Formation of the First Stars. I. The Primordial Star-forming Cloud. ApJ 564:23–51, DOI 10.1086/323947, `arXiv:astro-ph/0102503`

Bromm V, Yoshida N, Hernquist L, McKee CF (2009) The formation of the first stars and galaxies. Nature 459:49–54, DOI 10.1038/nature07990, `0905.0929`

Burrows A (2009) The Role of Dust Clouds in the Atmospheres of Brown Dwarfs. In:

T Henning, E Grün, & J Steinacker (ed) Astronomical Society of the Pacific Conference Series, Astronomical Society of the Pacific Conference Series, vol 414, pp 115–+, 0902.1777

Calura F, Pipino A, Matteucci F (2008) The cycle of interstellar dust in galaxies of different morphological types. A&A 479:669–685, DOI 10.1051/0004-6361:20078090, 0706.2197

Carilli CL, Bertoldi F, Omont A, Cox P, McMahon RG, Isaak KG (2001a) Radio Observations of Infrared-Luminous High-Redshift Quasi-Stellar Objects. AJ 122:1679–1687, DOI 10.1086/323104, arXiv:astro-ph/0106408

Carilli CL, Bertoldi F, Rupen MP, Fan X, Strauss MA, Menten KM, Kreysa E, Schneider DP, Bertarini A, Yun MS, Zylka R (2001b) A 250 GHz Survey of High-Redshift Quasars from the Sloan Digital Sky Survey. ApJ 555:625–632, DOI 10.1086/321519, arXiv:astro-ph/0103252

Cernuschi F, Marsicano FR, Kimel I (1965) On polarisation of stellar light. Annales d'Astrophysique 28:860–+

Chabrier G (2003a) Galactic Stellar and Substellar Initial Mass Function. PASP 115:763–795, DOI 10.1086/376392, arXiv:astro-ph/0304382

Chabrier G (2003b) The Galactic Disk Mass Function: Reconciliation of the Hubble Space Telescope and Nearby Determinations. ApJ 586:L133–L136, DOI 10.1086/374879, arXiv:astro-ph/0302511

Chabrier G (2005) The Initial Mass Function: from Salpeter 1955 to 2005. In: E Corbelli, F Palla, & H Zinnecker (ed) The Initial Mass Function 50 Years Later, Astrophysics and Space Science Library, vol 327, pp 41–+, arXiv:astro-ph/0409465

Charbonnel C, Meynet G, Maeder A, Schaller G, Schaerer D (1993) Grids of Stellar Models - Part Three - from 0.8 to 120-SOLAR-MASSES at Z=0.004. A&AS 101:415–+

Chary R, Stern D, Eisenhardt P (2005) Spitzer Constraints on the z = 6.56 Galaxy Lensed by Abell 370. ApJ 635:L5–L8, DOI 10.1086/499205, arXiv:astro-ph/0510827

Cherchneff I (2006) A chemical study of the inner winds of asymptotic giant branch stars. A&A 456:1001–1012, DOI 10.1051/0004-6361:20064827

Cherchneff I (2011) The formation of Polycyclic Aromatic Hydrocarbons in evolved circumstellar environments. In: EAS Publications Series, EAS Publications Series, vol 46, pp 177–189, DOI 10.1051/eas/1146019, 1010.2703

Cherchneff I, Dwek E (2009) The Chemistry of Population III Supernova Ejecta. I. Formation of Molecules in the Early Universe. ApJ 703:642–661, DOI 10.1088/0004-637X/703/1/642, 0907.3621

Cherchneff I, Dwek E (2010) The Chemistry of Population III Supernova Ejecta. II. The Nucleation of Molecular Clusters as a Diagnostic for Dust in the Early Universe. ApJ 713:1–24, DOI 10.1088/0004-637X/713/1/1, 1002.3060

Cherchneff I, Barker JR, Tielens AGGM (1991) Polycyclic aromatic hydrocarbon optical properties and contribution to the acceleration of stellar outflows. ApJ 377:541–552, DOI 10.1086/170383

Cherchneff I, Barker JR, Tielens AGGM (1992) Polycyclic aromatic hydrocarbon formation in carbon-rich stellar envelopes. ApJ 401:269–287, DOI 10.1086/172059

Chevalier RA (2005) Young Core-Collapse Supernova Remnants and Their Supernovae. ApJ 619:839–855, DOI 10.1086/426584, arXiv:astro-ph/0409013

Chevalier RA (2006) From progenitor to afterlife. ArXiv Astrophysics e-prints arXiv:astro-ph/0607422

Chevalier RA, Klein RI (1978) On the Rayleigh-Taylor instability in stellar explosions. ApJ 219:994–1007, DOI 10.1086/155864

Chu Y, Gruendl RA, Stockdale CJ, Rupen MP, Cowan JJ, Teare SW (2004) The Nature of SN 1961V. AJ 127:2850–2855, DOI 10.1086/383556, arXiv:astro-ph/0402473

Clayton DD (1979) Sudden grain nucleation and growth in supernova and nova ejecta. Ap&SS 65:179–189, DOI 10.1007/BF00643499

Clayton DD, Arnett D, Kane J, Meyer BS (1997) Type X Silicon Carbide Presolar Grains: Type IA Supernovae Condensates? ApJ 486:824–+, DOI 10.1086/304545

Clayton DD, Liu W, Dalgarno A (1999) Condensation of Carbon in Radioactive Supernova Gas. Science 283:1290–+, DOI 10.1126/science.283.5406.1290

Clayton DD, Deneault E, Meyer BS (2001) Condensation of Carbon in Radioactive Supernova Gas. ApJ 562:480–493, DOI 10.1086/323467

Crockett RM, Smartt SJ, Eldridge JJ, Mattila S, Young DR, Pastorello A, Maund JR, Benn CR, Skillen I (2007) A deeper search for the progenitor of the Type Ic supernova 2002ap. MNRAS 381:835–850, DOI 10.1111/j.1365-2966.2007.12283.x, 0706.0500

Crockett RM, Eldridge JJ, Smartt SJ, Pastorello A, Gal-Yam A, Fox DB, Leonard DC, Kasliwal MM, Mattila S, Maund JR, Stephens AW, Danziger IJ (2008) The type IIb SN 2008ax: the nature of the progenitor. MNRAS 391:L5–L9, DOI 10.1111/j.1745-3933.2008.00540.x, 0805.1913

Crockett RM, Smartt SJ, Pastorello A, Eldridge JJ, Stephens AW, Maund JR, Mattila S (2011) On the nature of the progenitors of three Type II-P supernovae: 2004et, 2006my and 2006ov. MNRAS 410:2767–2786, DOI 10.1111/j.1365-2966.2010.17652.x, 0912.3302

Crowther PA (2007) Physical Properties of Wolf-Rayet Stars. ARA&A 45:177–219, DOI 10.1146/annurev.astro.45.051806.110615, arXiv:astro-ph/0610356

Cucchiara A, Levan AJ, Fox DB, Tanvir NR, Ukwatta TN, Berger E, Krühler T, Küpcü Yoldaş A, Wu XF, Toma K, Greiner J, Olivares FE, Rowlinson A, Amati L, Sakamoto T, Roth K, Stephens A, Fritz A, Fynbo JPU, Hjorth J, Malesani D, Jakobsson P, Wiersema K, O'Brien PT, Soderberg AM, Foley RJ, Fruchter AS, Rhoads J, Rutledge RE, Schmidt BP, Dopita MA, Podsiadlowski P, Willingale R, Wolf C, Kulkarni SR, D'Avanzo P (2011) A Photometric Redshift of z ~ 9.4 for GRB 090429B. ApJ 736:7–+, DOI 10.1088/0004-637X/736/1/7, 1105.4915

Dabringhausen J, Kroupa P, Baumgardt H (2009) A top-heavy stellar initial mass function in starbursts as an explanation for the high mass-to-light ratios of ultra-compact dwarf galaxies. MNRAS 394:1529–1543, DOI 10.1111/j.1365-2966.2009.14425.x, 0901.0915

D'Antona F, Caloi V (2004) The Early Evolution of Globular Clusters: The Case of NGC 2808. ApJ 611:871–880, DOI 10.1086/422334, arXiv:astro-ph/0405016

D'Antona F, Mazzitelli I (1996) Hot Bottom Burning in Asymptotic Giant Branch Stars and the Turbulent Convection Model. ApJ 470:1093–+, DOI 10.1086/177933

Danziger IJ, Gouiffes C, Bouchet P, Lucy LB (1989) Supernova 1987A in the Large Magellanic Cloud. IAUC 4746:1–+

Dartois E, Muñoz Caro GM, Deboffle D, d'Hendecourt L (2004) Diffuse interstellar medium organic polymers. Photoproduction of the 3.4, 6.85 and 7.25 μm features. A&A 423:L33–L36, DOI 10.1051/0004-6361:200400032

Daulton TL, Bernatowicz TJ, Lewis RS, Messenger S, Stadermann FJ, Amari S (2002) Polytype Distribution in Circumstellar Silicon Carbide. Science 296:1852–1855, DOI 10.1126/science.1071136

Davé R (2008) The galaxy stellar mass-star formation rate relation: evidence for an evolving stellar initial mass function? MNRAS 385:147–160, DOI 10.1111/j.1365-2966.2008.12866.x, 0710.0381

Davidson K (1971) On the nature of Eta Carinae. MNRAS 154:415–427

De Breuck C, Neri R, Morganti R, Omont A, Rocca-Volmerange B, Stern D, Reuland M, van Breugel W, Röttgering H, Stanford SA, Spinrad H, Vigotti M, Wright M (2003) CO emission and associated H I absorption from a massive gas reservoir surrounding the z = 3 radio galaxy B3 J2330+3927. A&A 401:911–925, DOI 10.1051/0004-6361:20030171, arXiv:astro-ph/0302154

Decin L, Cherchneff I, Hony S, Dehaes S, De Breuck C, Menten KM (2008) Detection of "parent" molecules from the inner wind of AGB stars as tracers of non-equilibrium chemistry. A&A 480:431–438, DOI 10.1051/0004-6361:20078892, 0801.1118

Decin L, De Beck E, Brünken S, Müller HSP, Menten KM, Kim H, Willacy K, de Koter A, Wyrowski F (2010) Circumstellar molecular composition of the oxygen-rich AGB star IK Tauri. II. In-depth non-LTE chemical abundance analysis. A&A 516:A69+, DOI 10.1051/0004-6361/201014136, 1004.1914

Di Carlo E, Corsi C, Arkharov AA, Massi F, Larionov VM, Efimova NV, Dolci M, Napoleone N, Di Paola A (2008) Near-Infrared Observations of the Type Ib Supernova SN 2006jc: Evidence of Interactions with Dust. ApJ 684:471–480, DOI 10.1086/590051, 0712.3855

Doane JS, Mathews WG (1993) Stellar Evolution in the Starburst Galaxy M82: Evidence for a Top-heavy Initial Mass Function. ApJ 419:573–+, DOI 10.1086/173509

Donn B, Nuth JA (1985) Does nucleation theory apply to the formation of refractory circumstellar grains? ApJ 288:187–190, DOI 10.1086/162779

Dorschner J, Henning T (1995) Dust metamorphosis in the galaxy. A&A Rev. 6:271–333, DOI 10.1007/BF00873686

Dorschner J, Friedemann C, Guertler J, Duley WW (1980a) Laboratory spectra of protosilicates and the interstellar silicate absorption bands. Ap&SS 68:159–174, DOI 10.1007/BF00641652

Dorschner J, Friedemann C, Guertler J, Duley WW (1980b) Laboratory spectra of protosilicates and the interstellar silicate absorption bands. Ap&SS 68:159–174, DOI 10.1007/BF00641652

Douvion T, Lagage PO, Cesarsky CJ, Dwek E (2001a) Dust in the Tycho, Kepler and Crab supernova remnants. A&A 373:281–291, DOI 10.1051/0004-6361:20010447

Douvion T, Lagage PO, Pantin E (2001b) Cassiopeia A dust composition and heating. A&A 369:589–593, DOI 10.1051/0004-6361:20010053

Draine BT (1979) Time-dependent nucleation theory and the formation of interstellar grains. Ap&SS 65:313–335, DOI 10.1007/BF00648499

Draine BT (1985) Tabulated optical properties of graphite and silicate grains. ApJS 57:587–594, DOI 10.1086/191016

Draine BT (1990) Mass determinations from far-infrared observations. In: H A Thronson Jr & J M Shull (ed) The Interstellar Medium in Galaxies, Astrophysics and Space Science Library, vol 161, pp 483–492

Draine BT (2009) Interstellar Dust Models and Evolutionary Implications. In: T Henning, E Grün, & J Steinacker (ed) Astronomical Society of the Pacific Conference Series, Astronomical Society of the Pacific Conference Series, vol 414, pp 453–+, 0903.1658

Draine BT, Lee HM (1984) Optical properties of interstellar graphite and silicate grains. ApJ 285:89–108, DOI 10.1086/162480

Duley WW, Williams DA (1981) The infrared spectrum of interstellar dust - Surface functional groups on carbon. MNRAS 196:269–274

Dunne L, Eales SA (2001) The SCUBA Local Universe Galaxy Survey - II. 450-μm data: evidence for cold dust in bright IRAS galaxies. MNRAS 327:697–714, DOI 10.1046/j.1365-8711.2001.04789.x, arXiv:astro-ph/0106362

Dunne L, Eales S, Ivison R, Morgan H, Edmunds M (2003) Type II supernovae as a significant source of interstellar dust. Nature 424:285–287, DOI 10.1038/nature01792, `arXiv:astro-ph/0307320`

Dunne L, Maddox SJ, Ivison RJ, Rudnick L, Delaney TA, Matthews BC, Crowe CM, Gomez HL, Eales SA, Dye S (2009) Cassiopeia A: dust factory revealed via submillimetre polarimetry. MNRAS 394:1307–1316, DOI 10.1111/j.1365-2966.2009.14453.x, `0809.0887`

Dwek E (1998) The Evolution of the Elemental Abundances in the Gas and Dust Phases of the Galaxy. ApJ 501:643–+, DOI 10.1086/305829, `arXiv:astro-ph/9707024`

Dwek E (2004) The Detection of Cold Dust in Cassiopeia A: Evidence for the Formation of Metallic Needles in the Ejecta. ApJ 607:848–854, DOI 10.1086/382653, `arXiv:astro-ph/0401074`

Dwek E, Cherchneff I (2011) The Origin of Dust in the Early Universe: Probing the Star Formation History of Galaxies by Their Dust Content. ApJ 727:63–+, DOI 10.1088/0004-637X/727/2/63, `1011.1303`

Dwek E, Moseley SH, Glaccum W, Graham JR, Loewenstein RF, Silverberg RF, Smith RK (1992) Dust and gas contributions to the energy output of SN 1987A on day 1153. ApJ 389:L21–L24, DOI 10.1086/186339

Dwek E, Galliano F, Jones AP (2007) The Evolution of Dust in the Early Universe with Applications to the Galaxy SDSS J1148+5251. ApJ 662:927–939, DOI 10.1086/518430, `0705.3799`

Dwek E, Arendt RG, Bouchet P, Burrows DN, Challis P, Danziger IJ, De Buizer JM, Gehrz RD, Kirshner RP, McCray R, Park S, Polomski EF, Woodward CE (2008) Infrared and X-Ray Evidence for Circumstellar Grain Destruction by the Blast Wave of Supernova 1987A. ApJ 676:1029–1039, DOI 10.1086/529038, `0712.2759`

Dwek E, Galliano F, Jones A (2009) The Cycle of Dust in the Milky Way: Clues from the High-Redshift and Local Universe. In: T Henning, E Grün, & J Steinacker (ed) Cosmic Dust - Near and Far, Astronomical Society of the Pacific Conference Series, vol 414, pp 183–+, `0903.0006`

Edmunds MG (2001) An elementary model for the dust cycle in galaxies. MNRAS 328:223–236, DOI 10.1046/j.1365-8711.2001.04859.x

Ekström S, Meynet G, Maeder A (2008) Can Very Massive Stars Avoid Pair-Instability Supernovae? In: F Bresolin, P A Crowther, & J Puls (ed) IAU Symposium, IAU Symposium, vol 250, pp 209–216, DOI 10.1017/S1743921308020516, `0801.3397`

Eldridge JJ, Relaño M (2011) The red supergiants and Wolf-Rayet stars of NGC 604. MNRAS 411:235–246, DOI 10.1111/j.1365-2966.2010.17676.x, `1009.1871`

Eldridge JJ, Tout CA (2004) The progenitors of core-collapse supernovae. MNRAS 353:87–97, DOI 10.1111/j.1365-2966.2004.08041.x, `arXiv:astro-ph/0405408`

Eldridge JJ, Vink JS (2006) Implications of the metallicity dependence of Wolf-Rayet winds. A&A 452:295–301, DOI 10.1051/0004-6361:20065001, `arXiv:astro-ph/0603188`

Eldridge JJ, Genet F, Daigne F, Mochkovitch R (2006) The circumstellar environment of Wolf-Rayet stars and gamma-ray burst afterglows. MNRAS 367:186–200, DOI 10.1111/j.1365-2966.2005.09938.x, `arXiv:astro-ph/0509749`

Eldridge JJ, Izzard RG, Tout CA (2008) The effect of massive binaries on stellar populations and supernova progenitors. MNRAS 384:1109–1118, DOI 10.1111/j.1365-2966.2007.12738.x, `0711.3079`

Elias-Rosa N, Van Dyk SD, Li W, Miller AA, Silverman JM, Ganeshalingam M, Boden AF, Kasliwal MM, Vinkó J, Cuillandre J, Filippenko AV, Steele TN, Bloom JS, Griffith CV,

Kleiser IKW, Foley RJ (2010) The Massive Progenitor of the Type II-linear Supernova 2009kr. ApJ 714:L254–L259, DOI 10.1088/2041-8205/714/2/L254, 0912.2880

Elmegreen BG (2009) The Stellar Initial Mass Function in 2007: A Year for Discovering Variations. In: The Evolving ISM in the Milky Way and Nearby Galaxies

Elmhamdi A, Danziger IJ, Chugai N, Pastorello A, Turatto M, Cappellaro E, Altavilla G, Benetti S, Patat F, Salvo M (2003) Photometry and spectroscopy of the Type IIP SN 1999em from outburst to dust formation. MNRAS 338:939–956, DOI 10.1046/j.1365-8711.2003.06150.x, arXiv:astro-ph/0209623

Elmhamdi A, Danziger IJ, Cappellaro E, Della Valle M, Gouiffes C, Phillips MM, Turatto M (2004) SN Ib 1990I: Clumping and dust in the ejecta? A&A 426:963–977, DOI 10.1051/0004-6361:20041318, arXiv:astro-ph/0407145

Elvis M, Marengo M, Karovska M (2002) Smoking Quasars: A New Source for Cosmic Dust. ApJ 567:L107–L110, DOI 10.1086/340006, arXiv:astro-ph/0202002

Ercolano B, Barlow MJ, Sugerman BEK (2007) Dust yields in clumpy supernova shells: SN 1987A revisited. MNRAS 375:753–763, DOI 10.1111/j.1365-2966.2006.11336.x, arXiv:astro-ph/0611719

Erickson EF, Knacke RF, Tokunaga AT, Haas MR (1981) The 45 micron H2O ice band in the Kleinmann-Low Nebula. ApJ 245:148–153, DOI 10.1086/158795

Fabian D, Posch T, Mutschke H, Kerschbaum F, Dorschner J (2001) Infrared optical properties of spinels. A study of the carrier of the 13, 17 and 32 mu m emission features observed in ISO-SWS spectra of oxygen-rich AGB stars. A&A 373:1125–1138, DOI 10.1051/0004-6361:20010657

Fallest DW, Nozawa T, Nomoto K, Umeda H, Maeda K, Kozasa T, Lazzati D (2011) On the effects of microphysical grain properties on the yields of carbonaceous dust from type II SNe. ArXiv e-prints 1105.4631

Fan X, Strauss MA, Schneider DP, Becker RH, White RL, Haiman Z, Gregg M, Pentericci L, Grebel EK, Narayanan VK, Loh Y, Richards GT, Gunn JE, Lupton RH, Knapp GR, Ivezić Ž, Brandt WN, Collinge M, Hao L, Harbeck D, Prada F, Schaye J, Strateva I, Zakamska N, Anderson S, Brinkmann J, Bahcall NA, Lamb DQ, Okamura S, Szalay A, York DG (2003) A Survey of z>5.7 Quasars in the Sloan Digital Sky Survey. II. Discovery of Three Additional Quasars at z>6. AJ 125:1649–1659, DOI 10.1086/368246, arXiv:astro-ph/0301135

Feder D (1966) . Advanced in Physics 15:111

Ferrarotti AS, Gail H (2001) Dust Condensation in LBV and WN Stars. In: E R Schielicke (ed) Astronomische Gesellschaft Meeting Abstracts, Astronomische Gesellschaft Meeting Abstracts, vol 18, pp 49–+

Ferrarotti AS, Gail H (2002) Mineral formation in stellar winds. III. Dust formation in S stars. A&A 382:256–281, DOI 10.1051/0004-6361:20011580

Ferrarotti AS, Gail H (2006) Composition and quantities of dust produced by AGB-stars and returned to the interstellar medium. A&A 447:553–576, DOI 10.1051/0004-6361:20041198

Filippenko AV (1997) Optical Spectra of Supernovae. ARA&A 35:309–355, DOI 10.1146/annurev.astro.35.1.309

Filippenko AV, Barth AJ, Bower GC, Ho LC, Stringfellow GS, Goodrich RW, Porter AC (1995) Was Fritz Zwicky's "Type V" SN 1961V a Genuine Supernova? AJ 110:2261–+, DOI 10.1086/117687

Fink M, Hillebrandt W, Röpke FK (2007) Double-detonation supernovae of sub-Chandrasekhar mass white dwarfs. A&A 476:1133–1143, DOI 10.1051/0004-6361:20078438, 0710.5486

Foley RJ, Smith N, Ganeshalingam M, Li W, Chornock R, Filippenko AV (2007) SN 2006jc: A Wolf-Rayet Star Exploding in a Dense He-rich Circumstellar Medium. ApJ 657:L105–L108, DOI 10.1086/513145, arXiv:astro-ph/0612711

Foley RJ, Berger E, Fox O, Levesque EM, Challis PJ, Ivans II, Rhoads JE, Soderberg AM (2010) The Diversity of Massive Star Outbursts I: Observations of SN 2009ip, UGC 2773 OT2009-1, and Their Progenitors. ArXiv e-prints 1002.0635

Fox O, Skrutskie MF, Chevalier RA, Kanneganti S, Park C, Wilson J, Nelson M, Amirhadji J, Crump D, Hoeft A, Provence S, Sargeant B, Sop J, Tea M, Thomas S, Woolard K (2009) Near-Infrared Photometry of the Type IIn SN 2005ip: The Case for Dust Condensation. ApJ 691:650–660, DOI 10.1088/0004-637X/691/1/650, 0807.3555

Fox OD, Chevalier RA, Dwek E, Skrutskie MF, Sugerman BEK, Leisenring JM (2010) Disentangling the Origin and Heating Mechanism of Supernova Dust: Late-Time Spitzer Spectroscopy of the Type IIn SN 2005ip. ArXiv e-prints 1005.4682

Fox OD, Chevalier RA, Skrutskie MF, Soderberg AM, Filippenko AV, Ganeshalingam M, Silverman JM, Smith N, Steele TN (2011) A Spitzer Survey for Dust in Type IIn Supernovae. ArXiv e-prints 1104.5012

Fraser M, Takáts K, Pastorello A, Smartt SJ, Mattila S, Botticella M, Valenti S, Ergon M, Sollerman J, Arcavi I, Benetti S, Bufano F, Crockett RM, Danziger IJ, Gal-Yam A, Maund JR, Taubenberger S, Turatto M (2010) On the Progenitor and Early Evolution of the Type II Supernova 2009kr. ApJ 714:L280–L284, DOI 10.1088/2041-8205/714/2/L280, 0912.2071

Frenklach M, Feigelson ED (1989) Formation of polycyclic aromatic hydrocarbons in circumstellar envelopes. ApJ 341:372–384, DOI 10.1086/167501

Frenklach M, Carmer CS, Feigelson ED (1989) Silicon carbide and the origin of interstellar carbon grains. Nature 339:196–198, DOI 10.1038/339196a0

Freudling W, Corbin MR, Korista KT (2003) Iron Emission in z~6 QSOS. ApJ 587:L67–L70, DOI 10.1086/375338, arXiv:astro-ph/0303424

Fryer CL, Mazzali PA, Prochaska J, Cappellaro E, Panaitescu A, Berger E, van Putten M, van den Heuvel EPJ, Young P, Hungerford A, Rockefeller G, Yoon S, Podsiadlowski P, Nomoto K, Chevalier R, Schmidt B, Kulkarni S (2007) Constraints on Type Ib/c Supernovae and Gamma-Ray Burst Progenitors. PASP 119:1211–1232, DOI 10.1086/523768

Gail H (2003) Formation and Evolution of Minerals in Accretion Disks and Stellar Outflows. In: T K Henning (ed) Astromineralogy, Lecture Notes in Physics, Berlin Springer Verlag, vol 609, pp 55–120

Gail H, Keller R, Sedlmayr E (1984) Dust formation in stellar winds. I - A rapid computational method and application to graphite condensation. A&A 133:320–332

Gail H, Duschl WJ, Ferrarotti AS, Weis K (2005) Dust formation in LBV envelopes. In: R Humphreys & K Stanek (ed) The Fate of the Most Massive Stars, Astronomical Society of the Pacific Conference Series, vol 332, pp 317–+

Gail HP (2010) Formation and Evolution of Minerals in Accretion Disks and Stellar Outflows. In: T Henning (ed) Lecture Notes in Physics, Berlin Springer Verlag, Lecture Notes in Physics, Berlin Springer Verlag, vol 815, pp 61–141, DOI 10.1007/978-3-642-13259-9_2

Gal-Yam A, Leonard DC, Fox DB, Cenko SB, Soderberg AM, Moon D, Sand DJ, Li W, Filippenko AV, Aldering G, Copin Y (2007) On the Progenitor of SN 2005gl and the Nature of Type IIn Supernovae. ApJ 656:372–381, DOI 10.1086/510523, arXiv:astro-ph/0608029

Gal-Yam A, Mazzali P, Ofek EO, Nugent PE, Kulkarni SR, Kasliwal MM, Quimby RM, Filippenko AV, Cenko SB, Chornock R, Waldman R, Kasen D, Sullivan M, Beshore EC,

Drake AJ, Thomas RC, Bloom JS, Poznanski D, Miller AA, Foley RJ, Silverman JM, Arcavi I, Ellis RS, Deng J (2009) Supernova 2007bi as a pair-instability explosion. Nature 462:624–627, DOI 10.1038/nature08579, `1001.1156`

Gall C, Andersen AC, Hjorth J (2011a) Genesis and evolution of dust in galaxies in the early Universe. I. Modelling dust evolution in starburst galaxies. A&A 528:A13+, DOI 10.1051/0004-6361/201015286, `1011.3157`

Gall C, Andersen AC, Hjorth J (2011b) Genesis and evolution of dust in galaxies in the early Universe. II. Rapid dust evolution in quasars at $z \gtrsim 6$. A&A 528:A14+, DOI 10.1051/0004-6361/201015605, `1101.1553`

Gallagher JS III, Hunter DA, Tutukov AV (1984) Star formation histories of irregular galaxies. ApJ 284:544–556, DOI 10.1086/162437

Gallerani S, Maiolino R, Juarez Y, Nagao T, Marconi A, Bianchi S, Schneider R, Mannucci F, Oliva T, Willott CJ, Jiang L, Fan X (2010) The extinction law at high redshift and its implications. ArXiv e-prints `1006.4463`

Gautschy-Loidl R, Höfner S, Jørgensen UG, Hron J (2004) Dynamic model atmospheres of AGB stars. IV. A comparison of synthetic carbon star spectra with observations. A&A 422:289–306, DOI 10.1051/0004-6361:20035860

Gehrz R (1989) Sources of Stardust in the Galaxy. In: L J Allamandola & A G G M Tielens (ed) Interstellar Dust, IAU Symposium, vol 135, pp 445–+

Gomez HL, Dunne L, Ivison RJ, Reynoso EM, Thompson MA, Sibthorpe B, Eales SA, Delaney TM, Maddox S, Isaak K (2009) Accounting for the foreground contribution to the dust emission towards Kepler's supernova remnant. MNRAS 397:1621–1632, DOI 10.1111/j.1365-2966.2009.15061.x, `0905.2564`

Gomez HL, Vlahakis C, Stretch CM, Dunne L, Eales SA, Beelen A, Gomez EL, Edmunds MG (2010) Submillimetre variability of Eta Carinae: cool dust within the outer ejecta. MNRAS 401:L48–L52, DOI 10.1111/j.1745-3933.2009.00784.x, `0911.0176`

Goodrich RW, Stringfellow GS, Penrod GD, Filippenko AV (1989) SN 1961V - an extragalactic ETA Carinae analog. ApJ 342:908–916, DOI 10.1086/167646

Green DA, Tuffs RJ, Popescu CC (2004) Far-infrared and submillimetre observations of the Crab nebula. MNRAS 355:1315–1326, DOI 10.1111/j.1365-2966.2004.08414.x, `arXiv:astro-ph/0409469`

Greggio L (2005) The rates of type Ia supernovae. I. Analytical formulations. A&A 441:1055–1078, DOI 10.1051/0004-6361:20052926, `arXiv:astro-ph/0504376`

Greggio L, Renzini A (1983) The binary model for type I supernovae - Theoretical rates. A&A 118:217–222

Greif TH, Bromm V (2006) Two populations of metal-free stars in the early Universe. MNRAS 373:128–138, DOI 10.1111/j.1365-2966.2006.11017.x, `arXiv:astro-ph/0604367`

Greif TH, Glover SCO, Bromm V, Klessen RS (2010) The First Galaxies: Chemical Enrichment, Mixing, and Star Formation. ArXiv e-prints `1003.0472`

Groenewegen MAT, van der Veen WECJ, Matthews HE (1998a) IRC +10 216 revisited. II. The circumstellar CO shell. A&A 338:491–504, `arXiv:astro-ph/9807201`

Groenewegen MAT, Whitelock PA, Smith CH, Kerschbaum F (1998b) Dust shells around carbon Mira variables. MNRAS 293:18–+, DOI 10.1046/j.1365-8711.1998.01113.x

Groenewegen MAT, Wood PR, Sloan GC, Blommaert JADL, Cioni M, Feast MW, Hony S, Matsuura M, Menzies JW, Olivier EA, Vanhollebeke E, van Loon JT, Whitelock PA, Zijlstra AA, Habing HJ, Lagadec E (2007) Luminosities and mass-loss rates of carbon stars in the Magellanic Clouds. MNRAS 376:313–337, DOI 10.1111/j.1365-2966.2007.11428.x

Habergham SM, Anderson JP, James PA (2010) Type Ibc supernovae in disturbed galaxies: evidence for a top-heavy IMF. ArXiv e-prints `1005.0511`

Hanner M (1988) Grain optical properties. In: M S Hanner (ed) Infrared Observations of Comets Halley and Wilson and Properties of the Grains, pp 22–49

Heger A, Woosley SE (2002) The Nucleosynthetic Signature of Population III. ApJ 567:532–543, DOI 10.1086/338487, `arXiv:astro-ph/0107037`

Heger A, Fryer CL, Woosley SE, Langer N, Hartmann DH (2003) How Massive Single Stars End Their Life. ApJ 591:288–300, DOI 10.1086/375341, `arXiv:astro-ph/0212469`

Helling C, Dehn M, Woitke P, Hauschildt PH (2008) Consistent Simulations of Substellar Atmospheres and Nonequilibrium Dust Cloud Formation. ApJ 675:L105–L108, DOI 10.1086/533462, `0801.3733`

Henning T (ed) (2010a) Astromineralogy, Lecture Notes in Physics, Berlin Springer Verlag, vol 815

Henning T (2010b) Cosmic Silicates. ARA&A 48:21–46, DOI 10.1146/annurev-astro-081309-130815

Henning T, Jäger C, Mutschke H (2004) Laboratory Studies of Carbonaceous Dust Analogs. In: A N Witt, G C Clayton, & B T Draine (ed) Astrophysics of Dust, Astronomical Society of the Pacific Conference Series, vol 309, pp 603–+

Herant M, Benz W (1991) Hydrodynamical instabilities and mixing in SN 1987A - Two-dimensional simulations of the first 3 months. ApJ 370:L81–L84, DOI 10.1086/185982

Herant M, Woosley SE (1994) Postexplosion hydrodynamics of supernovae in red supergiants. ApJ 425:814–828, DOI 10.1086/174026

Herwig F (2004) Evolution and Yields of Extremely Metal-poor Intermediate-Mass Stars. ApJS 155:651–666, DOI 10.1086/425419, `arXiv:astro-ph/0407592`

Hildebrand RH (1983) The Determination of Cloud Masses and Dust Characteristics from Submillimetre Thermal Emission. QJRAS 24:267–+

Hillebrandt W, Niemeyer JC (2000) Type IA Supernova Explosion Models. ARA&A 38:191–230, DOI 10.1146/annurev.astro.38.1.191, `arXiv:astro-ph/0006305`

Hines DC, Rieke GH, Gordon KD, Rho J, Misselt KA, Woodward CE, Werner MW, Krause O, Latter WB, Engelbracht CW, Egami E, Kelly DM, Muzerolle J, Stansberry JA, Su KYL, Morrison JE, Young ET, Noriega-Crespo A, Padgett DL, Gehrz RD, Polomski E, Beeman JW, Haller EE (2004) Imaging of the Supernova Remnant Cassiopeia A with the Multiband Imaging Photometer for Spitzer (MIPS). ApJS 154:290–295, DOI 10.1086/422583

Hines DC, Krause O, Rieke GH, Fan X, Blaylock M, Neugebauer G (2006) Spitzer Observations of High-Redshift QSOs. ApJ 641:L85–L88, DOI 10.1086/504109, `arXiv:astro-ph/0604347`

Hirashita H, Nozawa T, Takeuchi TT, Kozasa T (2008) Extinction curves flattened by reverse shocks in supernovae. MNRAS 384:1725–1732, DOI 10.1111/j.1365-2966.2007.12834.x, `0801.2649`

Hjorth J, Sollerman J, Møller P, Fynbo JPU, Woosley SE, Kouveliotou C, Tanvir NR, Greiner J, Andersen MI, Castro-Tirado AJ, Castro Cerón JM, Fruchter AS, Gorosabel J, Jakobsson P, Kaper L, Klose S, Masetti N, Pedersen H, Pedersen K, Pian E, Palazzi E, Rhoads JE, Rol E, van den Heuvel EPJ, Vreeswijk PM, Watson D, Wijers RAMJ (2003) A very energetic supernova associated with the γ-ray burst of 29 March 2003. Nature 423:847–850, DOI 10.1038/nature01750, `arXiv:astro-ph/0306347`

Hofmeister AM (1997) Infrared reflectance spectra of fayalite, and absorption datafrom assorted olivines, including pressure and isotope effects. Physics and Chemistry of Minerals

24:535–546, DOI 10.1007/s002690050069

Höfner S (2006) Mass Loss: The Role of Grains. In: IAU Joint Discussion, IAU Joint Discussion, vol 11

Höfner S (2008) Winds of M-type AGB stars driven by micron-sized grains. A&A 491:L1–L4, DOI 10.1051/0004-6361:200810641

Höfner S (2009) Dust Formation and Winds around Evolved Stars: The Good, the Bad and the Ugly Cases. In: T Henning, E Grün, & J Steinacker (ed) Astronomical Society of the Pacific Conference Series, Astronomical Society of the Pacific Conference Series, vol 414, pp 3–+, 0903.5280

Höfner S, Andersen AC (2007) Winds of M- and S-type AGB stars: an unorthodox suggestion for the driving mechanism. A&A 465:L39–L42, DOI 10.1051/0004-6361:20066970, arXiv:astro-ph/0702445

Höfner S, Jörgensen UG, Loidl R, Aringer B (1998) Dynamic model atmospheres of AGB stars. I. Atmospheric structure and dynamics. A&A 340:497–507

Höfner S, Gautschy-Loidl R, Aringer B, Jørgensen UG (2003) Dynamic model atmospheres of AGB stars. III. Effects of frequency-dependent radiative transfer. A&A 399:589–601, DOI 10.1051/0004-6361:20021757

Hoyle F, Wickramasinghe NC (1970) Dust in Supernova Explosions. Nature 226:62–63, DOI 10.1038/226062a0

Hughes DH, Dunlop JS, Rawlings S (1997) High-redshift radio galaxies and quasars at submillimetre wavelengths: assessing their evolutionary status. MNRAS 289:766–782, arXiv:astro-ph/9705094

Hunter DJ, Valenti S, Kotak R, Meikle WPS, Taubenberger S, Pastorello A, Benetti S, Stanishev V, Smartt SJ, Trundle C, Arkharov AA, Bufano F, Cappellaro E, di Carlo E, Dolci M, Elias-Rosa N, Frandsen S, Fynbo JU, Hopp U, Larionov VM, Laursen P, Mazzali P, Navasardyan H, Ries C, Riffeser A, Rizzi L, Tsvetkov DY, Turatto M, Wilke S (2009) Extensive optical and near-infrared observations of the nearby, narrow-lined type Ic ¡ASTROBJ¿SN 2007gr¡/ASTROBJ¿: days 5 to 415. A&A 508:371–389, DOI 10.1051/0004-6361/200912896, 0909.3780

Iben I Jr, Renzini A (1981) Physical processes in red giants; Proceedings of the Second Workshop, Advanced School of Astronomy, Erice, Italy, September 3-13, 1980. In: I Iben Jr & A Renzini (ed) Physical Processes in Red Giants, Astrophysics and Space Science Library, vol 88

Iben I Jr, Tutukov AV (1984) Supernovae of type I as end products of the evolution of binaries with components of moderate initial mass (M not greater than about 9 solar masses). ApJS 54:335–372, DOI 10.1086/190932

Inserra C, Turatto M, Pastorello A, Benetti S, Cappellaro E, Pumo ML, Zampieri L, Agnoletto I, Bufano F, Botticella MT, Della Valle M, Elias Rosa N, Iijima T, Spiro S, Valenti S (2011) The Type IIP SN 2007od in UGC 12846: from a bright maximum to dust formation in the nebular phase. ArXiv e-prints 1102.5468

Isaak KG, Priddey RS, McMahon RG, Omont A, Peroux C, Sharp RG, Withington S (2002) The SCUBA Bright Quasar Survey (SBQS): 850-μm observations of the z >~ 4 sample. MNRAS 329:149–162, DOI 10.1046/j.1365-8711.2002.04966.x, arXiv:astro-ph/0109438

Ishihara D, Kaneda H, Furuzawa A, Kunieda H, Suzuki T, Koo B, Lee H, Lee J, Onaka T (2010) Origin of the dust emission from Tycho's SNR. A&A 521:L61+, DOI 10.1051/0004-6361/201015131, 1009.6047

Ivison RJ, Swinbank AM, Swinyard B, Smail I, Pearson CP, Rigopoulou D, Polehampton E, Baluteau J, Barlow MJ, Blain AW, Bock J, Clements DL, Coppin K, Cooray A, Danielson

A, Dwek E, Edge AC, Franceschini A, Fulton T, Glenn J, Griffin M, Isaak K, Leeks S, Lim T, Naylor D, Oliver SJ, Page MJ, Pérez Fournon I, Rowan-Robinson M, Savini G, Scott D, Spencer L, Valtchanov I, Vigroux L, Wright GS (2010) Herschel and SCUBA-2 imaging and spectroscopy of a bright, lensed submillimetre galaxy at z = 2.3. A&A 518:L35+, DOI 10.1051/0004-6361/201014548, 1005.1071

Iwamoto K, Nakamura T, Nomoto K, Mazzali PA, Danziger IJ, Garnavich P, Kirshner R, Jha S, Balam D, Thorstensen J (2000) The Peculiar Type IC Supernova 1997EF: Another Hypernova. ApJ 534:660–669, DOI 10.1086/308761

Jäger C, Molster FJ, Dorschner J, Henning T, Mutschke H, Waters LBFM (1998a) Steps toward interstellar silicate mineralogy. IV. The crystalline revolution. A&A 339:904–916

Jäger C, Mutschke H, Henning T (1998b) Optical properties of carbonaceous dust analogues. A&A 332:291–299

Jäger C, Dorschner J, Mutschke H, Posch T, Henning T (2003) Steps toward interstellar silicate mineralogy. VII. Spectral properties and crystallization behaviour of magnesium silicates produced by the sol-gel method. A&A 408:193–204, DOI 10.1051/0004-6361: 20030916

Jäger C, Huisken F, Mutschke H, Jansa IL, Henning T (2009a) Formation of Polycyclic Aromatic Hydrocarbons and Carbonaceous Solids in Gas-Phase Condensation Experiments. ApJ 696:706–712, DOI 10.1088/0004-637X/696/1/706, 0903.0775

Jäger C, Mutschke H, Henning T, Huisken F (2009b) Analogs of Cosmic Dust. In: T Henning, E Grün, & J Steinacker (ed) Cosmic Dust - Near and Far, Astronomical Society of the Pacific Conference Series, vol 414, pp 319–+

Jäger C, Mutschke H, Henning T, Huisken F (2011) From PAHs to Solid Carbon. In: EAS Publications Series, EAS Publications Series, vol 46, pp 293–304, DOI 10.1051/eas/ 1146031

Johnson JL, Greif TH, Bromm V (2007) Local Radiative Feedback in the Formation of the First Protogalaxies. ApJ 665:85–95, DOI 10.1086/519212, arXiv:astro-ph/0612254

Jones AP (2004) Dust Destruction Processes. In: A N Witt, G C Clayton, & B T Draine (ed) Astrophysics of Dust, Astronomical Society of the Pacific Conference Series, vol 309, pp 347–+

Jones AP, D'Hendecourt LB (2004) Interstellar Nanodiamonds. In: A N Witt, G C Clayton, & B T Draine (ed) Astrophysics of Dust, Astronomical Society of the Pacific Conference Series, vol 309, pp 589–+

Jones AP, Nuth JA (2011) Dust destruction in the ISM: a re-evaluation of dust lifetimes. A&A 530:A44+, DOI 10.1051/0004-6361/201014440

Jones AP, Tielens AGGM, Hollenbach DJ, McKee CF (1994) Grain destruction in shocks in the interstellar medium. ApJ 433:797–810, DOI 10.1086/174689

Juarez Y, Maiolino R, Mujica R, Pedani M, Marinoni S, Nagao T, Marconi A, Oliva E (2009) The metallicity of the most distant quasars. A&A 494:L25–L28, DOI 10.1051/ 0004-6361:200811415, 0901.0974

Justtanont K, Barlow MJ, Skinner CJ, Roche PF, Aitken DK, Smith CH (1996) Mid-infrared spectroscopy of carbon-rich post-AGB objects and detection of the PAH molecule chrysene. A&A 309:612–628

Karakas A, Lattanzio JC (2007) Stellar Models and Yields of Asymptotic Giant Branch Stars. Publications of the Astronomical Society of Australia 24:103–117, DOI 10.1071/ AS07021, 0708.4385

Karakas AI (2010) Updated stellar yields from asymptotic giant branch models. MNRAS 403:1413–1425, DOI 10.1111/j.1365-2966.2009.16198.x, 0912.2142

Karlsson T, Johnson JL, Bromm V (2008) Uncovering the Chemical Signature of the First Stars in the Universe. ApJ 679:6–16, DOI 10.1086/533520, `0709.4025`

Kawabata KS, Tanaka M, Maeda K, Hattori T, Nomoto K, Tominaga N, Yamanaka M (2009) Extremely Luminous Supernova 2006gy at Late Phase: Detection of Optical Emission from Supernova. ApJ 697:747–757, DOI 10.1088/0004-637X/697/1/747, `0902.1440`

Kawara K, Hirashita H, Nozawa T, Kozasa T, Oyabu S, Matsuoka Y, Shimizu T, Sameshima H, Ienaka N (2011) Supernova dust for the extinction law in a young infrared galaxy at z~ 1. MNRAS 412:1070–1080, DOI 10.1111/j.1365-2966.2010.17960.x, `1011.0511`

Kemper F, de Koter A, Waters LBFM, Bouwman J, Tielens AGGM (2002) Dust and the spectral energy distribution of the OH/IR star OH 127.8+0.0: Evidence for circumstellar metallic iron. A&A 384:585–593, DOI 10.1051/0004-6361:20020036, `arXiv:astro-ph/0201128`

Kifonidis K, Plewa T, Janka H, Müller E (2003) Non-spherical core collapse supernovae. I. Neutrino-driven convection, Rayleigh-Taylor instabilities, and the formation and propagation of metal clumps. A&A 408:621–649, DOI 10.1051/0004-6361:20030863, `arXiv:astro-ph/0302239`

Kitaura FS, Janka H, Hillebrandt W (2006) Explosions of O-Ne-Mg cores, the Crab supernova, and subluminous type II-P supernovae. A&A 450:345–350, DOI 10.1051/0004-6361:20054703, `arXiv:astro-ph/0512065`

Knapp GR, Young K, Lee E, Jorissen A (1998) Multiple Molecular Winds in Evolved Stars. I. A Survey of CO (2-1) and CO (3-2) Emission from 45 Nearby AGB Stars. ApJS 117:209–+, DOI 10.1086/313111, `arXiv:astro-ph/9711125`

Kochanek CS, Szczygiel DM, Stanek KZ (2010) The Supernova Impostor Impostor SN 1961V: Spitzer Shows That Zwicky Was Right (Again). ArXiv e-prints `1010.3704`

Koike C, Hasegawa H, Asada N, Hattori T (1981) The extinction coefficients in mid- and far-infrared of silicate and iron-oxide minerals of interest for astronomical observations. Ap&SS 79:77–85, DOI 10.1007/BF00655906

Koike C, Shibai H, Tuchiyama A (1993) Extinction of Olivine and Pyroxene in the Mid Infrared and Far Infrared. MNRAS 264:654–+

Koike C, Kaito C, Yamamoto T, Shibai H, Kimura S, Suto H (1995) Extinction spectra of corundum in the wavelengths from UV to FIR. Icar 114:203–214, DOI 10.1006/icar.1995.1055

Koike C, Tsuchiyama A, Shibai H, Suto H, Tanabé T, Chihara H, Sogawa H, Mouri H, Okada K (2000) Absorption spectra of Mg-rich Mg-Fe and Ca pyroxenes in the mid- and far-infrared regions. A&A 363:1115–1122

Koike C, Chihara H, Tsuchiyama A, Suto H, Sogawa H, Okuda H (2003) Compositional dependence of infrared absorption spectra of crystalline silicate. II. Natural and synthetic olivines. A&A 399:1101–1107, DOI 10.1051/0004-6361:20021831

Koike C, Imai Y, Chihara H, Suto H, Murata K, Tsuchiyama A, Tachibana S, Ohara S (2010) Effects of Forsterite Grain Shape on Infrared Spectra. ApJ 709:983–992, DOI 10.1088/0004-637X/709/2/983

Komatsu E, Smith KM, Dunkley J, Bennett CL, Gold B, Hinshaw G, Jarosik N, Larson D, Nolta MR, Page L, Spergel DN, Halpern M, Hill RS, Kogut A, Limon M, Meyer SS, Odegard N, Tucker GS, Weiland JL, Wollack E, Wright EL (2010) Seven-Year Wilkinson Microwave Anisotropy Probe (WMAP) Observations: Cosmological Interpretation. ArXiv e-prints `1001.4538`

Kotak R (2008) Core-Collapse Supernovae as Dust Producers. In: F Bresolin, P A Crowther, & J Puls (ed) IAU Symposium, IAU Symposium, vol 250, pp 437–442, DOI 10.1017/S1743921308020802

Kotak R, Vink JS (2006) Luminous blue variables as the progenitors of supernovae with quasi-periodic radio modulations. A&A 460:L5–L8, DOI 10.1051/0004-6361:20065800, `arXiv:astro-ph/0610095`

Kotak R, Meikle P, van Dyk SD, Höflich PA, Mattila S (2005) Early-Time Spitzer Observations of the Type II Plateau Supernova SN 2004dj. ApJ 628:L123–L126, DOI 10.1086/432719, `arXiv:astro-ph/0506407`

Kotak R, Meikle WPS, Farrah D, Gerardy CL, Foley RJ, Van Dyk SD, Fransson C, Lundqvist P, Sollerman J, Fesen R, Filippenko AV, Mattila S, Silverman JM, Andersen AC, Höflich PA, Pozzo M, Wheeler JC (2009) Dust and The Type II-Plateau Supernova 2004et. ApJ 704:306–323, DOI 10.1088/0004-637X/704/1/306, `0904.3737`

Kozasa T, Hasegawa H, Nomoto K (1989) Formation of dust grains in the ejecta of SN 1987A. ApJ 344:325–331, DOI 10.1086/167801

Kozasa T, Hasegawa H, Nomoto K (1991) Formation of dust grains in the ejecta of SN 1987A. II. A&A 249:474–482

Kozasa T, Nozawa T, Tominaga N, Umeda H, Maeda K, Nomoto K (2009) Dust in Supernovae; Formation and Evolution. ArXiv e-prints `0903.0217`

Krause O, Birkmann SM, Rieke GH, Lemke D, Klaas U, Hines DC, Gordon KD (2004) No cold dust within the supernova remnant Cassiopeia A. Nature 432:596–598, DOI 10.1038/nature03110, `arXiv:astro-ph/0412092`

Krause O, Birkmann SM, Usuda T, Hattori T, Goto M, Rieke GH, Misselt KA (2008) The Cassiopeia A Supernova Was of Type IIb. Science 320:1195–, DOI 10.1126/science.1155788, `0805.4557`

Kroupa P (2002) The Initial Mass Function of Stars: Evidence for Uniformity in Variable Systems. Science 295:82–91, DOI 10.1126/science.1067524, `arXiv:astro-ph/0201098`

Krumholz MR, Cunningham AJ, Klein RI, McKee CF (2010) Radiation Feedback, Fragmentation, and the Environmental Dependence of the Initial Mass Function. ApJ 713:1120–1133, DOI 10.1088/0004-637X/713/2/1120, `1001.0971`

Lagadec E, Zijlstra AA, Sloan GC, Matsuura M, Wood PR, van Loon JT, Harris GJ, Blommaert JADL, Hony S, Groenewegen MAT, Feast MW, Whitelock PA, Menzies JW, Cioni M (2007) Spitzer spectroscopy of carbon stars in the Small Magellanic Cloud. MNRAS 376:1270–1284, DOI 10.1111/j.1365-2966.2007.11517.x, `arXiv:astro-ph/0611071`

Lagadec E, Zijlstra AA, Sloan GC, Wood PR, Matsuura M, Bernard-Salas J, Blommaert JADL, Cioni M, Feast MW, Groenewegen MAT, Hony S, Menzies JW, van Loon JT, Whitelock PA (2009) Metal-rich carbon stars in the Sagittarius dwarf spheroidal galaxy. MNRAS 396:598–608, DOI 10.1111/j.1365-2966.2009.14736.x, `0903.1045`

Lakicevic M, van Loon JT, Patat F, Staveley-Smith L, Zanardo G (2011) The remnant of SN1987A revealed at (sub-)mm wavelengths. ArXiv e-prints `1107.1323`

Laor A, Draine BT (1993) Spectroscopic constraints on the properties of dust in active galactic nuclei. ApJ 402:441–468, DOI 10.1086/172149

Larson RB (1998) Early star formation and the evolution of the stellar initial mass function in galaxies. MNRAS 301:569–581, DOI 10.1046/j.1365-8711.1998.02045.x, `arXiv:astro-ph/9808145`

Larson RB (2006) Understanding the Stellar Initial Mass Function. In: Revista Mexicana de Astronomia y Astrofisica Conference Series, Revista Mexicana de Astronomia y Astrofisica, vol. 27, vol 26, pp 55–59, `arXiv:astro-ph/0602469`

Lattanzio JC, Wood P (2003) Evolution, Nucleosynthesis, and Pulsation of AGB Stars. In: H J Habing & H Olofsson (ed) Asymptotic giant branch stars, pp 23–104

Ledoux C, Bergeron J, Petitjean P (2002) Dust depletion and abundance pattern in damped Lyalpha systems: A sample of Mn and Ti abundances at z < 2.2. A&A 385:802–815, DOI 10.1051/0004-6361:20020198, `arXiv:astro-ph/0202134`

Lehnert MD, Nesvadba NPH, Cuby J, Swinbank AM, Morris S, Clément B, Evans CJ, Bremer MN, Basa S (2010) Spectroscopic confirmation of a galaxy at redshift z = 8.6. Nature 467:940–942, DOI 10.1038/nature09462, `1010.4312`

Leipski C, Meisenheimer K, Klaas U, Walter F, Nielbock M, Krause O, Dannerbauer H, Bertoldi F, Besel M, de Rosa G, Fan X, Haas M, Hutsemekers D, Jean C, Lemke D, Rix H, Stickel M (2010) Herschel/PACS far-infrared photometry of two z>4 quasars. ArXiv e-prints `1005.5016`

Leitch-Devlin MA, Williams DA (1985) Sticking coefficients for atoms and molecules at the surfaces of interstellar dust grains. MNRAS 213:295–306

Levesque EM, Massey P, Olsen KAG, Plez B, Josselin E, Maeder A, Meynet G (2005) The Effective Temperature Scale of Galactic Red Supergiants: Cool, but Not As Cool As We Thought. ApJ 628:973–985, DOI 10.1086/430901, `arXiv:astro-ph/0504337`

Levesque EM, Massey P, Olsen KAG, Plez B, Meynet G, Maeder A (2006) The Effective Temperatures and Physical Properties of Magellanic Cloud Red Supergiants: The Effects of Metallicity. ApJ 645:1102–1117, DOI 10.1086/504417, `arXiv:astro-ph/0603596`

Li Y, Hernquist L, Robertson B, Cox TJ, Hopkins PF, Springel V, Gao L, Di Matteo T, Zentner AR, Jenkins A, Yoshida N (2007) Formation of z~6 Quasars from Hierarchical Galaxy Mergers. ApJ 665:187–208, DOI 10.1086/519297, `arXiv:astro-ph/0608190`

Liffman K, Clayton DD (1989) Stochastic evolution of refractory interstellar dust during the chemical evolution of a two-phase interstellar medium. ApJ 340:853–868, DOI 10.1086/167440

Livio M (2000) The Progenitors of Type Ia Supernovae. In: J C Niemeyer & J W Truran (ed) Type Ia Supernovae, Theory and Cosmology, pp 33–+, `arXiv:astro-ph/9903264`

Lodders K, Fegley B Jr (1995) The origin of circumstellar silicon carbide grains found in meteorites. Meteoritics 30:661–+

Lucy LB, Danziger IJ, Gouiffes C, Bouchet P (1989) Dust Condensation in the Ejecta of SN 1987 A. In: G Tenorio-Tagle, M Moles, & J Melnick (ed) IAU Colloq. 120: Structure and Dynamics of the Interstellar Medium, Lecture Notes in Physics, Berlin Springer Verlag, vol 350, pp 164–+, DOI 10.1007/BFb0114861

Lucy LB, Danziger IJ, Gouiffes C (1991) Excitation by line coincidence in the spectrum of SN 1987A. A&A 243:223–229

Maguire K, di Carlo E, Smartt SJ, Pastorello A, Tsvetkov DY, Benetti S, Spiro S, Arkharov AA, Beccari G, Botticella MT, Cappellaro E, Cristallo S, Dolci M, Elias-Rosa N, Fiaschi M, Gorshanov D, Harutyunyan A, Larionov VM, Navasardyan H, Pietrinferni A, Raimondo G, di Rico G, Valenti S, Valentini G, Zampieri L (2010) Optical and near-infrared coverage of SN 2004et: physical parameters and comparison with other Type IIP supernovae. MNRAS 404:981–1004, DOI 10.1111/j.1365-2966.2010.16332.x, `0912.3111`

Maio U, Ciardi B, Dolag K, Tornatore L, Khochfar S (2010) The transition from population III to population II-I star formation. MNRAS 407:1003–1015, DOI 10.1111/j.1365-2966.2010.17003.x, `1003.4992`

Maiolino R, Schneider R, Oliva E, Bianchi S, Ferrara A, Mannucci F, Pedani M, Roca Sogorb M (2004) A supernova origin for dust in a high-redshift quasar. Nature 431:533–535, DOI 10.1038/nature02930, `arXiv:astro-ph/0409577`

Maíz-Apellániz J, Bond HE, Siegel MH, Lipkin Y, Maoz D, Ofek EO, Poznanski D (2004) The Progenitor of the Type II-P SN 2004dj in NGC 2403. ApJ 615:L113–L116, DOI

10.1086/426120, `arXiv:astro-ph/0408265`

Maness H, Martins F, Trippe S, Genzel R, Graham JR, Sheehy C, Salaris M, Gillessen S, Alexander T, Paumard T, Ott T, Abuter R, Eisenhauer F (2007) Evidence for a Long-standing Top-heavy Initial Mass Function in the Central Parsec of the Galaxy. ApJ 669:1024–1041, DOI 10.1086/521669, `0707.2382`

Mannucci F, Della Valle M, Panagia N (2006) Two populations of progenitors for Type Ia supernovae? MNRAS 370:773–783, DOI 10.1111/j.1365-2966.2006.10501.x, `arXiv:astro-ph/0510315`

Maoz D (2008) On the fraction of intermediate-mass close binaries that explode as Type Ia supernovae. MNRAS 384:267–277, DOI 10.1111/j.1365-2966.2007.12697.x, `0707.4598`

Marchenko SV (2006) Dust Production in the High-Redshift Universe. In: H J G L M Lamers, N Langer, T Nugis, & K Annuk (ed) Stellar Evolution at Low Metallicity: Mass Loss, Explosions, Cosmology, Astronomical Society of the Pacific Conference Series, vol 353, pp 299–+

Marigo P (2001) Chemical yields from low- and intermediate-mass stars: Model predictions and basic observational constraints. A&A 370:194–217, DOI 10.1051/0004-6361:20000247, `arXiv:astro-ph/0012181`

Massey P, Olsen KAG (2003) The Evolution of Massive Stars. I. Red Supergiants in the Magellanic Clouds. AJ 126:2867–2886, DOI 10.1086/379558, `arXiv:astro-ph/0309272`

Massey P, Plez B, Levesque EM, Olsen KAG, Clayton GC, Josselin E (2005) The Reddening of Red Supergiants: When Smoke Gets in Your Eyes. ApJ 634:1286–1292, DOI 10.1086/497065, `arXiv:astro-ph/0508254`

Mathis JS, Rumpl W, Nordsieck KH (1977) The size distribution of interstellar grains. ApJ 217:425–433, DOI 10.1086/155591

Matsuura M, Zijlstra AA, Bernard-Salas J, Menzies JW, Sloan GC, Whitelock PA, Wood PR, Cioni M, Feast MW, Lagadec E, van Loon JT, Groenewegen MAT, Harris GJ (2007) Spitzer Space Telescope spectral observations of AGB stars in the Fornax dwarf spheroidal galaxy. MNRAS 382:1889–1900, DOI 10.1111/j.1365-2966.2007.12501.x, `0709.3199`

Matsuura M, Barlow MJ, Zijlstra AA, Whitelock PA, Cioni M, Groenewegen MAT, Volk K, Kemper F, Kodama T, Lagadec E, Meixner M, Sloan GC, Srinivasan S (2009) The global gas and dust budget of the Large Magellanic Cloud: AGB stars and supernovae, and the impact on the ISM evolution. MNRAS 396:918–934, DOI 10.1111/j.1365-2966.2009.14743.x, `0903.1123`

Matsuura M, Dwek E, Meixner M, Otsuka M, Babler B, Barlow MJ, Roman-Duval J, Engelbracht C, Sandstrom K, Lakicevic M, van Loon JT, Sonneborn G, Clayton GC, Long KS, Lundqvist P, Nozawa T, Gordon KD, Hony S, Panuzzo P, Okumura K, Misselt KA, Montiel E, Sauvage M (2011) Herschel Detects a Massive Dust Reservoir in Supernova 1987A. ArXiv e-prints `1107.1477`

Matteucci F, Recchi S (2001) On the Typical Timescale for the Chemical Enrichment from Type Ia Supernovae in Galaxies. ApJ 558:351–358, DOI 10.1086/322472, `arXiv:astro-ph/0105074`

Mattila S, Meikle WPS, Lundqvist P, Pastorello A, Kotak R, Eldridge J, Smartt S, Adamson A, Gerardy CL, Rizzi L, Stephens AW, van Dyk SD (2008a) Massive stars exploding in a He-rich circumstellar medium - III. SN 2006jc: infrared echoes from new and old dust in the progenitor CSM. MNRAS 389:141–155, DOI 10.1111/j.1365-2966.2008.13516.x, `0803.2145`

Mattila S, Smartt SJ, Eldridge JJ, Maund JR, Crockett RM, Danziger IJ (2008b) VLT Detection of a Red Supergiant Progenitor of the Type II-P Supernova 2008bk. ApJ 688:L91–L94, DOI 10.1086/595587, 0809.0206

Mattila S, Smartt S, Maund J, Benetti S, Ergon M (2010) The Disappearance of the Red Supergiant Progenitor of Supernova 2008bk. ArXiv e-prints 1011.5494

Mattsson L (2011) Dust in the early Universe: evidence for non-stellar dust production or observational errors? MNRAS 414:781–791, DOI 10.1111/j.1365-2966.2011.18447.x, 1102.0570

Mattsson L, Höfner S (2011) Dust driven mass loss from carbon stars as function of stellar parameters - II. Effects of grain size on wind properties. ArXiv e-prints 1107.1771

Mattsson L, Wahlin R, Höfner S, Eriksson K (2008) Intense mass loss from C-rich AGB stars at low metallicity? A&A 484:L5–L8, DOI 10.1051/0004-6361:200809689, 0804.2482

Maund JR, Smartt SJ (2009) The Disappearance of the Progenitors of Supernovae 1993J and 2003gd. Science 324:486–, DOI 10.1126/science.1170198, 0903.3772

Maund JR, Smartt SJ, Kudritzki RP, Podsiadlowski P, Gilmore GF (2004) The massive binary companion star to the progenitor of supernova 1993J. Nature 427:129–131, arXiv:astro-ph/0401090

Maund JR, Smartt SJ, Schweizer F (2005) Luminosity and Mass Limits for the Progenitor of the Type Ic Supernova 2004gt in NGC 4038. ApJ 630:L33–L36, DOI 10.1086/491620, arXiv:astro-ph/0506436

Maund JR, Smartt SJ, Kudritzki R, Pastorello A, Nelemans G, Bresolin F, Patat F, Gilmore GF, Benn CR (2006) Faint supernovae and supernova impostors: case studies of SN 2002kg/NGC 2403-V37 and SN 2003gm. MNRAS 369:390–406, DOI 10.1111/j.1365-2966.2006.10308.x, arXiv:astro-ph/0603056

Maund JR, Fraser M, Ergon M, Pastorello A, Smartt SJ, Sollerman J, Benetti S, Botticella M, Bufano F, Danziger IJ, Kotak R, Magill L, Stephens AW, Valenti S (2011) The Yellow Supergiant Progenitor of the Type II Supernova 2011dh in M51. ArXiv e-prints 1106.2565

Mazzali PA, Deng J, Hamuy M, Nomoto K (2009) SN 2003bg: A Broad-Lined Type IIb Supernova with Hydrogen. ApJ 703:1624–1634, DOI 10.1088/0004-637X/703/2/1624, 0908.1773

McDonald I, van Loon JT, Decin L, Boyer ML, Dupree AK, Evans A, Gehrz RD, Woodward CE (2009) Giants in the globular cluster ω Centauri: dust production, mass-loss and distance. MNRAS 394:831–856, DOI 10.1111/j.1365-2966.2008.14370.x, 0812.0326

McDonald I, Boyer ML, van Loon JT, Zijlstra AA, Hora JL, Babler B, Block M, Gordon K, Meade M, Meixner M, Misselt K, Robitaille T, Sewiło M, Shiao B, Whitney B (2011) Fundamental Parameters, Integrated Red Giant Branch Mass Loss, and Dust Production in the Galactic Globular Cluster 47 Tucanae. ApJS 193:23–+, DOI 10.1088/0067-0049/193/2/23, 1101.1095

McKee C (1989) Dust Destruction in the Interstellar Medium. In: L J Allamandola & A G G M Tielens (ed) Interstellar Dust, IAU Symposium, vol 135, pp 431–+

McKee CF, Tan JC (2008) The Formation of the First Stars. II. Radiative Feedback Processes and Implications for the Initial Mass Function. ApJ 681:771–797, DOI 10.1086/587434, 0711.1377

Meikle P, Kotak R, Farrah D, Mattila S, van Dyk SD, Andersen AC, Fesen R, Filippenko AV, Foley RJ, Fransson C, Gerardy CL, Höflich PA, Lundqvist P, Pozzo M, Sollerman J, Wheeler JC (2011) Dust and the type II-Plateau supernova 2004dj. ArXiv e-prints 1103.2885

Meikle WPS, Mattila S, Pastorello A, Gerardy CL, Kotak R, Sollerman J, Van Dyk SD, Farrah D, Filippenko AV, Höflich P, Lundqvist P, Pozzo M, Wheeler JC (2007) A Spitzer Space Telescope Study of SN 2003gd: Still No Direct Evidence that Core-Collapse Supernovae are Major Dust Factories. ApJ 665:608–617, DOI 10.1086/519733, 0705.1439

Mennella V, Baratta GA, Colangeli L, Palumbo P, Rotundi A, Bussoletti E, Strazzulla G (1997) Ultraviolet Spectral Changes in Amorphous Carbon Grains Induced by Ion Irradiation. ApJ 481:545–+, DOI 10.1086/304035

Meynet G, Maeder A (2003) Stellar evolution with rotation. X. Wolf-Rayet star populations at solar metallicity. A&A 404:975–990, DOI 10.1051/0004-6361:20030512, arXiv:astro-ph/0304069

Michałowski MJ, Murphy EJ, Hjorth J, Watson D, Gall C, Dunlop JS (2010a) Dust grain growth in the interstellar medium of 5<z<6.5 quasars. ArXiv e-prints 1006.5466

Michałowski MJ, Watson D, Hjorth J (2010b) Rapid Dust Production in Submillimeter Galaxies at z > 4? ApJ 712:942–950, DOI 10.1088/0004-637X/712/2/942, 1002.2636

Miller AA, Smith N, Li W, Bloom JS, Chornock R, Filippenko AV, Prochaska JX (2010) New Observations of the Very Luminous Supernova 2006gy: Evidence for Echoes. AJ 139:2218–2229, DOI 10.1088/0004-6256/139/6/2218, 0906.2201

Molster F, Kemper C (2005) Crystalline Silicates. Space Science Reviews 119:3–28, DOI 10.1007/s11214-005-8066-x

Molster FJ, Waters LBFM (2003) The Mineralogy of Interstellar and Circumstellar Dust. In: T K Henning (ed) Astromineralogy, Lecture Notes in Physics, Berlin Springer Verlag, vol 609, pp 121–170

Molster FJ, Waters LBFM, Tielens AGGM (2002a) Crystalline silicate dust around evolved stars. II. The crystalline silicate complexes. A&A 382:222–240, DOI 10.1051/0004-6361:20011551, arXiv:astro-ph/0201304

Molster FJ, Waters LBFM, Tielens AGGM, Barlow MJ (2002b) Crystalline silicate dust around evolved stars. I. The sample stars. A&A 382:184–221, DOI 10.1051/0004-6361:20011550, arXiv:astro-ph/0201303

Molster FJ, Waters LBFM, Tielens AGGM, Koike C, Chihara H (2002c) Crystalline silicate dust around evolved stars. III. A correlations study of crystalline silicate features. A&A 382:241–255, DOI 10.1051/0004-6361:20011552, arXiv:astro-ph/0201305

Morgan HL, Edmunds MG (2003) Dust formation in early galaxies. MNRAS 343:427–442, DOI 10.1046/j.1365-8711.2003.06681.x, arXiv:astro-ph/0302566

Morgan HL, Dunne L, Eales SA, Ivison RJ, Edmunds MG (2003) Cold Dust in Kepler's Supernova Remnant. ApJ 597:L33–L36, DOI 10.1086/379639, arXiv:astro-ph/0309233

Moriya T, Tominaga N, Tanaka M, Maeda K, Nomoto K (2010) A Core-collapse Supernova Model for the Extremely Luminous Type Ic Supernova 2007bi: An Alternative to the Pair-instability Supernova Model. ApJ 717:L83–L86, DOI 10.1088/2041-8205/717/2/L83, 1004.2967

Mortlock DJ, Warren SJ, Venemans BP, Patel M, Hewett PC, McMahon RG, Simpson C, Theuns T, Gonzáles-Solares EA, Adamson A, Dye S, Hambly NC, Hirst P, Irwin MJ, Kuiper E, Lawrence A, Röttgering HJA (2011) A luminous quasar at a redshift of z = 7.085. Nature 474:616–619, DOI 10.1038/nature10159, 1106.6088

Murray SD, Lin DNC (1996) Coalescence, Star Formation, and the Cluster Initial Mass Function. ApJ 467:728–+, DOI 10.1086/177648

Mutschke H, Andersen AC, Clément D, Henning T, Peiter G (1999) Infrared properties of SiC particles. A&A 345:187–202, arXiv:astro-ph/9903031

Nagashima M, Lacey CG, Baugh CM, Frenk CS, Cole S (2005) The metal enrichment of the

intracluster medium in hierarchical galaxy formation models. MNRAS 358:1247–1266, DOI 10.1111/j.1365-2966.2005.08766.x, `arXiv:astro-ph/0408529`

Nakano S, Itagaki K, Puckett T, Gorelli R (2006) Possible Supernova in UGC 4904. Central Bureau Electronic Telegrams 666:1–+

Nath BB, Laskar T, Shull JM (2008) Dust Sputtering by Reverse Shocks in Supernova Remnants. ApJ 682:1055–1064, DOI 10.1086/589224, `0804.3472`

Nomoto K (1984) Evolution of 8-10 solar mass stars toward electron capture supernovae. I - Formation of electron-degenerate O + NE + MG cores. ApJ 277:791–805, DOI 10.1086/161749

Nomoto K (1987) Evolution of 8-10 solar mass stars toward electron capture supernovae. II - Collapse of an O + NE + MG core. ApJ 322:206–214, DOI 10.1086/165716

Nomoto K, Sugimoto D, Sparks WM, Fesen RA, Gull TR, Miyaji S (1982) The Crab Nebula's progenitor. Nature 299:803–805, DOI 10.1038/299803a0

Nomoto K, Tominaga N, Umeda H, Kobayashi C, Maeda K (2006) Nucleosynthesis yields of core-collapse supernovae and hypernovae, and galactic chemical evolution. Nuclear Physics A 777:424–458, DOI 10.1016/j.nuclphysa.2006.05.008, `arXiv:astro-ph/0605725`

Nomoto KI, Iwamoto K, Suzuki T (1995) The evolution and explosion of massive binary stars and Type Ib-Ic-IIb-IIL supernovae. Phys. Rep. 256:173–191, DOI 10.1016/0370-1573(94)00107-E

Norman ML (2010) Pop III Stellar Masses and IMF. In: D J Whalen, V Bromm, & N Yoshida (ed) American Institute of Physics Conference Series, American Institute of Physics Conference Series, vol 1294, pp 17–27, DOI 10.1063/1.3518848, `1011.4624`

Nowotny W, Lebzelter T, Hron J, Höfner S (2005) Atmospheric dynamics in carbon-rich Miras. II. Models meet observations. A&A 437:285–296, DOI 10.1051/0004-6361:20042572, `arXiv:astro-ph/0503653`

Nowotny W, Höfner S, Aringer B (2010) Line formation in AGB atmospheres including velocity effects. Molecular line profile variations of long period variables. A&A 514:A35+, DOI 10.1051/0004-6361/200911899, `1002.1849`

Nozawa T, Kozasa T, Umeda H, Maeda K, Nomoto K (2003) Dust in the Early Universe: Dust Formation in the Ejecta of Population III Supernovae. ApJ 598:785–803, DOI 10.1086/379011, `arXiv:astro-ph/0307108`

Nozawa T, Kozasa T, Habe A, Dwek E, Umeda H, Tominaga N, Maeda K, Nomoto K (2007) Evolution of Dust in Primordial Supernova Remnants: Can Dust Grains Formed in the Ejecta Survive and Be Injected into the Early Interstellar Medium? ApJ 666:955–966, DOI 10.1086/520621, `0706.0383`

Nozawa T, Kozasa T, Tominaga N, Maeda K, Umeda H, Nomoto K, Krause O (2010) Formation and Evolution of Dust in Type IIb Supernovae with Application to the Cassiopeia A Supernova Remnant. ApJ 713:356–373, DOI 10.1088/0004-637X/713/1/356, `0909.4145`

Nozawa T, Maeda K, Kozasa T, Tanaka M, Nomoto K, Umeda H (2011) Formation of Dust in the Ejecta of Type Ia Supernovae. ArXiv e-prints `1105.0973`

Ofek EO, Cameron PB, Kasliwal MM, Gal-Yam A, Rau A, Kulkarni SR, Frail DA, Chandra P, Cenko SB, Soderberg AM, Immler S (2007) SN 2006gy: An Extremely Luminous Supernova in the Galaxy NGC 1260. ApJ 659:L13–L16, DOI 10.1086/516749, `arXiv:astro-ph/0612408`

Olofsson H (1996) Circumstellar Molecular Envelopes of AGB and Post-AGB Objects. Ap&SS 245:169–200, DOI 10.1007/BF00642225

Olofsson H (1997) Molecules in Envelopes Around AGB-Stars. Ap&SS 251:31–39, DOI

10.1023/A:1000747630702

Omont A, Cox P, Bertoldi F, McMahon RG, Carilli C, Isaak KG (2001) A 1.2 mm MAMBO/IRAM-30 m survey of dust emission from the highest red-shift PSS quasars. A&A 374:371–381, DOI 10.1051/0004-6361:20010721, `arXiv:astro-ph/0107005`

Omont A, Beelen A, Bertoldi F, Cox P, Carilli CL, Priddey RS, McMahon RG, Isaak KG (2003) A 1.2 mm MAMBO/IRAM-30 m study of dust emission from optically luminous z ˜ 2 quasars. A&A 398:857–865, DOI 10.1051/0004-6361:20021652, `arXiv:astro-ph/0211655`

Origlia L, Rood RT, Fabbri S, Ferraro FR, Fusi Pecci F, Rich RM (2007) The First Empirical Mass-Loss Law for Population II Giants. ApJ 667:L85–L88, DOI 10.1086/521980, `0709.3271`

Origlia L, Rood RT, Fabbri S, Ferraro FR, Fusi Pecci F, Rich RM, Dalessandro E (2010) Dust is Forming Along the Red Giant Branch of 47 Tuc. ApJ 718:522–526, DOI 10.1088/0004-637X/718/1/522, `1005.4618`

Orofino V, Blanco A, Mennella V, Bussoletti E, Colangeli L, Fonti S (1991) Experimental extinction properties of granular mixtures of silicon carbide and amorphous carbon. A&A 252:315–319

O'Shea BW, Norman ML (2007) Population III Star Formation in a ΛCDM Universe. I. The Effect of Formation Redshift and Environment on Protostellar Accretion Rate. ApJ 654:66–92, DOI 10.1086/509250, `arXiv:astro-ph/0607013`

Ossenkopf V, Henning T, Mathis JS (1992) Constraints on cosmic silicates. A&A 261:567–578

Pakmor R, Kromer M, Röpke FK, Sim SA, Ruiter AJ, Hillebrandt W (2010) Sub-luminous type Ia supernovae from the mergers of equal-mass white dwarfs with mass ˜0.9M$_{solar}$. Nature 463:61–64, DOI 10.1038/nature08642, `0911.0926`

Palik ED (1985) Handbook of optical constants of solids. Academic Press Handbook Series, New York: Academic Press, 1985, edited by Palik, Edward D.

Pascoli G, Polleux A (2000) Condensation and growth of hydrogenated carbon clusters in carbon-rich stars. A&A 359:799–810

Pastorello A, Zampieri L, Turatto M, Cappellaro E, Meikle WPS, Benetti S, Branch D, Baron E, Patat F, Armstrong M, Altavilla G, Salvo M, Riello M (2004) Low-luminosity Type II supernovae: spectroscopic and photometric evolution. MNRAS 347:74–94, DOI 10.1111/j.1365-2966.2004.07173.x, `arXiv:astro-ph/0309264`

Pastorello A, Sauer D, Taubenberger S, Mazzali PA, Nomoto K, Kawabata KS, Benetti S, Elias-Rosa N, Harutyunyan A, Navasardyan H, Zampieri L, Iijima T, Botticella MT, di Rico G, Del Principe M, Dolci M, Gagliardi S, Ragni M, Valentini G (2006) SN 2005cs in M51 - I. The first month of evolution of a subluminous SN II plateau. MNRAS 370:1752–1762, DOI 10.1111/j.1365-2966.2006.10587.x, `arXiv:astro-ph/0605700`

Pastorello A, Smartt SJ, Mattila S, Eldridge JJ, Young D, Itagaki K, Yamaoka H, Navasardyan H, Valenti S, Patat F, Agnoletto I, Augusteijn T, Benetti S, Cappellaro E, Boles T, Bonnet-Bidaud J, Botticella MT, Bufano F, Cao C, Deng J, Dennefeld M, Elias-Rosa N, Harutyunyan A, Keenan FP, Iijima T, Lorenzi V, Mazzali PA, Meng X, Nakano S, Nielsen TB, Smoker JV, Stanishev V, Turatto M, Xu D, Zampieri L (2007) A giant outburst two years before the core-collapse of a massive star. Nature 447:829–832, DOI 10.1038/nature05825, `arXiv:astro-ph/0703663`

Pastorello A, Kasliwal MM, Crockett RM, Valenti S, Arbour R, Itagaki K, Kaspi S, Gal-Yam A, Smartt SJ, Griffith R, Maguire K, Ofek EO, Seymour N, Stern D, Wiethoff W (2008) The Type IIb SN 2008ax: spectral and light curve evolution. MNRAS 389:955–

966, DOI 10.1111/j.1365-2966.2008.13618.x, `0805.1914`

Patat F, Taubenberger S, Benetti S, Pastorello A, Harutyunyan A (2011) Asymmetries in the type IIn SN 2010jl. A&A 527:L6+, DOI 10.1051/0004-6361/201016217, `1011.5926`

Pei YC, Fall SM, Bechtold J (1991) Confirmation of dust in damped Lyman-alpha systems. ApJ 378:6–16, DOI 10.1086/170401

Perley DA, Bloom JS, Klein CR, Covino S, Minezaki T, Woźniak P, Vestrand WT, Williams GG, Milne P, Butler NR, Updike AC, Krühler T, Afonso P, Antonelli A, Cowie L, Ferrero P, Greiner J, Hartmann DH, Kakazu Y, Küpcü Yoldaş A, Morgan AN, Price PA, Prochaska JX, Yoshii Y (2010) Evidence for supernova-synthesized dust from the rising afterglow of GRB071025 at z ~ 5. MNRAS 406:2473–2487, DOI 10.1111/j.1365-2966.2010.16772.x

Pettini M, Smith LJ, Hunstead RW, King DL (1994) Metal enrichment, dust, and star formation in galaxies at high redshifts. 3: Zn and CR abundances for 17 damped Lyman-alpha systems. ApJ 426:79–96, DOI 10.1086/174041

Piovan L, Chiosi C, Merlin E, Grassi T, Tantalo R, Buonomo U, Cassarà LP (2011a) Formation and Evolution of the Dust in Galaxies. II. The Solar Neighbourhood. ArXiv e-prints `1107.4561`

Piovan L, Chiosi C, Merlin E, Grassi T, Tantalo R, Buonomo U, Cassarà LP (2011b) Formation and Evolution of the Dust in Galaxies. III. The Disk of the Milky Way. ArXiv e-prints `1107.4567`

Pipino A, Fan XL, Matteucci F, Calura F, Silva L, Granato G, Maiolino R (2011) The chemical evolution of elliptical galaxies with stellar and QSO dust production. A&A 525:A61+, DOI 10.1051/0004-6361/201014843, `1008.3875`

Pitman KM, Hofmeister AM (2006) Thin Film Absorbance Spectra of Forsterite and Fayalite Dust Grains. In: S Mackwell & E Stansbery (ed) 37th Annual Lunar and Planetary Science Conference, Lunar and Planetary Institute Science Conference Abstracts, vol 37, pp 1338–+

Pitman KM, Dijkstra C, Hofmeister AM, Speck AK (2010) IR absorbance spectra of olivine (Pitman+, 2010). VizieR Online Data Catalog 740:60,460–+

Poelarends AJT, Herwig F, Langer N, Heger A (2008) The Supernova Channel of Super-AGB Stars. ApJ 675:614–625, DOI 10.1086/520872, `0705.4643`

Posch T, Baier A, Mutschke H, Henning T (2007) Carbonates in Space: The Challenge of Low-Temperature Data. ApJ 668:993–1000, DOI 10.1086/521390, `0706.3963`

Pozzo M, Meikle WPS, Fassia A, Geballe T, Lundqvist P, Chugai NN, Sollerman J (2004) On the source of the late-time infrared luminosity of SN 1998S and other Type II supernovae. MNRAS 352:457–477, DOI 10.1111/j.1365-2966.2004.07951.x, `arXiv:astro-ph/0404533`

Pozzo M, Meikle WPS, Rayner JT, Joseph RD, Filippenko AV, Foley RJ, Li W, Mattila S, Sollerman J (2006) Optical and infrared observations of the TypeIIP SN2002hh from days 3 to 397. MNRAS 368:1169–1195, DOI 10.1111/j.1365-2966.2006.10204.x, `arXiv:astro-ph/0602372`

Priddey RS, McMahon RG (2001) The far-infrared-submillimetre spectral energy distribution of high-redshift quasars. MNRAS 324:L17–L22, DOI 10.1046/j.1365-8711.2001.04548.x, `arXiv:astro-ph/0102116`

Priddey RS, Isaak KG, McMahon RG, Robson EI, Pearson CP (2003) Quasars as probes of the submillimetre cosmos at z > 5 - I. Preliminary SCUBA photometry. MNRAS 344:L74–L78, DOI 10.1046/j.1365-8711.2003.07076.x, `arXiv:astro-ph/0308132`

Prieto JL, Kistler MD, Thompson TA, Yüksel H, Kochanek CS, Stanek KZ, Beacom JF, Martini P, Pasquali A, Bechtold J (2008) Discovery of the Dust-Enshrouded Progenitor

of SN 2008S with Spitzer. ApJ 681:L9–L12, DOI 10.1086/589922, 0803.0324

Puls J, Vink JS, Najarro F (2008) Mass loss from hot massive stars. A&A Rev. 16:209–325, DOI 10.1007/s00159-008-0015-8, 0811.0487

Raiteri CM, Villata M, Navarro JF (1996) Simulations of Galactic chemical evolution. I. O and Fe abundances in a simple collapse model. A&A 315:105–115

Ramstedt S, Schöier FL, Olofsson H, Lundgren AA (2008) On the reliability of mass-loss-rate estimates for AGB stars. A&A 487:645–657, DOI 10.1051/0004-6361:20078876, 0806.0517

Ramstedt S, Schöier FL, Olofsson H (2009) Circumstellar molecular line emission from S-type AGB stars: mass-loss rates and SiO abundances. A&A 499:515–527, DOI 10.1051/0004-6361/200911730, 0903.1672

Renzini A, Voli M (1981) Advanced evolutionary stages of intermediate-mass stars. I - Evolution of surface compositions. A&A 94:175–193

Reynolds SP (1985) An evolutionary history for the Crablike, pulsar-powered supernova remnant 0540-69.3. ApJ 291:152–155, DOI 10.1086/163050

Reynolds SP, Borkowski KJ, Hwang U, Hughes JP, Badenes C, Laming JM, Blondin JM (2007) A Deep Chandra Observation of Kepler's Supernova Remnant: A Type Ia Event with Circumstellar Interaction. ApJ 668:L135–L138, DOI 10.1086/522830, 0708.3858

Rho J, Kozasa T, Reach WT, Smith JD, Rudnick L, DeLaney T, Ennis JA, Gomez H, Tappe A (2008) Freshly Formed Dust in the Cassiopeia A Supernova Remnant as Revealed by the Spitzer Space Telescope. ApJ 673:271–282, DOI 10.1086/523835, 0709.2880

Rho J, Reach WT, Tappe A, Hwang U, Slavin JD, Kozasa T, Dunne L (2009) Spitzer Observations of the Young Core-Collapse Supernova Remnant 1E0102-72.3: Infrared Ejecta Emission and Dust Formation. ApJ 700:579–596, DOI 10.1088/0004-637X/700/1/579

Riechers DA, Walter F, Bertoldi F, Carilli CL, Aravena M, Neri R, Cox P, Weiß A, Menten KM (2009) Imaging Atomic and Highly Excited Molecular Gas in a $z = 6.42$ Quasar Host Galaxy: Copious Fuel for an Eddington-limited Starburst at the End of Cosmic Reionization. ApJ 703:1338–1345, DOI 10.1088/0004-637X/703/2/1338, 0908.0018

Rieke GH, Loken K, Rieke MJ, Tamblyn P (1993) Starburst modeling of M82 - Test case for a biased initial mass function. ApJ 412:99–110, DOI 10.1086/172904

Robson I, Priddey RS, Isaak KG, McMahon RG (2004) Submillimetre observations of $z > 6$ quasars. MNRAS 351:L29–L33, DOI 10.1111/j.1365-2966.2004.07923.x, arXiv:astro-ph/0405177

Rouleau F, Martin PG (1991) Shape and clustering effects on the optical properties of amorphous carbon. ApJ 377:526–540, DOI 10.1086/170382

Ryder SD, Murrowood CE, Stathakis RA (2006) A post-mortem investigation of the Type IIb supernova 2001ig. MNRAS 369:L32–L36, DOI 10.1111/j.1745-3933.2006.00168.x, arXiv:astro-ph/0603336

Sahu DK, Anupama GC, Srividya S, Muneer S (2006) Photometric and spectroscopic evolution of the Type IIP supernova SN 2004et. MNRAS 372:1315–1324, DOI 10.1111/j.1365-2966.2006.10937.x, arXiv:astro-ph/0608432

Sakon I, Onaka T, Wada T, Ohyama Y, Kaneda H, Ishihara D, Tanabé T, Minezaki T, Yoshii Y, Tominaga N, Nomoto K, Nozawa T, Kozasa T, Tanaka M, Suzuki T, Umeda H, Ohyabu S, Usui F, Matsuhara H, Nakagawa T, Murakami H (2009) Properties of Newly Formed Dust by SN 2006JC Based on Near- to Mid-Infrared Observation With AKARI. ApJ 692:546–555, DOI 10.1088/0004-637X/692/1/546, 0711.4801

Salpeter EE (1955) The Luminosity Function and Stellar Evolution. ApJ 121:161–+, DOI 10.1086/145971

Salvaterra R, Della Valle M, Campana S, Chincarini G, Covino S, D'Avanzo P, Fernández-

Soto A, Guidorzi C, Mannucci F, Margutti R, Thöne CC, Antonelli LA, Barthelmy SD, de Pasquale M, D'Elia V, Fiore F, Fugazza D, Hunt LK, Maiorano E, Marinoni S, Marshall FE, Molinari E, Nousek J, Pian E, Racusin JL, Stella L, Amati L, Andreuzzi G, Cusumano G, Fenimore EE, Ferrero P, Giommi P, Guetta D, Holland ST, Hurley K, Israel GL, Mao J, Markwardt CB, Masetti N, Pagani C, Palazzi E, Palmer DM, Piranomonte S, Tagliaferri G, Testa V (2009) GRB090423 at a redshift of z˜8.1. Nature 461:1258–1260, DOI 10.1038/nature08445, 0906.1578

Sandstrom K, Bolatto A, Leroy A, Stanimirovic S, Simon JD, Staveley-Smith L, Shah R (2008) The Far-IR Radio Continuum Correlation in the Small Magellanic Cloud. In: R-R Chary, H I Teplitz, & K Sheth (ed) Infrared Diagnostics of Galaxy Evolution, Astronomical Society of the Pacific Conference Series, vol 381, pp 268–+

Scalo J (1998) The IMF Revisited: A Case for Variations. In: G Gilmore & D Howell (ed) The Stellar Initial Mass Function (38th Herstmonceux Conference), Astronomical Society of the Pacific Conference Series, vol 142, pp 201–+, arXiv:astro-ph/9712317

Scalo J (2005) Fifty years of IMF variation: the intermediate-mass stars. In: E Corbelli, F Palla, & H Zinnecker (ed) The Initial Mass Function 50 Years Later, Astrophysics and Space Science Library, vol 327, pp 23–+, arXiv:astro-ph/0412543

Scalo JM (1986) The stellar initial mass function. FCPh 11:1–278

Schaerer D, Meynet G, Maeder A, Schaller G (1993) Grids of stellar models. II - From 0.8 to 120 solar masses at Z = 0.008. A&AS 98:523–527

Schaller G, Schaerer D, Meynet G, Maeder A (1992) New grids of stellar models from 0.8 to 120 solar masses at Z = 0.020 and Z = 0.001. A&AS 96:269–331

Schneider R, Ferrara A, Salvaterra R (2004) Dust formation in very massive primordial supernovae. MNRAS 351:1379–1386, DOI 10.1111/j.1365-2966.2004.07876.x, arXiv:astro-ph/0307087

Schneider R, Omukai K, Inoue AK, Ferrara A (2006) Fragmentation of star-forming clouds enriched with the first dust. MNRAS 369:1437–1444, DOI 10.1111/j.1365-2966.2006.10391.x, arXiv:astro-ph/0603766

Schöier FL, Olofsson H (2001) Models of circumstellar molecular radio line emission. Mass loss rates for a sample of bright carbon stars. A&A 368:969–993, DOI 10.1051/0004-6361:20010072, arXiv:astro-ph/0101477

Schwartz PR (1982) The spectral dependence of dust emissivity at millimeter wavelengths. ApJ 252:589–593, DOI 10.1086/159585

Schwarzschild M, Spitzer L (1953) On the evolution of stars and chemical elements in the early phases of a galaxy. The Observatory 73:77–79

Scoville N, Young JS (1983) The molecular gas distribution in M51. ApJ 265:148–+, DOI 10.1086/160660

Sedlmayr E (1994) From Molecules to Grains. In: U G Jorgensen (ed) IAU Colloq. 146: Molecules in the Stellar Environment, Lecture Notes in Physics, Berlin Springer Verlag, vol 428, pp 163–+, DOI 10.1007/3-540-57747-5_42

Sharp CM, Wasserburg GJ (1995) Molecular equilibria and condensation temperatures in carbon-rich gases. GeCoA 59:1633–1652, DOI 10.1016/0016-7037(95)00069-C

Shigeyama T, Nomoto K (1990) Theoretical light curve of SN 1987A and mixing of hydrogen and nickel in the ejecta. ApJ 360:242–256, DOI 10.1086/169114

Sibthorpe B, Ade PAR, Bock JJ, Chapin EL, Devlin MJ, Dicker S, Griffin M, Gundersen JO, Halpern M, Hargrave PC, Hughes DH, Jeong W, Kaneda H, Klein J, Koo B, Lee H, Marsden G, Martin PG, Mauskopf P, Moon D, Netterfield CB, Olmi L, Pascale E, Patanchon G, Rex M, Roy A, Scott D, Semisch C, Truch MDP, Tucker C, Tucker GS, Viero MP, Wiebe DV (2009) AKARI and BLAST Observations of the Cassiopeia A Supernova

Remnant and Surrounding Interstellar Medium. ArXiv e-prints 0910.1094

Siess L (2007) Evolution of massive AGB stars. II. model properties at non-solar metallicity and the fate of Super-AGB stars. A&A 476:893–909, DOI 10.1051/0004-6361:20078132

Siess L (2008) The most massive AGB stars. In: L Deng & K L Chan (ed) IAU Symposium, IAU Symposium, vol 252, pp 297–307, DOI 10.1017/S1743921308023077

Silvia DW, Smith BD, Shull JM (2010) Numerical Simulations of Supernova Dust Destruction. I. Cloud-crushing and Post-processed Grain Sputtering. ApJ 715:1575–1590, DOI 10.1088/0004-637X/715/2/1575, 1001.4793

Sloan GC, Kraemer KE, Wood PR, Zijlstra AA, Bernard-Salas J, Devost D, Houck JR (2008) The Magellanic Zoo: Mid-Infrared Spitzer Spectroscopy of Evolved Stars and Circumstellar Dust in the Magellanic Clouds. ApJ 686:1056–1081, DOI 10.1086/591437, 0807.2998

Sloan GC, Matsuura M, Zijlstra AA, Lagadec E, Groenewegen MAT, Wood PR, Szyszka C, Bernard-Salas J, van Loon JT (2009) Dust Formation in a Galaxy with Primitive Abundances. Science 323:353–, DOI 10.1126/science.1165626

Smartt SJ (2009) Progenitors of Core-Collapse Supernovae. ARA&A 47:63–106, DOI 10.1146/annurev-astro-082708-101737, 0908.0700

Smartt SJ, Maund JR, Hendry MA, Tout CA, Gilmore GF, Mattila S, Benn CR (2004) Detection of a Red Supergiant Progenitor Star of a Type II-Plateau Supernova. Science 303:499–503, DOI 10.1126/science.1092967, arXiv:astro-ph/0401235

Smartt SJ, Eldridge JJ, Crockett RM, Maund JR (2009) The death of massive stars - I. Observational constraints on the progenitors of Type II-P supernovae. MNRAS 395:1409–1437, DOI 10.1111/j.1365-2966.2009.14506.x, 0809.0403

Smith LJ, Gallagher JS (2001) M82-F: a doomed super star cluster? MNRAS 326:1027–1040, DOI 10.1046/j.1365-8711.2001.04627.x, arXiv:astro-ph/0104429

Smith N, Owocki SP (2006) On the Role of Continuum-driven Eruptions in the Evolution of Very Massive Stars and Population III Stars. ApJ 645:L45–L48, DOI 10.1086/506523, arXiv:astro-ph/0606174

Smith N, Humphreys RM, Gehrz RD (2001) Post-Eruption Detection of Variable 12 in NGC 2403 (SN 1954j): Another η Carinae Variable. PASP 113:692–696, DOI 10.1086/320812

Smith N, Gehrz RD, Hinz PM, Hoffmann WF, Hora JL, Mamajek EE, Meyer MR (2003) Mass and Kinetic Energy of the Homunculus Nebula around η Carinae. AJ 125:1458–1466, DOI 10.1086/346278

Smith N, Li W, Foley RJ, Wheeler JC, Pooley D, Chornock R, Filippenko AV, Silverman JM, Quimby R, Bloom JS, Hansen C (2007) SN 2006gy: Discovery of the Most Luminous Supernova Ever Recorded, Powered by the Death of an Extremely Massive Star like η Carinae. ApJ 666:1116–1128, DOI 10.1086/519949, arXiv:astro-ph/0612617

Smith N, Foley RJ, Bloom JS, Li W, Filippenko AV, Gavazzi R, Ghez A, Konopacky Q, Malkan MA, Marshall PJ, Pooley D, Treu T, Woo J (2008a) Late-Time Observations of SN 2006gy: Still Going Strong. ApJ 686:485–491, DOI 10.1086/590141, 0802.1743

Smith N, Foley RJ, Filippenko AV (2008b) Dust Formation and He II λ4686 Emission in the Dense Shell of the Peculiar Type Ib Supernova 2006jc. ApJ 680:568–579, DOI 10.1086/587860, 0704.2249

Smith N, Silverman JM, Chornock R, Filippenko AV, Wang X, Li W, Ganeshalingam M, Foley RJ, Rex J, Steele TN (2009) Coronal Lines and Dust Formation in SN 2005ip: Not the Brightest, but the Hottest Type IIn Supernova. ApJ 695:1334–1350, DOI 10.1088/0004-637X/695/2/1334, 0809.5079

Smith N, Chornock R, Silverman JM, Filippenko AV, Foley RJ (2010a) Spectral Evolution of the Extraordinary Type IIn Supernova 2006gy. ApJ 709:856–883, DOI 10.1088/

0004-637X/709/2/856, 0906.2200

Smith N, Miller A, Li W, Filippenko AV, Silverman JM, Howard AW, Nugent P, Marcy GW, Bloom JS, Ghez AM, Lu J, Yelda S, Bernstein RA, Colucci JE (2010b) Discovery of Precursor Luminous Blue Variable Outbursts in Two Recent Optical Transients: The Fitfully Variable Missing Links UGC 2773-OT and SN 2009ip. AJ 139:1451–1467, DOI 10.1088/0004-6256/139/4/1451, 0909.4792

Soderberg AM, Chakraborti S, Pignata G, Chevalier RA, Chandra P, Ray A, Wieringa MH, Copete A, Chaplin V, Connaughton V, Barthelmy SD, Bietenholz MF, Chugai N, Stritzinger MD, Hamuy M, Fransson C, Fox O, Levesque EM, Grindlay JE, Challis P, Foley RJ, Kirshner RP, Milne PA, Torres MAP (2010) A relativistic type Ibc supernova without a detected γ-ray burst. Nature 463:513–515, DOI 10.1038/nature08714, 0908.2817

Stanimirović S, Bolatto AD, Sandstrom K, Leroy AK, Simon JD, Gaensler BM, Shah RY, Jackson JM (2005) Spitzer Space Telescope Detection of the Young Supernova Remnant 1E 0102.2-7219. ApJ 632:L103–L106, DOI 10.1086/497985, arXiv:astro-ph/0509786

Stockdale CJ, Rupen MP, Cowan JJ, Chu Y, Jones SS (2001) The Fading Radio Emission from SN 1961V: Evidence for a Type II Peculiar Supernova? AJ 122:283–287, DOI 10.1086/321136, arXiv:astro-ph/0104235

Sugerman BEK, Ercolano B, Barlow MJ, Tielens AGGM, Clayton GC, Zijlstra AA, Meixner M, Speck A, Gledhill TM, Panagia N, Cohen M, Gordon KD, Meyer M, Fabbri J, Bowey JE, Welch DL, Regan MW, Kennicutt RC (2006) Massive-Star Supernovae as Major Dust Factories. Science 313:196–200, DOI 10.1126/science.1128131, arXiv:astro-ph/0606132

Szalai T, Vinkó J, Balog Z, Gáspár A, Block M, Kiss LL (2011) Dust formation in the ejecta of the type II-P supernova 2004dj. A&A 527:A61+, DOI 10.1051/0004-6361/201015624, 1012.2035

Tanvir NR, Fox DB, Levan AJ, Berger E, Wiersema K, Fynbo JPU, Cucchiara A, Krühler T, Gehrels N, Bloom JS, Greiner J, Evans PA, Rol E, Olivares F, Hjorth J, Jakobsson P, Farihi J, Willingale R, Starling RLC, Cenko SB, Perley D, Maund JR, Duke J, Wijers RAMJ, Adamson AJ, Allan A, Bremer MN, Burrows DN, Castro-Tirado AJ, Cavanagh B, de Ugarte Postigo A, Dopita MA, Fatkhullin TA, Fruchter AS, Foley RJ, Gorosabel J, Kennea J, Kerr T, Klose S, Krimm HA, Komarova VN, Kulkarni SR, Moskvitin AS, Mundell CG, Naylor T, Page K, Penprase BE, Perri M, Podsiadlowski P, Roth K, Rutledge RE, Sakamoto T, Schady P, Schmidt BP, Soderberg AM, Sollerman J, Stephens AW, Stratta G, Ukwatta TN, Watson D, Westra E, Wold T, Wolf C (2009) A γ-ray burst at a redshift of z~8.2. Nature 461:1254–1257, DOI 10.1038/nature08459, 0906.1577

Tegmark M, Silk J, Rees MJ, Blanchard A, Abel T, Palla F (1997) How Small Were the First Cosmological Objects? ApJ 474:1–+, DOI 10.1086/303434, arXiv:astro-ph/9603007

Temim T, Gehrz RD, Woodward CE, Roellig TL, Smith N, Rudnick L, Polomski EF, Davidson K, Yuen L, Onaka T (2006) Spitzer Space Telescope Infrared Imaging and Spectroscopy of the Crab Nebula. AJ 132:1610–1623, DOI 10.1086/507076, arXiv:astro-ph/0606321

Thompson TA, Prieto JL, Stanek KZ, Kistler MD, Beacom JF, Kochanek CS (2009) A New Class of Luminous Transients and a First Census of their Massive Stellar Progenitors. ApJ 705:1364–1384, DOI 10.1088/0004-637X/705/2/1364, 0809.0510

Thronson HA Jr, Telesco CM (1986) Star formation in active dwarf galaxies. ApJ 311:98–112, DOI 10.1086/164756

Tian WW, Leahy DA (2011) Tycho SN 1572: A Naked Ia Supernova Remnant Without an

Associated Ambient Molecular Cloud. ApJ 729:L15+, DOI 10.1088/2041-8205/729/2/L15, 1012.5673

Tielens AGGM (1998) Interstellar Depletions and the Life Cycle of Interstellar Dust. ApJ 499:267–+, DOI 10.1086/305640

Tinsley BM (1980) Evolution of the stars and gas in galaxies. In: Gordon CW, Canuto V (eds) Fundamentals of Cosmic Physics, vol 5, pp 287–388

Todini P, Ferrara A (2001) Dust formation in primordial Type II supernovae. MNRAS 325:726–736, DOI 10.1046/j.1365-8711.2001.04486.x, arXiv:astro-ph/0009176

Truelove JK, McKee CF (1999) Evolution of Nonradiative Supernova Remnants. ApJS 120:299–326, DOI 10.1086/313176

Trundle C, Kotak R, Vink JS, Meikle WPS (2008) SN 2005 gj: evidence for LBV supernovae progenitors? A&A 483:L47–L50, DOI 10.1051/0004-6361:200809755, 0804.2392

Tumlinson J (2006) Chemical Evolution in Hierarchical Models of Cosmic Structure. I. Constraints on the Early Stellar Initial Mass Function. ApJ 641:1–20, DOI 10.1086/500383, arXiv:astro-ph/0507442

Umana G, Buemi CS, Trigilio C, Hora JL, Fazio GG, Leto P (2009) The Dusty Nebula Surrounding HR Car: A Spitzer View. ApJ 694:697–703, DOI 10.1088/0004-637X/694/1/697, 0901.2447

Umeda H, Nomoto K (2002) Nucleosynthesis of Zinc and Iron Peak Elements in Population III Type II Supernovae: Comparison with Abundances of Very Metal Poor Halo Stars. ApJ 565:385–404, DOI 10.1086/323946, arXiv:astro-ph/0103241

Valiante R, Schneider R, Bianchi S, Andersen AC (2009) Stellar sources of dust in the high-redshift Universe. MNRAS 397:1661–1671, DOI 10.1111/j.1365-2966.2009.15076.x, 0905.1691

Valiante R, Schneider R, Salvadori S, Bianchi S (2011) The origin of dust in high redshift QSOs: the case of SDSS J1148+5251. ArXiv e-prints 1106.1418

van den Hoek LB, Groenewegen MAT (1997) New theoretical yields of intermediate mass stars. A&AS 123:305–328, DOI 10.1051/aas:1997162

Van Dyk SD, Peng CY, King JY, Filippenko AV, Treffers RR, Li W, Richmond MW (2000) SN 1997bs in M66: Another Extragalactic η Carinae Analog? PASP 112:1532–1541, DOI 10.1086/317727, arXiv:astro-ph/0009027

Van Dyk SD, Filippenko AV, Li W (2002) Possible Recovery of SN 1961V in Hubble Space Telescope Archival Images. PASP 114:700–707, DOI 10.1086/341695, arXiv:astro-ph/0203508

Van Dyk SD, Filippenko AV, Chornock R, Li W, Challis PM (2005) Supernova 1954J (Variable 12) in NGC 2403 Unmasked. PASP 117:553–562, DOI 10.1086/430238, arXiv:astro-ph/0503324

Van Dyk SD, Li W, Filippenko AV, Humphreys RM, Chornock R, Foley R, Challis PM (2006) The Type IIn Supernova 2002kg: The Outburst of a Luminous Blue Variable Star in NGC 2403. ArXiv Astrophysics e-prints arXiv:astro-ph/0603025

Van Dyk SD, Davidge TJ, Elias-Rosa N, Taubenberger S, Li W, Howerton S, Pignata G, Morrell N, Hamuy M, Filippenko AV (2010) Supernova 2008bk and Its Red Supergiant Progenitor. ArXiv e-prints 1011.5873

van Loon JT, Cohen M, Oliveira JM, Matsuura M, McDonald I, Sloan GC, Wood PR, Zijlstra AA (2008) Molecules and dust production in the Magellanic Clouds. A&A 487:1055–1073, DOI 10.1051/0004-6361:200810036, 0806.3557

Vassiliadis E, Wood PR (1993) Evolution of low- and intermediate-mass stars to the end of the asymptotic giant branch with mass loss. ApJ 413:641–657, DOI 10.1086/173033

Ventura P, D'Antona F (2009) Massive AGB models of low metallicity: the implications for the self-enrichment scenario in metal-poor globular clusters. A&A 499:835–846, DOI 10.1051/0004-6361/200811139

Vinkó J, Sárneczky K, Balog Z, Immler S, Sugerman BEK, Brown PJ, Misselt K, Szabó GM, Csizmadia S, Kun M, Klagyivik P, Foley RJ, Filippenko AV, Csák B, Kiss LL (2009) The Young, Massive, Star Cluster Sandage-96 After the Explosion of Supernova 2004dj in NGC 2403. ApJ 695:619–635, DOI 10.1088/0004-637X/695/1/619, 0812.1589

Vlahakis C, Dunne L, Eales S (2005) The SCUBA Local Universe Galaxy Survey - III. Dust along the Hubble sequence. MNRAS 364:1253–1285, DOI 10.1111/j.1365-2966.2005.09666.x, arXiv:astro-ph/0510768

Wachter A, Winters JM, Schröder K, Sedlmayr E (2008) Dust-driven winds and mass loss of C-rich AGB stars with subsolar metallicities. A&A 486:497–504, DOI 10.1051/0004-6361:200809893, 0805.3656

Wagner RM, Vrba FJ, Henden AA, Canzian B, Luginbuhl CB, Filippenko AV, Chornock R, Li W, Coil AL, Schmidt GD, Smith PS, Starrfield S, Klose S, Tichá J, Tichý M, Gorosabel J, Hudec R, Simon V (2004) Discovery and Evolution of an Unusual Luminous Variable Star in NGC 3432 (Supernova 2000ch). PASP 116:326–336, DOI 10.1086/382997, arXiv:astro-ph/0404035

Walter F, Carilli C, Bertoldi F, Menten K, Cox P, Lo KY, Fan X, Strauss MA (2004) Resolved Molecular Gas in a Quasar Host Galaxy at Redshift z=6.42. ApJ 615:L17–L20, DOI 10.1086/426017, arXiv:astro-ph/0410229

Wanajo S, Nomoto K, Janka H, Kitaura FS, Müller B (2009) Nucleosynthesis in Electron Capture Supernovae of Asymptotic Giant Branch Stars. ApJ 695:208–220, DOI 10.1088/0004-637X/695/1/208, 0810.3999

Wang R, Carilli CL, Neri R, Riechers DA, Wagg J, Walter F, Bertoldi F, Menten KM, Omont A, Cox P, Fan X (2010) Molecular Gas in z ˜ 6 Quasar Host Galaxies. ApJ 714:699–712, DOI 10.1088/0004-637X/714/1/699, 1002.1561

Wang X, Yang Y, Zhang T, Ma J, Zhou X, Li W, Lou Y, Li Z (2005) The Progenitor of SN 2004dj in a Star Cluster. ApJ 626:L89–L92, DOI 10.1086/431903, arXiv:astro-ph/0505305

Webbink RF (1984) Double white dwarfs as progenitors of R Coronae Borealis stars and Type I supernovae. ApJ 277:355–360, DOI 10.1086/161701

Weingartner JC, Draine BT (2001) Dust Grain-Size Distributions and Extinction in the Milky Way, Large Magellanic Cloud, and Small Magellanic Cloud. ApJ 548:296–309, DOI 10.1086/318651, arXiv:astro-ph/0008146

Weis K, Bomans DJ (2005) SN 2002kg - the brightening of LBV V37 in NGC 2403. A&A 429:L13–L16, DOI 10.1051/0004-6361:200400105, arXiv:astro-ph/0411504

Wesson R, Barlow MJ, Ercolano B, Andrews JE, Clayton GC, Fabbri J, Gallagher JS, Meixner M, Sugerman BEK, Welch DL, Stock DJ (2010) The destruction and survival of dust in the shell around SN2008S. MNRAS 403:474–482, DOI 10.1111/j.1365-2966.2009.15871.x, 0907.0246

Whelan J, Iben I Jr (1973) Binaries and Supernovae of Type I. ApJ 186:1007–1014, DOI 10.1086/152565

Williams BJ, Borkowski KJ, Reynolds SP, Raymond JC, Long KS, Morse J, Blair WP, Ghavamian P, Sankrit R, Hendrick SP, Smith RC, Points S, Winkler PF (2008) Ejecta, Dust, and Synchrotron Radiation in SNR B0540-69.3: A More Crab-Like Remnant than the Crab. ApJ 687:1054–1069, DOI 10.1086/592139, 0807.4155

Willson LA (2007) What Do We Really Know about Mass Loss on the AGB? In: F Kerschbaum, C Charbonnel, & R F Wing (ed) Why Galaxies Care About AGB Stars: Their

Importance as Actors and Probes, Astronomical Society of the Pacific Conference Series, vol 378, pp 211–+

Wilson TL, Batrla W (2005) An alternate estimate of the mass of dust in Cassiopeia A. A&A 430:561–566, DOI 10.1051/0004-6361:20041220, `arXiv:astro-ph/0412533`

Winters JM, Le Bertre T, Jeong KS, Helling C, Sedlmayr E (2000) A systematic investigation of the mass loss mechanism in dust forming long-period variable stars. A&A 361:641–659

Woitke P (2006) Too little radiation pressure on dust in the winds of oxygen-rich AGB stars. A&A 460:L9–L12, DOI 10.1051/0004-6361:20066322, `arXiv:astro-ph/0609392`

Wooden DH, Rank DM, Bregman JD, Witteborn FC, Tielens AGGM, Cohen M, Pinto PA, Axelrod TS (1993) Airborne spectrophotometry of SN 1987A from 1.7 to 12.6 microns - Time history of the dust continuum and line emission. ApJS 88:477–507, DOI 10.1086/191830

Woosley SE, Weaver TA (1986) The physics of supernova explosions. ARA&A 24:205–253, DOI 10.1146/annurev.aa.24.090186.001225

Woosley SE, Weaver TA (1995) The Evolution and Explosion of Massive Stars. II. Explosive Hydrodynamics and Nucleosynthesis. ApJS 101:181–+, DOI 10.1086/192237

Yang X, Chen P, He J (2004) Molecular and dust features of 29 SiC carbon AGB stars. A&A 414:1049–1063, DOI 10.1051/0004-6361:20031673

Yoshida N, Omukai K, Hernquist L, Abel T (2006) Formation of Primordial Stars in a ΛCDM Universe. ApJ 652:6–25, DOI 10.1086/507978, `arXiv:astro-ph/0606106`

Yoshida N, Oh SP, Kitayama T, Hernquist L (2007a) Early Cosmological H II/He III Regions and Their Impact on Second-Generation Star Formation. ApJ 663:687–707, DOI 10.1086/518227, `arXiv:astro-ph/0610819`

Yoshida N, Omukai K, Hernquist L (2007b) Formation of Massive Primordial Stars in a Reionized Gas. ApJ 667:L117–L120, DOI 10.1086/522202, `0706.3597`

Yoshida N, Omukai K, Hernquist L (2008) Protostar Formation in the Early Universe. Science 321:669–, DOI 10.1126/science.1160259, `0807.4928`

Yoshida T, Umeda H (2011) A progenitor for the extremely luminous Type Ic supernova 2007bi. MNRAS 412:L78–L82, DOI 10.1111/j.1745-3933.2011.01008.x, `1101.0635`

Yun MS, Carilli CL (2002) Radio-to-Far-Infrared Spectral Energy Distribution and Photometric Redshifts for Dusty Starburst Galaxies. ApJ 568:88–98, DOI 10.1086/338924, `arXiv:astro-ph/0112074`

Zeidler S, Posch T, Mutschke H, Richter H, Wehrhan O (2011) Near-infrared absorption properties of oxygen-rich stardust analogs. The influence of coloring metal ions. A&A 526:A68+, DOI 10.1051/0004-6361/201015219, `1101.0695`

Zhukovska S, Gail H, Trieloff M (2008) Evolution of interstellar dust and stardust in the solar neighbourhood. A&A 479:453–480, DOI 10.1051/0004-6361:20077789, `0706.1155`

Zijlstra AA, Matsuura M, Wood PR, Sloan GC, Lagadec E, van Loon JT, Groenewegen MAT, Feast MW, Menzies JW, Whitelock PA, Blommaert JADL, Cioni M, Habing HJ, Hony S, Loup C, Waters LBFM (2006) A Spitzer mid-infrared spectral survey of mass-losing carbon stars in the Large Magellanic Cloud. MNRAS 370:1961–1978, DOI 10.1111/j.1365-2966.2006.10623.x, `arXiv:astro-ph/0602531`